

115

Beaufort Sea
Ice Design Criteria

Acquisition of Data
on EIFs

The Environmental Studies Research Funds are financed from special levies on the oil and gas industry and are administered by the National Energy Board for the Minister of Energy, Mines and Resources, and for the Minister of Indian Affairs and Northern Development.

The Environmental Studies Research Funds and any person acting on their behalf assume no liability arising from the use of the information contained in this document. The opinions expressed are those of the authors and do not necessarily reflect those of the Environmental Studies Research Funds agencies. The use of trade names or identification of specific products does not constitute an endorsement or recommendation for use.

**Environmental Studies Research Funds Report No. 115
October 1992**

**BEAUFORT SEA
ICE DESIGN CRITERIA
ACQUISITION OF DATA
ON EIFs**

by

***CANATEC Consultants Ltd.*
#1730, 700 - 6th Avenue SW
Calgary, Alberta
T2P 0T8**

Scientific Advisor: B.D. Wright

Pilkington, G.R., M.C. Hill, M. Metge, D. McGonigal, Beaufort Sea Ice Design Criteria. 1992. Environmental Studies Research Funds. Report No. 115. Calgary. xiii + 154 pages.

Published under the auspices of the Environmental Studies Research Funds

ISBN #0-921652-15-1

©1992 - *CANATEC Consultants Ltd.*

Abstract

The objectives of this project were to develop an extreme ice features (EIF) data base using 1991 AES SAR and other available remotely sensed data, and, if possible, identify the means of continuing the data base in the future. Further, statistical analyses were carried out on the EIF data obtained, and an estimate made of the impact rate of EIFs against structures in the Southern Beaufort Sea.

An EIF is defined here as an ice feature which causes extreme design loads on an offshore production platform (i.e. greater than 300,000 tonnes). This definition results in an EIF being a feature consisting of, for example, a piece of ice at least 20 m thick and 500 m in diameter, frozen into a multi-year floe at least 5 m thick and 2 km in diameter surrounded by pack ice at least 1.5 m thick. Multi-year hummock fields (MYHFs), ice islands (IIs), and re-entrant ice (REs) thus constitute a part or all of an EIF, particularly when frozen solidly to old landfast or re-entrant ice.

This study summarizes the information on EIFs in the literature and uses this to form an initial data base. Data from the STAR-1 and STAR-2 Synthetic Aperture Radar (SAR) systems were systematically analyzed for EIFs and the resulting EIFs were added into a database.

An analysis of the available radar data and SPOT (Satellite pour l'Observation de la Terre) satellite visual-imagery data indicated that a spatial resolution of 15 metres or better is required to identify EIFs. Thus one can use 12 or 15 m resolution Synthetic Aperture Radar (SAR) data, but not 25 m SAR or SLAR (Side Looking Airborne Radar) data. Aerial photography and 10 m SPOT imagery are also suitable. The SAR data is the most useful as it provides all weather coverage, 50 to 128 km swath width, and identification of old and first year ice in winter. Aerial photography provides an image swath width of 3 to 6 km, and 10 m SPOT data about 60 km swath width. SPOT images are mostly useful in summer when

the ice melt provides the necessary contrast to permit identification of surface features. Aerial photography is good in winter and provides the height of features when stereo is used.

Using three years of recent SAR data, covering 334,600 km², 114 MYHFs, REs and IIs were identified, for an areal density of $6.4 \times 10^{-4}/\text{km}^2$. Of these, 40% were greater than 2 km and so the density of EIFs is $2.6 \times 10^{-4}/\text{km}^2$. This EIF density suggests a return period of at least 123 and 54 years for impact with offshore structures at 70 and 71° latitude in the Southern Beaufort Sea, respectively. If we count only EIFs within 50 km of the shore of the Queen Elizabeth Islands, the density of EIFs increases to $6.8 \times 10^{-4}/\text{km}^2$ for return periods of at least 53 and 23 years for 70 and 71° latitude, respectively. These return period estimates are very rough and must be used with caution.

Recommendations are also provided for future collection of EIF data using SAR, aerial photography and SPOT images, the processing of the data and the further enhancement of the data base.

Résumé

Les objectifs du projet étaient l'élaboration d'une base de données sur les formations glacielles extrêmes (FGE) regroupant les données de télédétection du RAAS du SEA prises en 1991 et d'autres. Il fallait aussi examiner le moyen de poursuivre, si possible, l'étoffement de cette base de données. De plus, on a effectué des analyses statistiques des données ainsi obtenues, et procédé à une estimation des incidences de ces formations sur des structures dans le sud de la mer de Beaufort.

On entend ici par FGE une formation glacielle qui peut exercer une charge considérable sur une plate-forme de production en mer (plus de 300 000 tonnes). Il s'agirait donc par exemple d'un morceau de glace d'au moins 20 m d'épaisseur et 500 m de diamètre, pris dans un floe de glace de plusieurs années d'au moins 5 m d'épaisseur et 2 km de diamètre, lui-même entouré de pack d'au moins 1,5 m d'épaisseur. Les champs de hummocks de glace de plusieurs années, les îles de glace et la glace soudée à la plate-forme constituent donc tout ou partie d'une FGE, surtout s'ils sont solidement soudés à de la vieille glace de rivage ou elle-même soudée à la plate-forme.

L'étude résume les renseignements sur les FGE déjà publiés et s'en sert comme base de données initiale. On a systématiquement recherché dans les données provenant des systèmes de radar à antenne synthétique (RAAS) STAR-1 et STAR-2 la présence de FGE, et celles qu'on a détectées ont été ajoutées sous forme de base de données.

Après analyse des données radar et de celles du satellite SPOT (Satellite pour l'observation de la Terre) dans le visuel, on a constaté qu'il fallait avoir, pour détecter les FGE, une résolution spatiale d'au moins 15 mètres. On peut donc utiliser les données de RAAS de résolution 12 ou 15 mètres, mais pas celles d'un RAAS ou d'un RAAL à résolution de 25 mètres. Les photographies aériennes

et l'imagerie SPOT à résolution de 10 m s'y prêtent aussi. Les données de RAAS sont les plus utiles : couverture par tous les temps, largeur de couloir de 50 à 128 km, détection de la glace vieille et de la glace de première année en hiver. Les photographies aériennes ont un couloir de 3 à 6 km, et les données du SPOT à résolution de 10 m en ont un d'environ 60 km. L'imagerie SPOT sert surtout en été, lorsque la fonte assure le contraste nécessaire pour qu'on puisse déterminer les caractéristiques de la surface. La photographie aérienne est utile en hiver, et donne, en stéréo, la hauteur des reliefs.

À partir de trois ans de données RAAS récentes, couvrant 334 600 km², on a repéré 114 champs de hummocks de glace de plusieurs années, éléments de glace soudée à la plate-forme et îles de glace, soit une densité de $6,4 \times 10^{-4}/\text{km}^2$. Sur ces 114 éléments, 40 % dépassaient 2 km; la densité de FGE est donc de $2,6 \times 10^{-4}/\text{km}^2$. Ce chiffre semble indiquer une période de retour des impacts sur les structures d'au moins 123 et 54 ans, aux latitudes 70 et 71 du sud de la mer de Beaufort, respectivement. Si l'on ne compte que les FGE situées à moins de 50 km des rives des îles Queen-Elizabeth, leur densité passe à $6,8 \times 10^{-4}/\text{km}^2$, avec des périodes de retour de 53 et 23 ans, aux latitudes ci-dessus respectivement. Ces évaluations de périodes de retour sont très sommaires et doivent être utilisées avec circonspection.

On formule également des recommandations visant la collecte future de données sur les FGE au moyens de photographies aériennes du RAAS et de l'imagerie SPOT, le traitement de ces données et l'amélioration ultérieure de la base de données.

Acknowledgements

The authors of this report greatly appreciate the assistance provided by the Scientific Authority, Brian Wright of Gulf Canada Resources Inc. (now with B. Wright & Associates). His direction and advice in all parts of the project were invaluable. The help provided by the ESRF Senior Program Officer, Brian Nesbitt, the Director Physical Environment with the National Energy Board, Oleh Mycyk, and the staff of the Ice Climatology section of the Atmospheric Environment Services in Ottawa, David Mudry, Terry Mullane and Fred Richardson, is also very much appreciated.

The authors acknowledge AES for modifying their STAR-2 flight plan, providing imagery over the test area, and the digital data tape along with Gulf Canada Resources Ltd. and Canadian Marine Drilling Ltd. who allowed use of their library material for the literature review. RadarSat International Inc. (Susan Ross and Monica Meneghetti) showed considerable patience in finding SPOT imagery for the project. Tiit Romat of the Department of National Defence kindly offered to provide aerial photography for the area of interest, while Dave Maloley of Polar Continental Shelf Project offered to provide ground truthing of the SAR data near Hobson's Choice Ice Island. Scott Paterson of Intera-Kenting and Chuck Livingstone of the Canadian Centre for Remote Sensing also provided useful discussions.

TABLE OF CONTENTS

| | |
|---|------|
| Abstract | iii |
| Acknowledgements | vii |
| TABLE OF CONTENTS | viii |
| List of Tables | xi |
| List of Figures | xii |
| CHAPTER 1 | |
| INTRODUCTION | 1-1 |
| CHAPTER 2 | |
| SUMMARY, CONCLUSIONS AND RECOMMENDATIONS | 2-1 |
| 2.1 SUMMARY AND CONCLUSIONS | 2-1 |
| 2.2 RECOMMENDATIONS | 2-5 |
| CHAPTER 3 | |
| WHAT IS AN "EXTREME ICE FEATURE"? | 3-1 |
| 3.1 INTRODUCTION | 3-2 |
| 3.2 CONTEXT | 3-2 |
| 3.3 TYPES OF STRUCTURE AND WATER DEPTH | 3-3 |
| 3.4 EXPLORATION OR PRODUCTION PLATFORMS? | 3-4 |
| 3.5 LIMITS TO GLOBAL LOADS | 3-6 |
| CHAPTER 4 | |
| REVIEW OF LITERATURE AND EXISTING INFORMATION | 4-1 |
| 4.1 SUMMARY | 4-1 |
| 4.2 LITERATURE REVIEW | 4-1 |
| 4.2.1 Ice Islands | 4-1 |
| 4.2.2 Multi-Year Hummock Fields (MYHFs) | 4-5 |
| 4.2.3 Ice Plugs | 4-7 |
| 4.2.4 Multi-Year Landfast Ice (MYLF) | 4-8 |
| 4.3 DATA SOURCES | 4-8 |
| 4.4 DATA BASE | 4-11 |
| 4.4.1 Relevant Parameters | 4-11 |

TABLE OF CONTENTS (cont'd)

CHAPTER 5

| | |
|---|-----|
| PROPOSED STAR-2 FLIGHT PLAN AND GROUND TRUTHING | 5-1 |
| 5.1 OBJECTIVES | 5-1 |
| 5.2 PROPOSED FLIGHT PLAN | 5-2 |
| 5.3 GROUND TRUTHING | 5-2 |

CHAPTER 6

| | |
|---|-----|
| OTHER SOURCES OF DATA | 6-1 |
| 6.1 INTRODUCTION | 6-1 |
| 6.2 AERIAL PHOTOGRAPHY | 6-1 |
| 6.2.1 Department of National Defence (DND) | 6-1 |
| 6.2.2 National Research Council (NRC) | 6-4 |
| 6.2.3 Intera Technologies Ltd., Calgary | 6-5 |
| 6.3 SAR DATA | 6-5 |
| 6.3.1 Intera Technologies Ltd., Calgary | 6-5 |
| 6.4 SPOT (Satellite pour l'observation de la terre) | 6-7 |

CHAPTER 7

| | |
|--|------|
| INTERPRETATION OF EIFs FROM SAR, 1988 - 1991 | 7-1 |
| 7.1 INTRODUCTION | 7-1 |
| 7.2 METHODOLOGY | 7-1 |
| 7.2.1 Notes on the 1988 STAR-2/SPOT Interpretation | 7-2 |
| 7.2.2 SAR Interpretation Key | 7-4 |
| 7.3 INTERPRETATION OF ARCHIVE SAR, 1988-1989 | 7-13 |
| 7.4 INTERPRETATION OF JANUARY 1991 STAR-2 | 7-15 |

CHAPTER 8

| | |
|---------------------------------|------|
| DATA SUMMARY AND ANALYSIS | 8-1 |
| 8.1 INTRODUCTION | 8-1 |
| 8.2 DATA TABLES AND MAPS | 8-1 |
| 8.2.1 Tables | 8-1 |
| 8.2.2 Maps | 8-4 |
| 8.3 ANALYSES | 8-9 |
| 8.3.1 Feature Size Distribution | 8-10 |
| 8.3.2 Areal Density | 8-17 |
| 8.3.3 Major/minor axis ratio | 8-18 |
| 8.3.4 Landfast Ice | 8-18 |
| 8.3.5 Ice Plugs | 8-25 |

TABLE OF CONTENTS (cont'd)

| | | |
|-------|--|------|
| 8.4 | INTERACTION PROBABILITIES WITH EIFs IN THE SOUTHERN BEAUFORT SEA | 8-25 |
| 8.4.1 | Introduction | 8-25 |
| 8.4.2 | Assumptions | 8-25 |
| 8.4.3 | Impact Rate | 8-27 |

CHAPTER 9

| | | |
|-------|--|-----|
| | RECOMMENDATIONS FOR FUTURE DATA COLLECTION | 9-1 |
| 9.1 | GENERAL | 9-1 |
| 9.2 | GENERAL SURVEY DETAILS | 9-1 |
| 9.2.1 | Area of interest | 9-1 |
| 9.2.2 | Frequency of Survey | 9-1 |
| 9.3 | SAR SURVEY (Aircraft/Satellite) | 9-3 |
| 9.3.1 | General | 9-3 |
| 9.3.2 | Resolution and Swath Width | 9-3 |
| 9.3.3 | Flight Path | 9-3 |
| 9.3.4 | Date of Flight | 9-4 |
| 9.4 | AERIAL PHOTOGRAPHY | 9-4 |
| 9.4.1 | Aircraft | 9-4 |
| 9.4.2 | Satellite | 9-5 |
| 9.5 | THE DATA | 9-5 |

| | | |
|------------|------------------|------|
| CHAPTER 10 | REFERENCES | 10-1 |
|------------|------------------|------|

| | | |
|------------|--|-----|
| APPENDIX A | Survey Fax and Recipients of Fax | A-1 |
|------------|--|-----|

| | | |
|------------|------------------------------|-----|
| APPENDIX B | Results of SPOT Survey | B-1 |
|------------|------------------------------|-----|

| | | |
|------------|---------------------|-----|
| APPENDIX C | EIF Data Base | C-1 |
|------------|---------------------|-----|

| | | |
|------------|-----------------------|-----|
| APPENDIX D | Ice Terminology | D-1 |
|------------|-----------------------|-----|

LIST OF TABLES

| <u>Table</u> | <u>Description</u> | <u>Page</u> |
|--------------|---|-------------|
| Table 3.1 | Extreme Ice Feature dimensions vs structure resistance | 3-9 |
| Table 4.1 | Raw Data Sources with Potential for EIF Data | 4-9 |
| Table 4.2 | EIFs Data Base, 1946-1988 | 4-12 |
| Table 6.1 | Archival SAR Data available through INTERA | 6-6 |
| Table 6.2 | Latitude and Longitude ranges of Hobson's Choice ice island positions, 1988 - 1990 | 6-9 |
| Table 6.3 | Results of SPOT imagery 1988 search | 6-10 |
| Table 6.4 | Results of SPOT imagery 1990 search | 6-11 |
| Table 8.1 | Sample of the extreme ice features data extracted from SAR imagery | 8-2 |
| Table 8.2 | Areal Density of EIFs | 8-17 |
| Table 8.3 | Inferred fast ice movements along the outer coasts of the Queen Elizabeth Islands 1974 - 1991 | 8-23 |

LIST OF FIGURES

| <u>Figure</u> | <u>Description</u> | <u>Page</u> |
|---------------|---|-------------|
| Fig. 1.1 | Location Map | 1-4 |
| Fig. 3.1 | Classification Scheme for Arctic Offshore Structures | 3-5 |
| Fig. 3.2 | The Different Types of Ice Floe Interactions | 3-7 |
| Fig. 3.3 | Extreme Ice Feature Impact | 3-8 |
| Fig. 4.1 | Map of Ice Island Sightings in the Arctic Ocean | 4-18 |
| Fig. 4.2 | Ice Island Fragments - West of Banks Island | 4-19 |
| Fig. 4.3 | Northern Ellesmere Island Showing Remaining Ice Shelves in 1977 and Possible Ice Shelf Extremities | 4-20 |
| Fig. 4.4 | Northern Ellesmere Island Showing Remaining Ice Shelves in 1984 | 4-21 |
| Fig. 4.5 | Drift of Ice Island T-3 in the Beaufort Gyre 1950-79 | 4-22 |
| Fig. 4.6 | Mean Velocities of Ice Drift in the Arctic Ocean | 4-23 |
| Fig. 4.7 | Aerial Views of a Multi-Year Hummock Field, Prince Patrick Island 1980 | 4-24 |
| Fig. 4.8 | Ground Truthing Sites April 1980 | 4-25 |
| Fig. 4.9 | Aerial Photography Flight Lines April 1980 | 4-26 |
| Fig. 4.10 | Floe Size Distributions of "Extremely Bumpy" Floes (MYHFs) April 1980 | 4-27 |
| Fig. 4.11 | Aerial Photography of MYHF, March 1980 | 4-28 |
| Fig. 4.12 | Aerial Photography of Second Year Hummock Field April 1984 | 4-29 |
| Fig. 4.13 | Areas of Multi-year Landfast Ice, Queen Elizabeth Islands | 4-30 |
| Fig. 5.1 | Flight Paths for AES Round Robin January 1991 | 5-3 |
| Fig. 5.2 | Detail of STAR-2 Flight paths over test area, January 1991 | 5-4 |
| Fig. 5.3 | Extensions of regular STAR-2 flight lines, January 1991 | 5-5 |
| Fig. 5.4 | Proposed path of additional 15 m resolution STAR-2 flight line for collection of statistical data during January 1991 Round Robin | 5-6 |
| Fig. 5.5 | EIFs, Surface Truth Report Form | 5-8 |
| Fig. 6.1 | Map of 1982 air photo flight lines and area of multi- year hummock fields | 6-3 |
| Fig. 6.2 | SPOT satellite orbit paths over the study area | 6-8 |
| Fig. 7.1 | Detail of STAR-2 image of 19 February 1988, used during intercomparison with SPOT imagery | 7-3 |
| Fig. 7.2 | Detail of SPOT image of 27 July 1988 | 7-6 |
| Fig. 7.3 | Detail of STAR-1, 12 m pixel image of 24 March 1989 | 7-7 |
| Fig. 7.4 | Detail of STAR-2, 15 m pixel image of January 1991 | 7-8 |
| Fig. 7.5 | Detail of STAR-2, 25 m pixel image of January 1991 | 7-9 |

LIST OF FIGURES continued

| <u>Figure</u> | <u>Description</u> | <u>Page</u> |
|---------------|--|-------------|
| Fig. 8.1 | EIFs Locations, Winter 1988 | 8-5 |
| Fig. 8.2 | EIFs Locations, Winter 1989 | 8-6 |
| Fig. 8.3 | EIFs Locations, Winter 1991 | 8-7 |
| Fig. 8.4 | EIFs Locations, All Years of Record | 8-8 |
| Fig. 8.5 | Exceedence Probability Plot EIFs, 1946-1988 | 8-11 |
| Fig. 8.6 | EIFs New Data Sources | 8-12 |
| Fig. 8.7 | Exceedence Probability, 1988-1991 MY Hummock Fields greater than 2 km | 8-13 |
| Fig. 8.8 | Exceedence Probability, 1988-1991 Ice Islands greater than 2 km | 8-14 |
| Fig. 8.9 | Exceedence Probability, 1988-1991 Re-entrant ice greater than 2 km | 8-15 |
| Fig. 8.10 | Shape vs Size, MY Hummock Fields, 1988-1991 | 8-19 |
| Fig. 8.11 | Shape vs Size, Ice Islands, 1988-1991 | 8-20 |
| Fig. 8.12 | Shape vs Size, Re-entrant Ice, 1988-1991 | 8-21 |
| Fig. 8.13 | Detail of AES composite series ice chart used to monitor changes in fast ice limits | 8-22 |
| Fig. 8.14 | Multi-Year Fast Ice Extent | 8-24 |
| Fig. 9.1 | Area of EIFs Interest | 9-2 |

CHAPTER 1 INTRODUCTION

The objective of this project was to acquire information and develop statistics on extreme ice features relevant to Beaufort Sea development structures, and included the following phases as follows:

- a) Develop a field data acquisition plan in conjunction with the Atmospheric Environment Services Ice Branch which 1) utilizes the remote sensing tools (particularly STAR-2 and mapping cameras) aboard their reconnaissance aircraft and 2) takes advantage of systematic AES round robin ice reconnaissance flights for high quality, low cost data acquisition on an opportunity basis.
- b) Implement the plan on a pilot basis during the 1990/92 period, quality control and archive the data products.
- c) Review existing information on extreme ice features and undertake a statistical analysis of extreme ice features from the data base collected during the 1990/91 period.
- d) Recommend an approach for ongoing systematic AES data acquisition on extreme features, follow-up quality control, analysis and archiving until a reliable extreme ice feature data base is in place.

Ice islands and multi-year hummock fields are extreme ice features (EIFs) which originate on the northwest coast of the Queen Elizabeth Islands and in the adjacent pack ice of the Arctic Basin and then drift southwards with the Beaufort Gyre. Since they are the most formidable ice features found in the Beaufort Sea, potential EIF impacts may govern the design of offshore production platforms and the burial depth of subsea pipeline sections. Ice islands are usually more massive, but are rare. Multi-year hummock fields can be as thick as ice islands, are more numerous, and, if embedded in a large multi-year floe, can generate extremely large forces.

The initial project concept was to use high resolution STAR-2 synthetic aperture radar (SAR) imagery obtained during regular AES reconnaissance missions as a low cost, analytic data source for definitions of EIFs. The STAR-2 aircraft entered service with AES in the fall of 1989 carrying a SAR with two modes of operation:

- a) a "wide swath" mode which provides coverage of the ice over 100 km wide swaths on both sides of the aircraft's flight path; in this mode, the resolution (or pixel size) is 25 m.
- b) a "narrow swath" mode which provides coverage over 64 km wide swaths on both sides of the aircraft's path; in this mode the resolution (or pixel size) is 15 m.

In most years, the STAR-2 aircraft flies over the Queen Elizabeth Islands and provides complete SAR coverage of the ice in various channels. The first part of this project was to identify changes to the aircraft's overall Arctic Islands flight plan that would provide good coverage of the areas where EIFs might be found (i.e. the northwestern coastline of the Archipelago from Ellesmere Island to Prince Patrick Island). As noted earlier, EIFs form along this coastline and, from there, can drift southwards into areas of potential production in the Beaufort Sea.

This report covers all aspects of the project, including a review of pre-existing literature on EIFs (Chapter 4), a description of the 1991 data acquisition plan and results (Chapter 5), alterations to the original work plan and a description of other sources of imagery identified during the course of the work (Chapter 6), development of SAR interpretation keys for EIFs, additions to the EIF data base (Chapter 7), and analysis of the EIF data in statistical terms of relevance to Beaufort Sea production (Chapter 8). Recommendations regarding on-going maintenance of, and additions to, the EIF data base are provided (Chapter 9).

This report also addresses the question "What is an extreme ice feature?". In order to establish some context for the definition of EIFs in ice engineering terms, Chapter 3

discusses the sizes of ice features of interest in this study on the basis of design loads on a gravity-based offshore production structure.

Figure 1.1 shows a location map for the area of interest to this study.

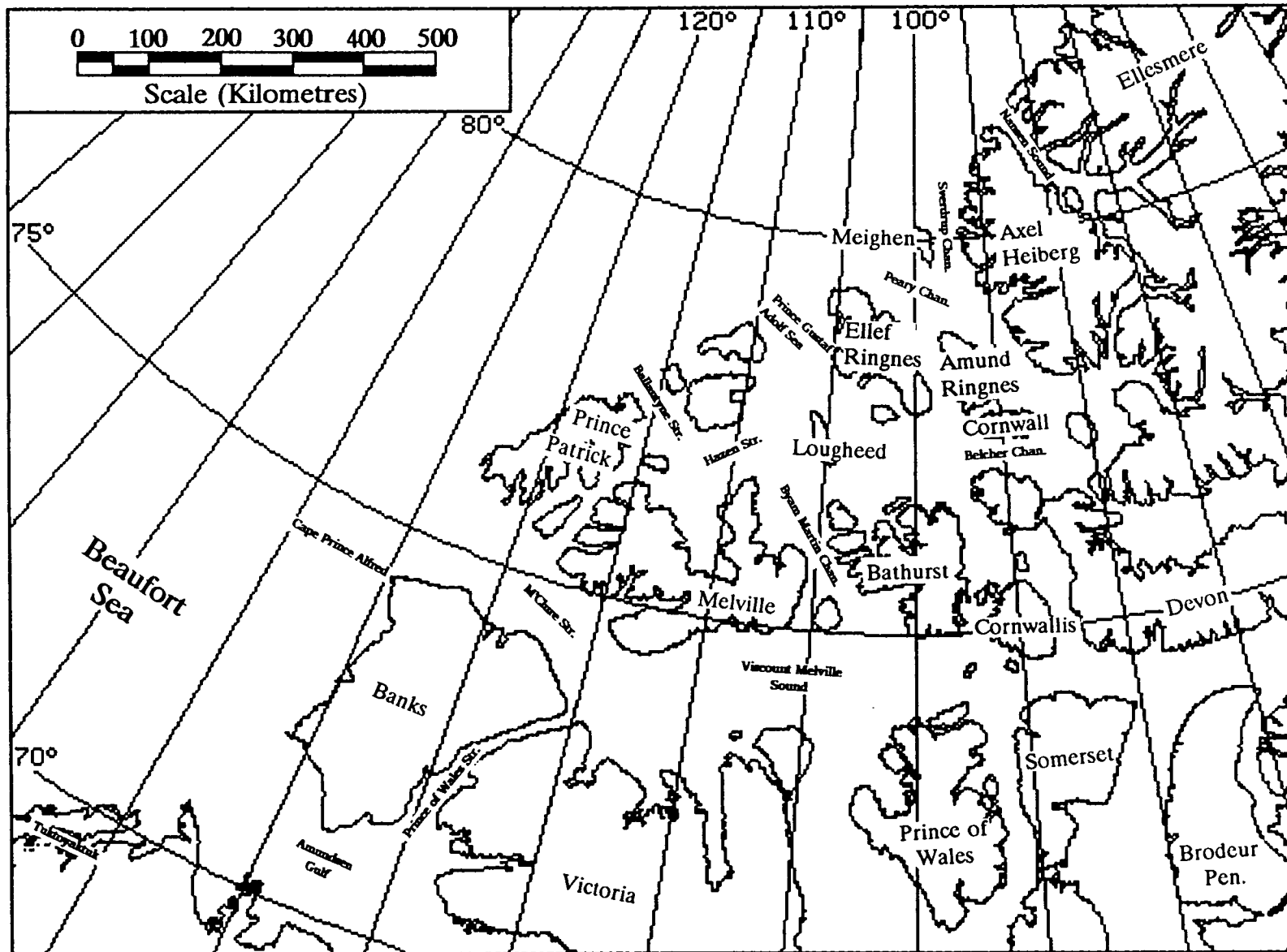


Figure 1.1 Location Map

CHAPTER 2

SUMMARY, CONCLUSIONS AND RECOMMENDATIONS

2.1 SUMMARY AND CONCLUSIONS

- i) Flight plan modifications for AES's January 1991 STAR-2 Round Robin were developed to address the requirements of this EIF study and submitted to AES. However, only part of the flight plan modifications that were requested could be accommodated by AES due to aircraft range limitations and AES priorities.

- ii) The relevant SAR imagery obtained from the Round Robin was for a test area over Peary Channel, in which there were ice island fragments and multi-year hummock fields. These data provided an excellent opportunity to determine the limitations of the STAR-2 at its two resolutions (15 and 25 m), the effect of ice feature location relative to the aircraft (i.e., near field or far field), and the direction of overflight (i.e., North-South vs. East-West) relative to these ice features.

The STAR-2 data indicated that

- a) MYHFs, ice islands and re-entrant ice could be identified in 15 m resolution data. Only ice islands could be identified in 25 m data.
- b) In the STAR-2 15 m data, there appeared to be no obvious degradation of the image, whether it was located near-to or far-from the aircraft flight path. However, a section of imagery on the near edge and far edge of the imagery should be removed before analysis.
- c) In the STAR-2 15 m imagery, the orientation of flight path did not appear to affect the identification of EIFs. However, linear features were generally evident in the SAR due to the raster scan, and these must be taken into consideration.

- iii) A number of organizations were contacted to try and co-ordinate ground-truthing of the SAR data for this project, but only Polar Continental Shelf Project personnel were planning to be in the right region. An arrangement was made with the Polar Continental Shelf Project (PCSP) office to surface truth ice features near the Hobson's Choice ice island in the spring. They were provided with a kit containing STAR-2 data, an identification of ice features to be surface truthed, and explicit data reporting forms. Unfortunately, they were not able to do any ground truthing, due to a reduction of their program and other commitments.
- iv) A context for an "Extreme Ice Feature" definition, was developed in this study. Here the definition of "extreme" relates to the potential load magnitudes that an ice feature could produce on an offshore production platform. Potential loads greater than 300,000 tonnes are considered "extreme" and would be caused by, for example, ice floes consisting of an ice feature in excess of 20 m thick and 500 m diameter embedded in a multi-year floe over 5 m thick and 2 km in diameter, and surrounded by pack ice over 1.5 m thick. In this study, we have searched for MYHF, very rough multi-year floes, ice islands, and re-entrant ice in excess of 2 km in diameter.
- v) A literature search identified public domain information on EIFs which include ice islands and multi-year hummock fields. Ice islands originate from the ice shelves of Ellesmere Island; their exact numbers are not known. Thirty-five ice islands currently in the Arctic Ocean are included in the EIF data base table provided in this report. The largest multi-year hummock fields (MYHFs) appear to originate along the eastern edge of the Beaufort Gyre. Ice plugs and multi-year landfast ice can freeze solidly to ice islands and MYHFs, and so greatly increase the driving force which the pack ice can apply to such features.
- vi) Initially, the study plan included a detailed analysis of EIF data from the AES STAR-2 imagery acquired in January, 1991. However, as only limited STAR-2 imagery was obtained for the reasons mentioned in i) above, other data sources, both archived and

potential, were considered and assessed in terms of suitability. These additional data sources were:

- SAR data from AES, Intera Technologies Ltd., and Industry

It soon became evident that SLAR and 25 m resolution SAR data do not have adequate resolution for the identification of extreme ice features. High resolution SAR data taken by the Intera STAR-1 aircraft in 1988 and 1989 were analysed in detail; these provided good coverage of the area of interest. Other SAR data in Intera's archives were also reviewed but not considered worth pursuing for this project.

- SPOT (Satellite pour l'observation de la Terre)

Panchromatic images from the SPOT satellite have a resolution of 10 m, and each image covers an area of 60 by 60 km. A SPOT sample was obtained and identified as a good source of ice information for this type of study, although it did not allow identification of old and first year ice types that can be determined from the tone in SAR images in winter. However, SPOT images were found to be useful for "surface truthing" of SAR imagery acquired over the same area.

- Aerial Photography

Aerial photography is an excellent source of imagery for the identification of EIFs. The Department of National Defence (DND) offered to acquire aerial photography for this project, however, they were unable to fly over the area of interest. National Research Council Canada (NRC) also notified us that they had tentative plans to mount a camera in an aircraft which could be used to collect "ground truth" data for this project. However, the budget was not available and photography in the area of interest was not obtained. In summary, neither of these possible data sources provided information for this project, but DND holds promise for future collaboration.

- vii) A comparison of Intera's February 1988 STAR-1 SAR and a July 1988 SPOT image for the Peary Channel revealed the same ice islands, ice island fragments, re-entrant ice, and features interpreted as MYHFs from their surface appearance. Keys were developed from this SAR and SPOT data intercomparison that were used with the SAR data for other areas and years, allowing an interpretation of over 334,600 km² of imagery. With these keys, we are confident that EIFs can be reliably recognized in high resolution (15 m or better) SAR imagery, although a ground truthing program to verify this is clearly advisable.
- viii) Comparison of STAR-2 imagery from the AES 1991 round-robin flight and STAR-1 data from 1988 and 1989 indicated that both the 12 m resolution data and 15 m data can be used for the recognition of EIFs, but the former are better. According to Intera this should not have been the case, and may have been due to the tuning and/or operation of the STAR-2 SAR instrument. It is not possible to clearly identify MYHFs and re-entrant ice in 25 m resolution STAR-2 SAR data, although these data do allow the recognition of ice islands, and certainly regions of old and first year ice.
- ix) Forty-two EIFs were found in the literature, and used to form an initial EIF data base. A further 155 EIFs were identified in the 1988, 1989 and 1991 STAR-1 and STAR-2 data between the Ward Hunt ice shelf and Banks Island. The old and new data sets have not been added together, as the former are observations of opportunity and the latter a systematic search of 334,600 km² of good imagery.
- x) The 1988, 1989 and 1991 SAR data covering the area from 77° to 80° north latitude indicate a density of EIFs of 0.64/1000 km², and 0.26/1000 km² greater than 2 km.
- xi) A simple analysis of the migration of EIFs into the southern Beaufort Sea indicated the measured density of EIFs adjacent to Prince Patrick Island would result in an EIF impact return period of at least 123 years at 70° and 54 years at 71° latitude for a

structure 200 m wide. There are large uncertainties in these numbers, and they should be used with caution.

2.2 RECOMMENDATIONS

The following recommendations are provided.

- i) Although development may not occur in the Canadian Beaufort Sea for a decade or more, it is felt to be important to continue the effort to collect information on EIFs, as the impact of such features with a structure will represent a significant design consideration for the structure. It is recommended that every opportunity be made to collect EIF data by on-going programs, such as DND's air photo flights, and AES's "Round Robin" STAR-2 flights.
- ii) High resolution SAR data (12 or 15 m resolution) should be acquired over the western edge of the Queen Elizabeth Islands every 1 or 2 years to maintain the EIF data acquisition effort, and so improve the statistical definition of EIF return periods of relevance to operations in the Canadian Beaufort Sea.
- iii) The SAR imagery should be analysed for EIFs and a ground truthing program conducted to verify the interpretation of the EIFs identified in the SAR data. Ideally, this should be specifically organized and directed to the MYHF program. Otherwise, ground truth sources of opportunity, e.g., field parties in the region, might provide the necessary ground truthing data. This report provides a list of groups who occasionally carry out field programs in the area of interest. When a SAR or air photo program is planned, these groups should be contacted regarding their activities and provided with an "interpretation kit", should they be in a position to acquire suitable data.
- iv) This report provides keys for the interpretation of EIFs from SAR data based on our knowledge of EIFs, and a comparison with SPOT imagery. These keys should be

used as provided, but confirmed with ground truthing data when the opportunity arises.

- v) Aerial photography is an option to SAR data, and DND's offer to provide imagery should be pursued.
- vi) The 10 m SPOT data is also a good, alternative source of data.
- vii) ERS 1 and future RADARSAT data should be considered as a potential source of data.
- viii) EIFs identified in future programs should be entered into the data base provided here, using the procedures outlined in this report. It is important to indicate the area of data analyzed, so that an EIF number density can be obtained. Observations of isolated features should be entered into the "old" data base, and EIFs based on a systematic analysis of SAR or air photo data should be entered into the "new" data base.
- ix) An improved model for calculating the impact rate of EIFs with offshore structures in the southern Beaufort Sea should be developed as the uncertainty in this aspect is as great as the uncertainty in the EIF statistics.

CHAPTER 3

WHAT IS AN "EIF"?

3.1 INTRODUCTION

The term "extreme ice feature" has been widely used and is generally understood, in the ice community, to mean:

- relatively rare (infrequent) and "large" ice features such as ice islands, ice plugs or multi-year hummock fields.

In 1986, a workshop on EIFs, sponsored by NRC, was held in Banff and attracted over 80 technical representatives involved with Arctic offshore engineering. At this meeting, there was no clear definition of what makes an ice feature "extreme", and the issue of definition was mostly avoided. For the purpose of his presentation, Croasdale (1986) defined an EIF as:

- greater than 15-20 m thick
- tabular or ridge-like
- discrete (i.e., limited in area and existing within thinner ice)

The definition above is somewhat vague and raises a number of questions such as:

- are all ice islands and all multi-year hummock fields EIFs, independent of their size?
- how large a floe does a multi-year hummock field need to be embedded into, to make it an EIF?
- does the definition change for a summer or winter scenario (i.e., with or without pack ice pressure)?
- how does the definition of EIFs relate to the type of structure concerned (e.g., exploration or production platforms)?

The following section addresses these questions and attempts to provide a more precise definition of EIFs.

3.2 CONTEXT

There is no single "correct" definition of an EIF. Literally, an EIF could mean an extremely thick ice feature, an extremely wide feature or extremely massive feature, or, to press the point, an extremely cold or an extremely flat feature! We must therefore agree on the context within which we want to define "extreme ice features".

The word "extreme" does imply that such ice features must be relatively rare or infrequent, i.e., a very common type of ice feature such as a first year ice floe or even an "average" multi-year ice floe cannot be considered to be an "extreme ice feature".

In this study of extreme Beaufort Sea ice features, the main emphasis was put (in the terms of reference) on how such ice features will affect the design of offshore structures in the southern Beaufort Sea. There is also some interest on how extremely thick ice features might cause seabed scouring and therefore affect the design of buried offshore pipelines. However, since this project is largely aimed at using surface remote sensing to establish statistics and a data base of EIFs, and since keel depth information cannot be obtained this way, the issue of seabed scouring by deep keels will be considered secondary. However, the two issues (seabed scour and forces on structures) may not be totally different. For significant deep scours to occur, an ice feature must exert a large, sustained force on the seabed which is limited by the same factors limiting the force between a floe and a structure (i.e., ice strength, momentum and driving forces).

In summary, the definition of EIFs for this study will be within the context of global ice load design criteria for offshore structures in the southern Beaufort Sea. In other words, an extreme ice feature must be capable of exerting an "extreme" global load on a structure (i.e.,

a load equal to or greater than the "design" load for the structure).¹

3.3 TYPES OF STRUCTURE AND WATER DEPTH

Figure 3.1 illustrates the large variety of offshore structures which could be considered for the Beaufort Sea. Of course, an EIF for a floating platform would be very different from an EIF for a caisson retained island.

The present study is concerned only with bottom founded structures designed to support exploration or production facilities. Floating structures are not dealt with here, largely because even very common and relatively small ice features (e.g., first-year ice) can threaten floating structures.

At this stage of offshore "development" in the Southern Beaufort Sea, the main types of bottom founded platforms which have been used or are being planned are artificial islands (including caisson retained islands), quasi-vertical, and sloping caisson structures. These structures may be protected against "extreme" ice features through large, inherent sliding resistances or by sand/gravel berms. These three types of structures are quite similar, and the geometry of the structure depends more on the water depth and on its purpose (production or exploration) than on its type. The water depth, in turn, controls the thickness or depth of the EIF which could impact the structure. Structures in shallow waters cannot be exposed to inordinately thick ice features, since such features would ground out before hitting the structure.

We are therefore concerned here with EIFs in terms of the global design ice loads on bottom founded structures in relatively deep water.

¹ Note that local ice pressure design issues are clearly left out.

3.4 EXPLORATION OR PRODUCTION PLATFORMS?

A typical exploration platform in the southern Beaufort Sea is about 100 metres in diameter and designed to withstand 25 year return period ice loads between 50,000 and 100,000 tonnes. As the effective ice failure pressure is about 1 MPa, such a load could be caused by an ice floe 5 to 10 m thick.

For the purpose of this project, we will use 75,000 tonnes as the design load on an exploration platform.

Production platforms are usually much larger than exploration structures since they must accommodate surface facilities. They are typically 200 m in diameter and must be designed to withstand 100 year return period loads of about 200,000 to 300,000 tonnes. Using an ice failure pressure of 0.75 MPa for large area interactions, a load of 300,000 tonnes could be caused by an ice feature 20 m thick.

For the purpose of this project, we will use 300,000 tonnes as the extreme load on the production structure. It should be noted that the typical values chosen above are within the range generally quoted in the literature (e.g. Croasdale, 1986). However, these values could be quite different, depending on the type of structure, the location, ice thickness, failure pressure, and many other factors. These values are only "order of magnitude" indicators.

The above load ranges indicate that a typical exploration structure is designed to withstand impacts by multi-year ice floes 5 m to 10 m thick. Since 5 m is the average thickness of multi-year floes, 5 to 10 m of ice cannot be considered "extreme". In other words, an ice feature which can exert an "extreme" ice force (greater than design) on an exploration platform is not a particularly rare ice feature in the Arctic Ocean and therefore is not considered an "EIF".

Hence, for this study, an EIF will be defined as a feature which can exert extreme global loads on a bottom founded production platform.

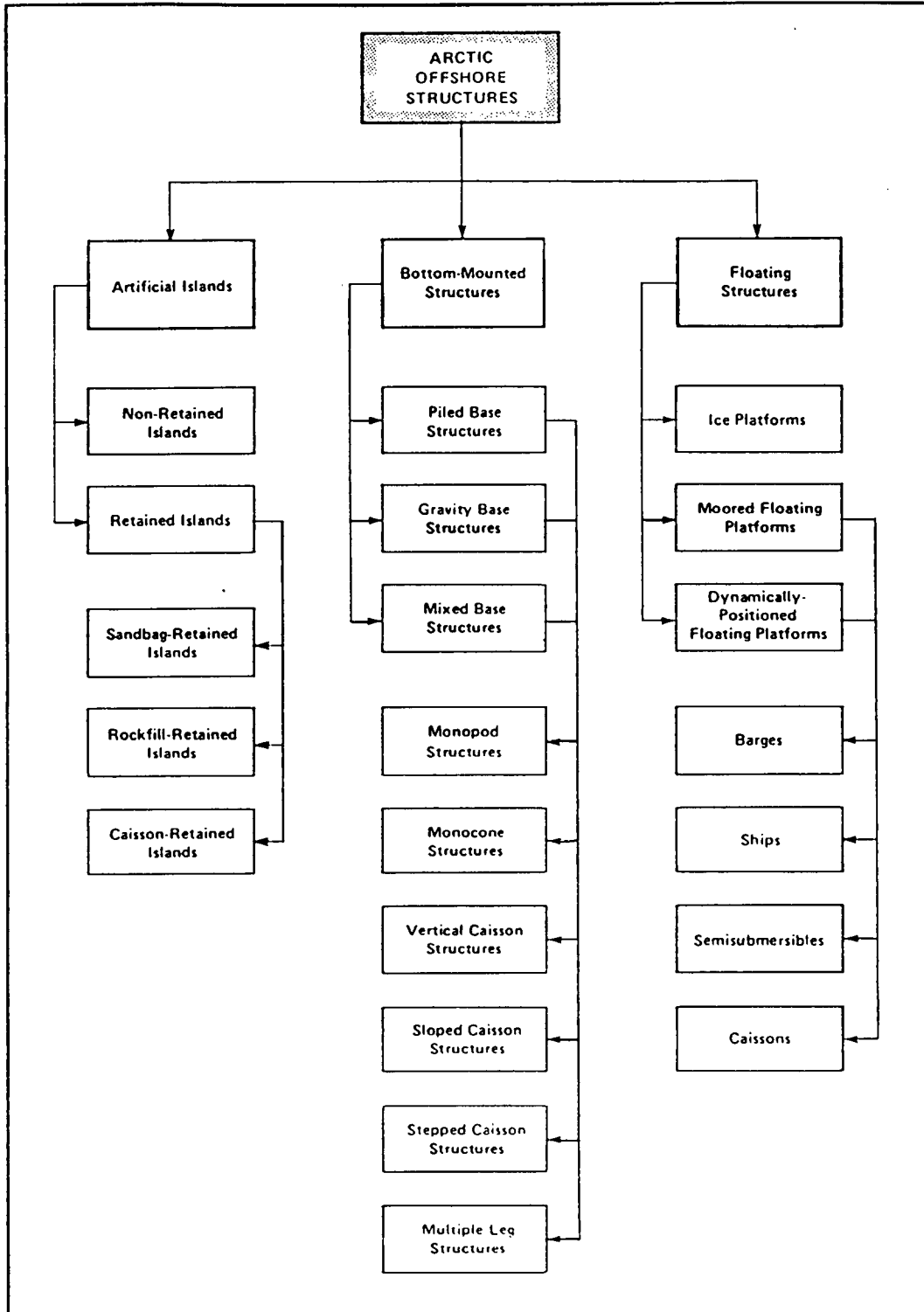


Figure 3.1: Classification Scheme for Arctic Offshore Structures

3.5 LIMITS TO GLOBAL LOADS

The concepts of limit stress, limit momentum and limit driving force were introduced by Croasdale (see for example, Croasdale 1987).

In order for an ice feature to exert an "extreme" load on a structure, it must fail locally at the ice/structure interface (limit stress mode) and, it must have sufficient momentum or sufficient driving force to generate this "extreme" load (Figure 3.2).

The limit momentum case generally corresponds to the summer scenario, while the limit driving force case generally corresponds to the winter scenario. The two cases are not totally separate, since, in the limit momentum case for example, some significant driving forces (wind, current, other floes) can add to the force caused by the momentum.

In the winter scenario, Croasdale assumes that the force driving the extreme multi-year floe is limited by the first year pack ice failing in "ridge building" at its trailing edge. If the multi-year floe is frozen into the first year ice, then the multi-year pack ice bond will withstand a much higher stress than the "ridge building" stress.

Figure 3.3 shows a structure being impacted by an "extreme ice feature", and typical ice force values. The values are based on the EIS (1982) ice pressure curve, Sanderson's (1988) pressure versus area curve, and recently published experience on Gulf's Molikpaq (Jefferies and Wright 1988). The force or failure stress values indicated in Figure 3.3 are given here only as "order of magnitude" indicators and should not be construed as accurate or exact.

Assuming a structure resistance of 300,000 tonnes, an "extreme ice feature" is (using the values in Figure 3.3) a multi-year floe

- 1) which is at least 2 km wide in winter (or 20 km wide in summer),
- 2) which incorporates a thick feature (hummock field, ridge, ice island or ice plug) at least 20 m thick and 480 m wide.

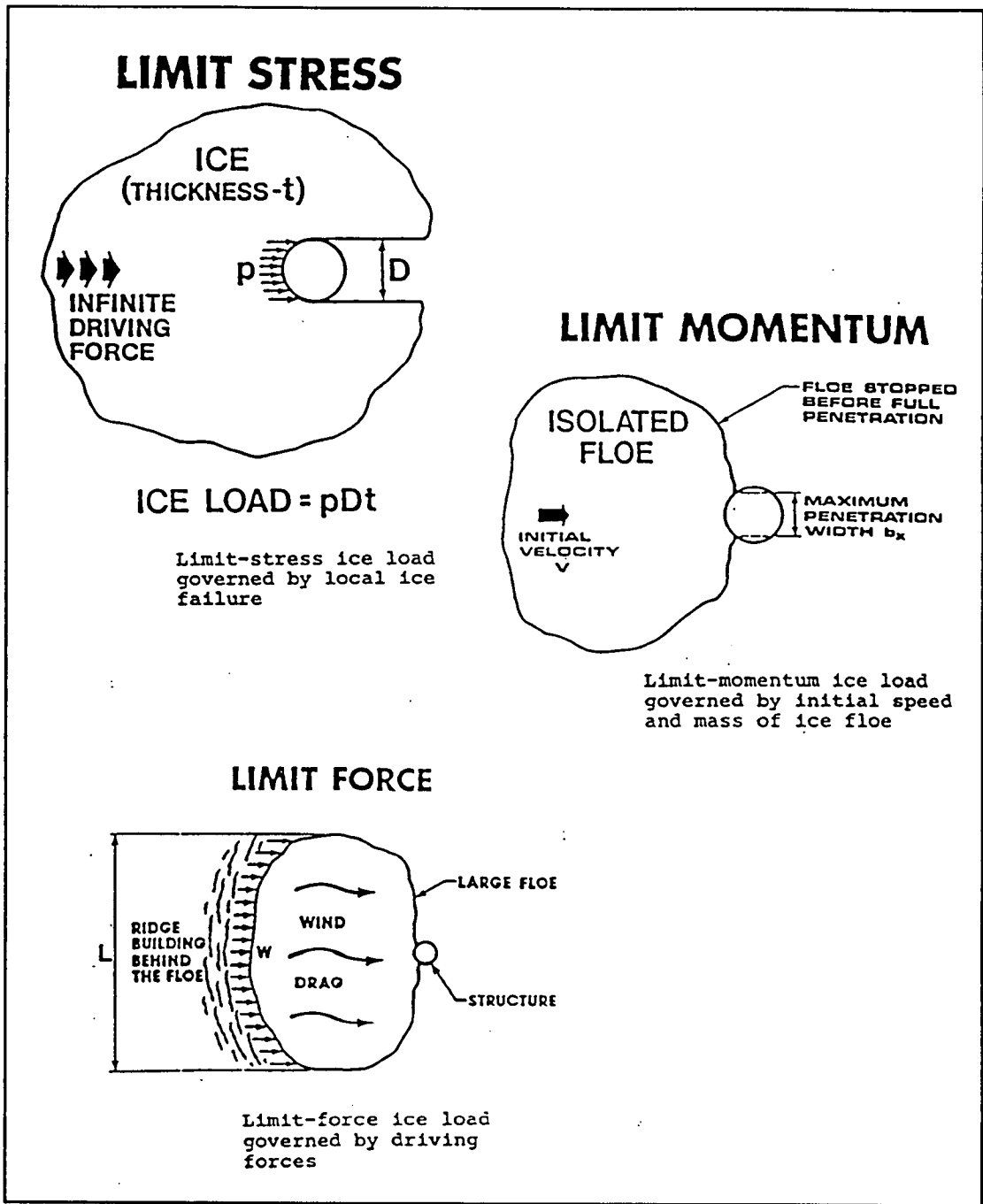


Figure 3.2: The Different Types of Ice Floe Interactions (Source: Croasdale 1986)

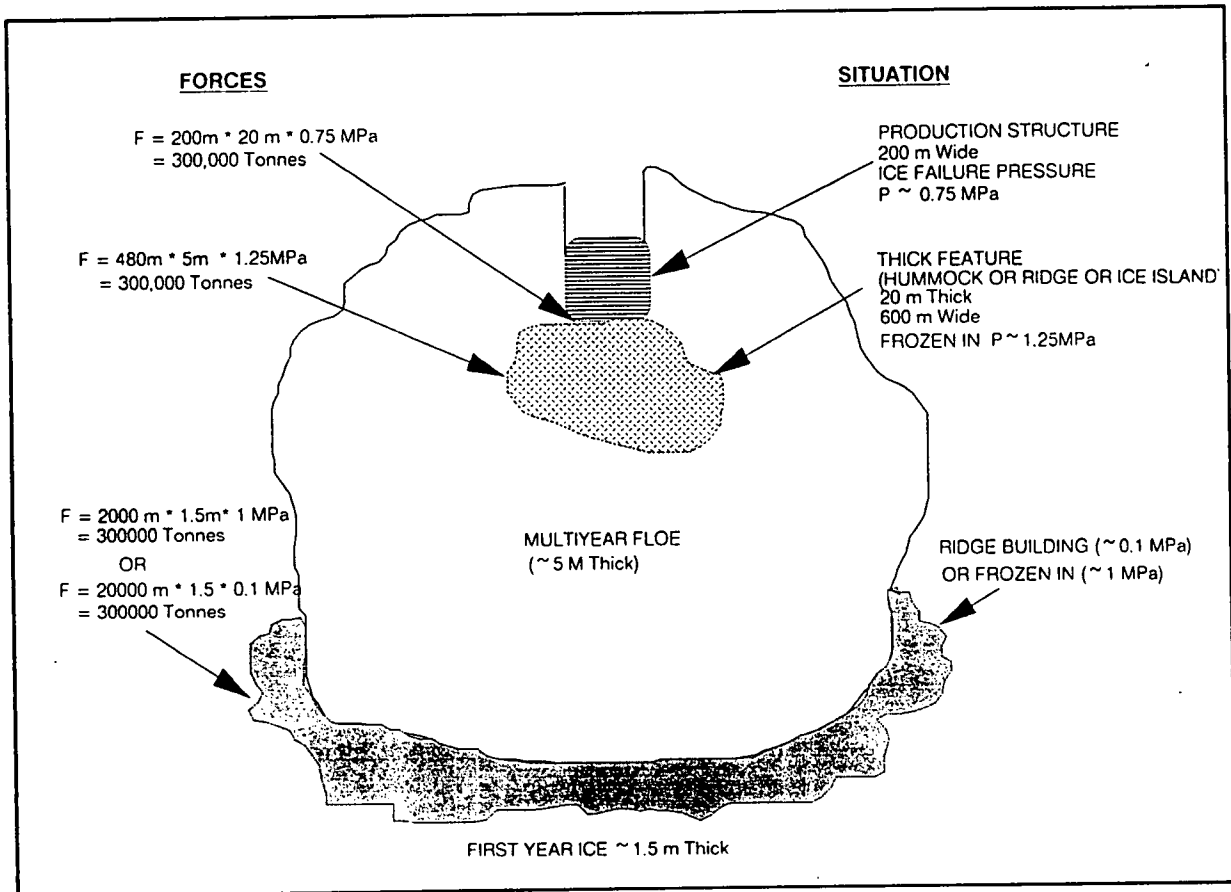


Figure 3.3: Extreme Ice Feature Impact

If different structure resistances are assumed, the definition of an extreme ice feature also changes as shown in Table 3.1.

Table 3.1: Representative extreme ice feature dimensions vs. structure resistance

| Structure Resistance (tonnes) | Thick Feature Ice Thickness (m) | Thick Feature Ice Width (m) | M.Y. Floe Diameter (km) |
|-------------------------------|---------------------------------|-----------------------------|-------------------------|
| 200,000 | 13 m | 320 | 1.3 |
| 300,000 | 20 m | 480 | 2.0 |
| 400,000 | 27 m | 640 | 2.7 |

In this analysis of remotely sensed data, the range of areal sizes indicated here has been used to define "extreme" ice features. Ice thickness is not available to us, but any ice island and moderate to rough MYHF are included, since they are undoubtedly 15 - 25 m thick in places.

Note that all three conditions must be exceeded to result in the ice loads indicated. For example, an isolated MYHF or ice island which may be 20 m thick over its entire area, if it is not over 1.3 km in dimension it will not result in loads over 200,000 tonnes, even though it is well over the 320 m "Thick Feature Ice Width" indicated in the Table.

CHAPTER 4

REVIEW OF LITERATURE AND EXISTING INFORMATION

4.1 SUMMARY

The effort in this task was directed towards identifying where EIFs were most likely to be found based on previous field studies, and compiling a database of existing information. While the precise definition of an EIF was being developed, it was agreed that they would include Ice Islands, Multi-year Hummock Fields (MYHF), Ice Plugs, and Multi-year Landfast Ice (MYLF); see Appendix C for ice terminology.

Reviews of the literature and of various field studies were undertaken. As expected, it was found that the most likely area to encounter significant numbers of EIFs is along the northwest edge of the Queen Elizabeth Islands in a swath one or two hundred kilometres in width, from the edge of the landfast ice (and some of the northwest channels) out into the pack ice of the Arctic Ocean. This swath stretches from Banks Island to the ice shelves of Ellesmere Island. Most EIFs are believed to originate in this region, and practically all that enter the southern Beaufort Sea transit the region of the Beaufort Sea adjacent to Prince Patrick Island.

4.2 LITERATURE REVIEW

4.2.1 Ice Islands

Ice Islands are the most formidable extreme ice features found in the Beaufort Sea. They were first sighted in the late 1940s on Royal Canadian Air Force reconnaissance flights. Figure 4.1 shows ice island drift patterns in the Arctic Ocean. These features break off, or "calve" from the ice shelves of the north coast of Ellesmere Island. The resulting ice islands are tabular blocks of ice, initially 40 to 60 metres thick and often tens of kilometres across.

The largest recorded ice island, T-2, measured 27 km x 29 km (Koenig et al. 1952). The largest ice island presently known to exist in the Arctic Ocean is Hobson's Choice which measures 5.7 km x 8.7 km with an average thickness of 42.5 metres (Jeffries et al. 1988).

At break-off, and with subsequent drift in the pack ice and/or grounding near shore, small ice island fragments tens to hundreds of metres across can be produced. Figure 4.2 shows grounded fragments of an ice island west of Banks Island seen in 1980. The actual number of all such fragments may be large - in the order of thousands (Spedding, 1977), however, the number of ice island features large enough to pose a hazard to an offshore production structure is much smaller.

In 1972, 433 ice island fragments were sighted along the Alaskan Arctic coast. It was postulated these had resulted from the grounding and breakup of a single large ice island. Of these 433 fragments, only 10 were greater than 400 metres in diameter. In 1977, Spedding estimated from the literature that a total of 41 ice islands greater than 400 metres across might still be drifting in the Arctic Basin. The basis for choosing 400 metres diameter is unclear, but an ice island would certainly need to be about that size to generate "extreme feature ice loads" (see Table 3.1).

Recent Events

Since 1977, there have been a number of sightings of ice islands from recent ice shelf calvings. These include eight "new" ice islands (including Hobson's Choice), sighted April 1983 and recorded on SLAR, which calved from Ward Hunt ice shelf in 1982/83, and nine "old" ice islands sighted July 1984 near Ward Hunt ice shelf and recorded on air photographs (Jeffries et al. 1988). Between 1983 and May 1986, these eight "new" ice islands appear to have fragmented into some 23 - 25 fragments and drifted 500 km west. Therefore, some 32 to 34 ice islands were identified during that period including both "old" and "new" features.

The total population of known ice island fragments therefore increased during the 1980's to 32 to 34 features. These events are reflected in the Data Table of Section 4.4. Seven fragments were smaller than 0.06 km^2 (300 x 200 m) and are not included in the table as they are not considered "extreme" according to the definition in Section 4.

Future Trends

The future supply of ice islands has been estimated in a number of studies (Spedding 1977, Wadhams 1979, Jeffries 1985b). The prevailing opinion is that, since the overall extent of the ice shelves has decreased considerably during this century, the area and frequency of calvings will decrease. The original ice shelf area of 7450 km² (Spedding 1977) has been reduced to 1300 - 1400 km² today (Figures 4.3 and 4.4).

Jeffries (1986) notes that two of the remaining ice shelves, Ayles and Alfred Ernest, have moved seaward in recent years, and could yield new ice islands. Jeffries (1988) has shown that the average size of the ice islands breaking off has decreased since 1946.

Decay Rate

The rate of deterioration and loss of ice islands from the Arctic Basin must also be considered. Ice islands escape from the region by drifting through the channels of the Queen Elizabeth Islands, by being carried with the Transpolar Drift Stream to the Atlantic Ocean or, by grounding, break-up and melting in place. Some features however may drift with the Beaufort Gyre for decades before escaping. Ice Island T-3 is believed to have made at least three circuits of the Beaufort Gyre between its discovery in 1950 and its departure via the Transpolar Drift Stream between 1979 and 1984 (Sackinger et al., 1990; see Figure 4.5). From this example, it can be seen that an ice island can take up to 10 years to make one circuit of the Gyre. Figure 4.6 illustrates the drift velocities of the Gyre.

Various authors (Crary, 1958, De Paoli et al., 1982) have suggested that the chance of an ice island escaping the Gyre on any circuit is between 50% and 70%. On the basis of 50% release or escape rate every ten years, Jeffries (1985b) estimated that the total number of ice islands greater than 300 metres across would be 9 by 1982 and 4 by 1992. This, however, does not take into account the most recent sightings. The trend is clear, however, and the number of dangerous extreme ice features of this sort is expected to be low and decreasing in the near future.

Summary

The literature review revealed a number of trends regarding the formation, drift and behaviour of ice islands which would naturally influence the choice of location for ongoing, regional SAR coverage for the purpose of compiling a data base and improving statistics on extreme ice features. The key points are:

- 1) Ice Islands calve from the ice shelves of northern Ellesmere Island at unpredictable intervals.
- 2) They drift slowly with the general motion of the pack ice of the Beaufort Gyre, until they reach M'Clure Strait. It may take 3 to 5 years, if not longer, for an ice island to progress from Ellesmere Island to M'Clure Strait.
- 3) South of M'Clure Strait, the drift rates increase dramatically. Ice can traverse the Canadian Beaufort Sea (>300 km) in the space of one winter.
- 4) They rarely enter the southern Beaufort Sea, however, occasionally they drift into the offshore drilling areas and ground out in the 40 - 60 m water depth range. Usually, they fragment during the grounding process.
- 5) In 7 to 10 years, a total circuit of the Beaufort Gyre may be made and an ice island may arrive back near its starting point.
- 6) Some have drifted at the outer fringes of the Beaufort Gyre, i.e., drifting within a few hundred kilometres of the shores of the Arctic Islands. This would be the easiest place to detect them.
- 7) South of M'Clure Strait there is a dispersal and acceleration (see Fig. 4.6) of the pack. Detection of EIFs would be more difficult here due to the faster speed and more sparse aerial distribution.

4.2.2 Multi-Year Hummock Fields (MYHFs)

A hummock is defined in World Meteorological Organization Sea-Ice Nomenclature as "A hillock of broken ice which has been forced upwards by pressure. May be fresh or weathered" (WMO 1970). Multi-year hummock fields are generally considered to be very rough multi-year floes containing a series of densely packed parallel ridges. Some hummock fields are known to form at the edges of landfast ice along the western shores of the Queen Elizabeth Islands (Hudson et al. 1980). This area appears to be the main source of multi-year hummock fields. In this region, from Prince Patrick Island to northern Ellesmere Island, the pack ice drift repeatedly converges towards the shore and the resulting pressure creates parallel rows of massive, grounded shear ridges at the edge of the landfast ice. Figure 4.7 shows such a feature at the edge of the landfast ice off Prince Patrick Island. These ridges, being grounded, remain in place for several years, until their top and bottom surfaces ablate enough for the keels to lift off the sea floor. By this time, the ridges are consolidated to well below sea level, and possibly to the base of the keel in some cases. The resulting "hummock field" is typically 300 m by 1000 m in extent and comprised of rows of multi-year ridges which may be up to about 50 m deep (Hudson et al. 1980). A hummock field may be solidly frozen to an area of thick (10 m), multi-year (formally landfast) ice when it finally breaks free and moves into the gyre. De Paoli et al., (1982) suggest that this formation process does not account for all MYHFs counted in surveys. They cite Hibler's (1980) conclusion that heavy ridging due to convergence of the pack comparable to that which occurs against the Queen Elizabeth Islands, will take place near the North Pole. This suggests that MYHFs may also form in the pack ice between Ellesmere Island and the North Pole.

Given the prevailing motion of the Beaufort Gyre, it is expected that the MYHFs would be found mainly in a corridor 100 - 200 kilometres wide from northern Ellesmere Island to the south of Prince Patrick Island. This width is based upon the extent of previous surveys (Hudson et al. 1980, Eley and Hudson 1982, LeSchack 1978) as well as the drift of ice island T-3 (see Figure 4.5). Since it is the features closer to shore in this corridor which will be more likely to enter the southern Beaufort Sea, this area would be the best choice for future surveys.

The total population of MYHFs within a 50 km wide corridor has been estimated by De Paoli et al. (1982) as between 1200 and 3000. These numbers come from two sources:

- a) Hudson et al. (1980) and Eley and Hudson (1982) found (from aerial photographic surveys) that one floe in a hundred could be considered a MYHF (they used the term "very bumpy"). This translated into 1.6 MYHFs greater than 500 m diameter per 100 km². Considering the 50 km wide coastal corridor from Ellesmere Island to the northern tip of Banks Island, (a distance of 1500 km) the area in question was 75,000 km². This yielded the number 1200 MYHFs. (If we consider a 100 km wide strip then the population doubles to 2400.) The 500 m diameter was chosen as a cutoff, because at the time it was believed that smaller floes would do not exert extreme loads on a structure.

- b) The second population estimate of 3000 was derived from under ice submarine data (LeSchack 1978). A data track from submarine USS Sargo in 1960 along the western shores of the Queen Elizabeth Islands from M'Clure Strait to Peary Channel yielded 64 MYHFs with an average diameter of 1 km. An assumption of 50 parallel runs at 1 km spacing, each 1500 km long, would yield a population of 3000 MYHFs. For this part of their study, De Paoli et al. defined a MYHF as a floe with a diameter greater than 500 m with an average floe depth of greater than 10 metres.

Clearly, the number of MYHFs may be large, much larger than ice islands, and the risk of collision with a structure is correspondingly higher. At the Kopanoar drill site, an estimated interaction return period for an ice island is 1100 years, and about one year for MYHFs (De Paoli et al. 1982). Unlike ice islands with a decreasing source, MYHFs are formed continually and there is no reason to expect a diminishing supply ignoring the effects of global warming. Previous methods of estimating populations have limitations and it is believed that the wide area coverage and high resolution of SAR will produce much more reliable data.

Ground truthing of MYHFs has been sparse. The only documented cases having been found in Hudson et al. (1980), Wright et al. (1983) and Dickins (1982a). These are summarized in the Data Table of Section 4.4. In Hudson et al. (1980), thirteen features were documented, four of which were true MYHFs. Figure 4.8 shows the location of these features. Aerial photography lines (Figure 4.9) yielded floe-size distributions of MYHFs for different regions (Figure 4.10). In Wright et al. (1983) five multi-year floes were studied in detail, the first of which (Figure 4.11) could be considered a MYHF. In Dickins (1982a), a total of fourteen multi-year floes were documented west of Banks Island, one of which had the characteristics of a MYHF. Two other studies are of interest. McGonigal (1985a), documented some thirteen fragments of extremely rough second-year hummock fields, eight of which could be considered extreme. Large numbers of these features contained within the summer pack and believed to have been formed offshore Alaska by a process similar to that for MYHFs, invaded the southern Beaufort Sea in August 1983 and halted drilling operation for one and a half months. In time, these would have become MYHFs. However, most drifted out of the region the following summer. This unusual event was documented with SLAR, aerial photography, and ground truthing. McGonigal (1985b) documented eight ice features from the same population which were grounded in water depths between 19 and 25 metres. Figure 4.12 shows a photograph of one of these features.

4.2.3 Ice Plugs

These are thick, old areas of ice which form within the fiords and inlets of the Queen Elizabeth Islands (Walker and Wadhams 1979). Such plugs grow to thicknesses of 5 to 10 metres (Sadler and Serson 1981). They could enter the Beaufort Gyre and from there, the southern Beaufort Sea. They appear to be readily visible in SAR data (Hill 1990) – see Chapter 5 - partly because they can be very large in extent (10 - 20 km). However, they are relatively rare, with known occurrences being in Nansen Sound, Sverdrup Channel, and certain fiords of northern Greenland.

Ice plugs were originally felt to be candidates for inclusion in the category of EIF, but this has been reconsidered because potential load levels are lower than "extreme". The average ice thickness is only 5 m to 10 m and this can be expected to decrease markedly once a fragment breaks away from a sheltered channel, due to the different thermal and precipitation regime of the Arctic basin.

4.2.4 Multi-Year Landfast Ice (MYLF)

Multi-year landfast ice exists along the western shores of the Queen Elizabeth Islands (see Figure 4.13). Landsat imagery interpretation of these areas, by Arsenault (1981b), showed that a significant amount of the MYLF breaks off yearly. It was found that, on average, 340 km² of MYLF broke off each year along this coast. Hudson et al. (1980) found that this ice was 6 - 10 metres thick. While the landfast ice may not be an extreme ice feature in itself, a wide expanse of MYLF may often be attached to a MYHF. This increases the mass and area of the MYHF and influences the potential pack ice forces that such features could exert on a structure.

The most recent incident found in this literature search involved the calving of a large piece of multi-year landfast sea ice (also called a re-entrant or recent ice shelf) from Milne Ice Shelf around February 1988 (Jeffries and Sackinger 1990a). This event was captured on the SAR image of 22 February 1988. The "re-entrant" was known to be 10 metres thick in places with dimensions of 7.2 x 3.6 km. Attached to this was a larger area of younger, thinner, multi-year landfast sea ice. The entire feature had dimensions of 12 x 24 km.

4.3 DATA SOURCES

Potential data sources which could augment the EIF data base exist in the form of SAR, SLAR, satellite and aerial photograph imagery. Some of these sources are listed in Table 4.1. Not listed are some proprietary sources and foreign language (e.g., Russian) sources which could not be reviewed within the scope of this project.

TABLE 4.1 Raw Data Sources with Potential for EIF Data

| | Date | Data Type | Location | Reference | Comments |
|---|----------------------|-------------------|---|---|---|
| 1 | 1973-78 | Air Photography | S. Beaufort | Esso | 1974 multi-year invasion. EIF potential. Proprietary to Esso. |
| 2 | 1980 | Air Photography | S. Beaufort to 72°N | Gulf. Wright et al., 1983 | Air photos of South Edge of polar pack. EIF potential. |
| 3 | 1980, 81 | SLAR | Western Arctic Islands | CRRS reports for Dome by Arsenault, 1981a, 1981b | Identifies Ice Shelves and MYLF. Potential for EIF. |
| 4 | 1982 | SAR | Bering, Chukchi & Alaskan Beaufort Seas | AOGA Proj. 177, Intera, 1983 | Proprietary. EIF potential. |
| 5 | 1982 | SLAR | Chukchi Sea | F.G. Bercha for Gulf | Katie's Floeberg EIF potential. |
| 6 | 1982 | SAR | Alaskan Beaufort | AOGA 144, Intera, 1982 | Proprietary. EIF potential. |
| 7 | 1983/84 | Air Photography | S. Beaufort | Gulf McGonigal, 1985a, 1985b | Air photos of 2nd year hummock fields. |
| 8 | 1983 1984 1985 | SAR SAR SAR | S. Beaufort | Gulf/Dome Operational SAR missions | Invasion of 2nd year hummock fields, multi-year floes present. Potential for EIFs. Originals located at Gulf and Amoco. |
| 9 | 1986/87 | SAR (STAR-1) | Canadian Arctic | Canadian Arctic Marine Ice Atlas deBastiani, 1987 | Limited coverage of EIF areas. Low potential for EIF. |

TABLE 4.1 Raw Data Sources with Potential for EIF Data (concluded)

| | Date | Data Type | Location | Reference | Comments |
|----|-------------|--------------------------------|----------------------|---|--|
| 10 | 1987/88 | SAR (STAR-1) | Canadian Arctic | Canadian Arctic Marine Ice Atlas deBastiani, 1990 | Valuable data. Used in this study - see Section 8. |
| 11 | 22/2/88 | SAR (STAR-1, 12 m resolution) | N. Ellesmere Island | deBastiani, 1990, Jeffries & Sackinger, 1990a | Can identify Ice Shelf Calving |
| 12 | 28/7/88 | SPOT-1 Satellite, PLA sensor | Ellef Ringnes Island | Sackinger et al., 1990 | Visual image. Can identify Ice Islands. High potential for EIFs. |
| 13 | 8/8/88 | SPOT-1 Satellite, PLA sensor | N. Ellesmere Island | Jeffries & Sackinger, 1990a | Visual image. Can identify ice shelf and re-entrant. Potential for EIFs. |
| 14 | 24/3/89 | SAR (STAR 1) (12 m resolution) | Peary Channel | Hill, 1990 | Scale 1:250,000. High resolution. Can identify II, MYHF, Ice Plug. |
| 15 | 4/2/90 | SAR (STAR 2) (25 m resolution) | West Banks Island | AES Round Robin | Scale 1:250,000. Low resolution. Low potential for EIF. |

4.4 DATA BASE

4.4.1 Relevant Parameters

Ideally, one wants to know as much about a single EIF as possible when assessing the potential interaction behaviour and loads on a structure. The list below was used as a guide for producing Table 4.2 which forms the basis of the EIF data base from information acquired prior to this study.

- Source Report
- Date of Sighting - Location (Lat, Long) - Water Depth
- Ice type - Stage of Evolution
- Size (length, width, surface area)
- Elevation Data (mean freeboard, maximum keel depth, keel profiles)
- Mass
- Velocity
- Roughness

For a more concise data base on the occurrence of MYHFs, we rely on statistics, using frequency histograms to describe regional distributions of EIFs.

Table 4.2: Extreme Ice Features Data Base, 1946-1988, page 1.

| General Area | Feature Type | Feature I.D. | Date | Lat. N | Long. W. | Water Depth | Size | | |
|----------------------|--|--------------------|---------|---------|----------|--------------|-------------|------------|-------------------------|
| | | | | | | | Length (km) | Width (km) | Area (km ²) |
| Hudson et al. 1980 | | | | | | | | | |
| PPI | MYHF (floating) | Site #2 | 1/4/80 | 76 26.5 | 123 52.5 | | 1 | 0.25 | 3 km Dia. Floe |
| PPI | MYHF (grounded) | Site #3 | 2/4/80 | 77 17 | 119 30 | 40 | 1.8 | 0.3 | |
| PPI | MYHF (floating) | Site #4 | 3/4/80 | 77 27 | 118 45 | 32 m 36 m | 1 | 0.5 | |
| PPI | II (grounded) | Site #7 | 6/4/80 | 77 22 | 119 40 | > 100 m | 1.5 | 1 | 2 km X 2 km floe |
| Borden I | II (grounded) | Site #8 | 9/4/80 | 78 54 | 110 42 | 30 m | 0.26 | 0.2 | |
| Banks I | II (grounded) | Site #12 | 13/4/80 | 73 33 | 124 54 | 23.2 | 0.18 | 0.14 | |
| PPI | MY Floe with ridge (floating) | Site #14 | 8/4/80 | 77 35 | 118 00 | | | | 1.5 km Diam floe |
| Borden I | MY Pile-up ride-up grounded not consol | Site #8 | 9/4/80 | 78 50.2 | 110 33 | > 40 | | | |
| Borden I | Shear Ridge (grounded) MYLF | Site #9 Site #9 | 9/4/80 | 78.52.5 | 111 2 | 52 47 | | | |
| Wright et al. 1983 | | | | | 132 51 | | | 0.8 | |
| South Beaufort Sea | MYHF (floating) | Floe #1 | 17/3/80 | 72.16.5 | | | 1.1 | | |
| DICKINS 1982 | | | | | | | | | |
| West of Banks Island | MYHF (floating) | Floe #10 | | 73 | 128 | | | | 550 m Diam. |

Table 4.2: Extreme Ice Features Data Base, 1946-1988, page 1 concluded.

| Thickness | | | Freeboard | | | Roughness | Mass x 10 ⁶ tons | Comments |
|------------------------|--------------------------|-------------------|-----------|---------|----------------|-----------|--------------------------------|--|
| Mean (m) | Max (m) | Profile | Mean (m) | Max (m) | Profile | | | |
| | | | | | | | | |
| 25 est. thick sect. | | | 3.9 | 12.2 | Two | High | 4.6 | Measured thickness 7 m, 12.5 m |
| 25 est. | | | 4 | | | High | 15 | |
| 30 est. | 49 | Two | 5 est. | 20 | Two | High | 15 | |
| 20 est. | | | 3 | | | High | 30 Hummock Section | Rough Section in MY floe 2 x 2 km |
| 35 est. | | | 5 | | | Smooth | 1.6 | |
| 28 | | | 5 | | | Smooth | 0.7 | |
| | 43 sail & keel (est.) | | 5 est. | 10 sail | | | 8 | |
| | | | | 23 sail | | | | |
| 7 | 70 10 est. | One | | 18 | One One | | | |
| | | | | | | | | |
| 10.5 | > 20 | 1 by drillhole | | | | High | 8 | |
| | | | | | | | | |
| 7 | > 20 | | 5.5 | | | High | | |

Table 4.2: Extreme Ice Features Data Base, 1946-1988, page 2.

| General Area | Feature Type | Feature I.D. | Date | Lat. N. | Long. W. | Water Depth | Size | | |
|---------------|--------------|--------------|---------|---------|----------|-------------|-------------|------------|-------------------------|
| | | | | | | | Length (km) | Width (km) | Area (km ²) |
| JEFFRIES 1985 | | | | | | | | | |
| | Ice Island | T-1 | 14/8/46 | | | | 29 | 24 | 610 |
| | Ice Island | T-2 | 21/7/50 | | | | 29 | 27 | 697 |
| | Ice Island | T-3 | 29/7/50 | | | | 14 | 7 | 560+ |
| | Ice Island | T-4 | 7/47 | | | | | | 610 |
| | Ice Island | T-5 | 28/6/48 | | | | 11 | 10 | 100 |
| | Ice Island | NP-6 | 1956 | | | | 13 | 9 | 65 |
| | Ice Island | ARLIS 11 | 23/5/61 | | | | 6 | 4 | 14.5 |
| | Ice Island | WH-1 | 10/6/62 | | | | 16 | 9 | 73.5 |
| | Ice Island | WH-2 | 10/6/62 | | | | 9 | 8 | 68 |
| | Ice Island | WH-3 (NP-18) | 10/6/62 | | | | 13 | 9 | 105 |
| | Ice Island | WH-4 | 10/6/62 | | | | 13 | 9 | 93 |
| | Ice Island | WH-5 | 10/6/62 | | | | 18 | 8 | 133 |
| | Ice Island | WH-6 | 3/4/67 | | | | 12 | 5 | 60 Est. |
| | Ice Island | Peisters | 4/74 | | | | 12 | 5 | 60 Est. |
| | Ice Island | NP-23 | 12/75 | | | | 7 | 3 | 20 Est. |
| | Ice Island | WH-7 | 3/4/67 | | | | 23 | 10 | 200 Est. |

Table 4.2: Extreme Ice Features Data Base, 1946-1988, page 2 concluded.

| Thickness | | | Free-board | | | Roughness | Mass X 10 ⁶ tons | Comments |
|-------------|---------|---------|-------------|------------|---------|-----------|--------------------------------|--|
| Mean (m) | Max (m) | Profile | Mean (m) | Max (m) | Profile | | | |
| | | | | | | | | |
| 20 Est. | | | | | | | | Exited via Archipelago |
| | | | | | | | | Exited via TransPolar |
| 40 | 53 | | | | | | | Exited via TransPolar |
| 20 Est. | | | | | | | | Exited via Robson Ch. |
| | | | | | | | | |
| 8 | 12 | | | | | | | |
| 12 | 25 | | | | | | | Exited via TransPolar |
| 20 Est. | | | | | | | | Exited via M'Clure Str. |
| 20 Est. | | | | | | | | Exited via TransPolar |
| 20 Est. | | | | | | | | Broke in two parts. Same as Russian Station NP-18 |
| 20 Est. | | | | | | | | Broke up North of Barrow in 1968. Fragments grounded S.E. of Barrow |
| 20 Est. | | | | | | | | Exited via Robeson Ch. |
| 40 Est. | | | | | | | | Same Feature |
| 40 Est. | | | | | | | | Same Feature |
| | | | | | | | | Same Feature |
| 40 Est. | | | | | | | | Its breakup is postulated as cause of 1972 ice island invasion of Alaska's offshore 433 fragments 10>400 m |

Table 4.2: Extreme Ice Features Data Base, 1946-1988, page 3.

| General Area | Feature Type | Feature I.D. | Date | Lat. N. | Long. W. | Water Depth | Size | | |
|---------------------------------------|-----------------|--------------|-------------|---------|----------|-------------|-------------|------------|-------------------------|
| | | | | | | | Length (km) | Width (km) | Area (km ²) |
| JEFFRIES 1985 | | | | | | | | | |
| | Ice Island | Alert No 1 | 20/5/67 | | | | 1.6 | 1.6 | 2.5 |
| | Ice Island | NP-18 | 10/68 | | | | | | 104 |
| | Ice Island | NP-19 | 1969 | | | | | | 80 |
| | Ice Island | ZIMIS | 31/3/81 | | | | 7.2 | 2 | 14 |
| | Ice Island | NP-21 | | | | | | | 62 |
| | Ice Island | NP-22 | 9/73 | | | | | | 10 |
| | Ice Island | NP-24 | Spring 1978 | | | | 17 | 8 | 130 |
| | Ice Island | WH-8 | 23/4/83 | | | | 10.5 | 3.9 | 26 |
| | Ice Island | WH-9 | 23/4/83 | | | | 3.9 | 2.7 | 7.1 |
| | Ice Island | WH-10 | 23/4/83 | | | | 2.4 | 2.1 | 2.8 |
| | Ice Island | WH-11 | 23/4/83 | | | | 4.5 | 1 | 1.9 |
| | Ice Island | WH-12 | 21/5/83 | | | | 2.7 | 0.6 | |
| | Ice Island | WH-13 | 21/5/83 | | | | 2.7 | 1 | |
| | Ice Island | WH-14 | 21/5/83 | | | | 2.4 | 0.75 | |
| | Ice Island | Beta | 19/10/83 | | | | | | |
| | Ice Island | WH-15 | 23/7/84 | | | | 0.5 | 0.25 | 0.125 |
| | Ice Island | WH-16 | 23/7/85 | | | | 4 | 15 | 0.06 |
| JEFFRIES AND SACKING ER 1987 | | | | | | | | | |
| | MYLF Re-entrant | | 22/2/88 | | | | 7.2 | 3.6 | |

Table 4.2: Extreme Ice Features Data Base, 1946-1988, page 3 concluded.

| Thickness | | | Free-board | | | Roughness | Mass $\times 10^6$ tons | Comments |
|-----------|---------|---------|------------|---------|---------|-----------|----------------------------|--|
| Mean (M) | Max (N) | Profile | Mean (M) | Max (N) | Profile | | | |
| | | | | | | | | |
| | | | | | | | | |
| 30 | | | | | | | | |
| 35 | | | | | | | | |
| 12 | 15 | | | | | | | |
| | | | | | | | | |
| 30 | | | | | | | | |
| 30 | | | | | | | | |
| 42.5 | | | | | | | 702 | Hobson's Choice (SLAR-1 in Jeffries '87) |
| 40 Est. | | | | | | | 172 | SLAR 2 in J-67 |
| 40 Est. | | | | | | | 59 | SLAR 3 in J-67 |
| 40 Est. | | | | | | | 71 | SLAR 4 in J-67 |
| 40 Est. | | | | | | | | Related to SLAR 5,6,7,8 in Jeffries '87 |
| 40 Est. | | | | | | | | Related to SLAR 5,6,7,8 in Jeffries '87 |
| 40 Est. | | | | | | | | |
| | | | | | | | | |
| 40 Est. | | | | | | | | |
| 40 Est. | | | | | | | | |
| | | | | | | | | |
| 10 | | | | | | | | Re-entrant calved from Milne Ice Shelf |

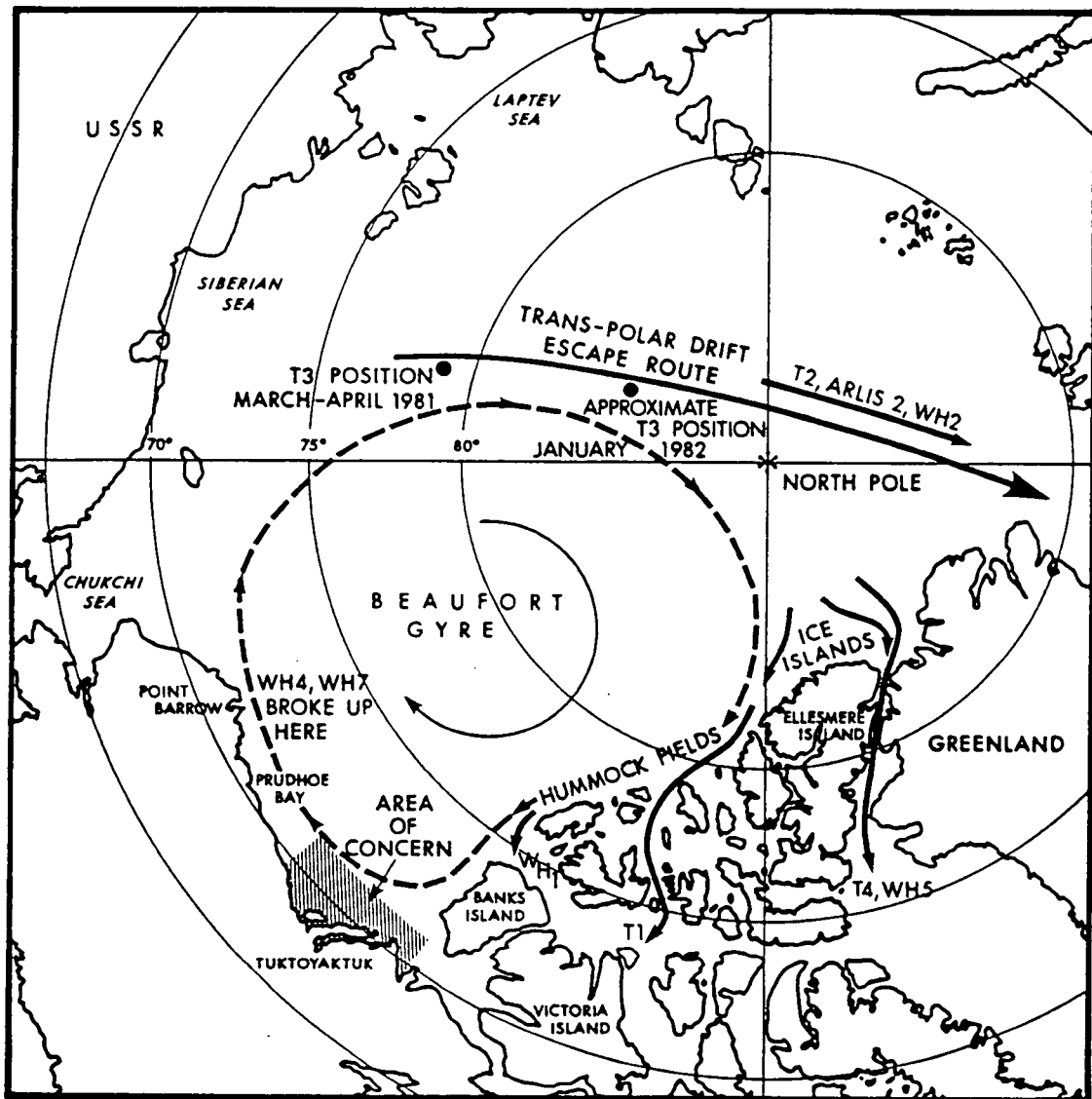


Figure 4.1: Ice Island Drift Patterns in the Arctic Ocean
 (Source: De Paoli et al., 1982)



Figure 4.2: Ice Island Fragments (on right) - West of Banks Island (Source: Hudson et al., 1980)

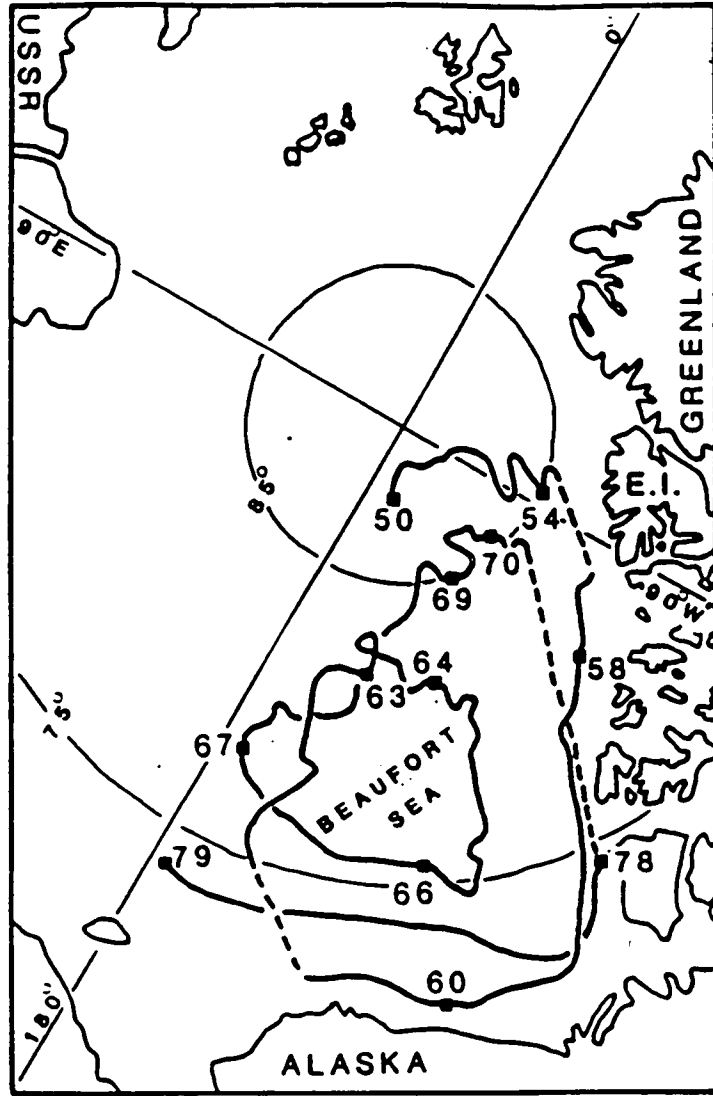


Figure 4.5: Drift of Ice Island T-3 in the Beaufort Gyre 1950-1979
 (Source: Jeffries, 1985a)

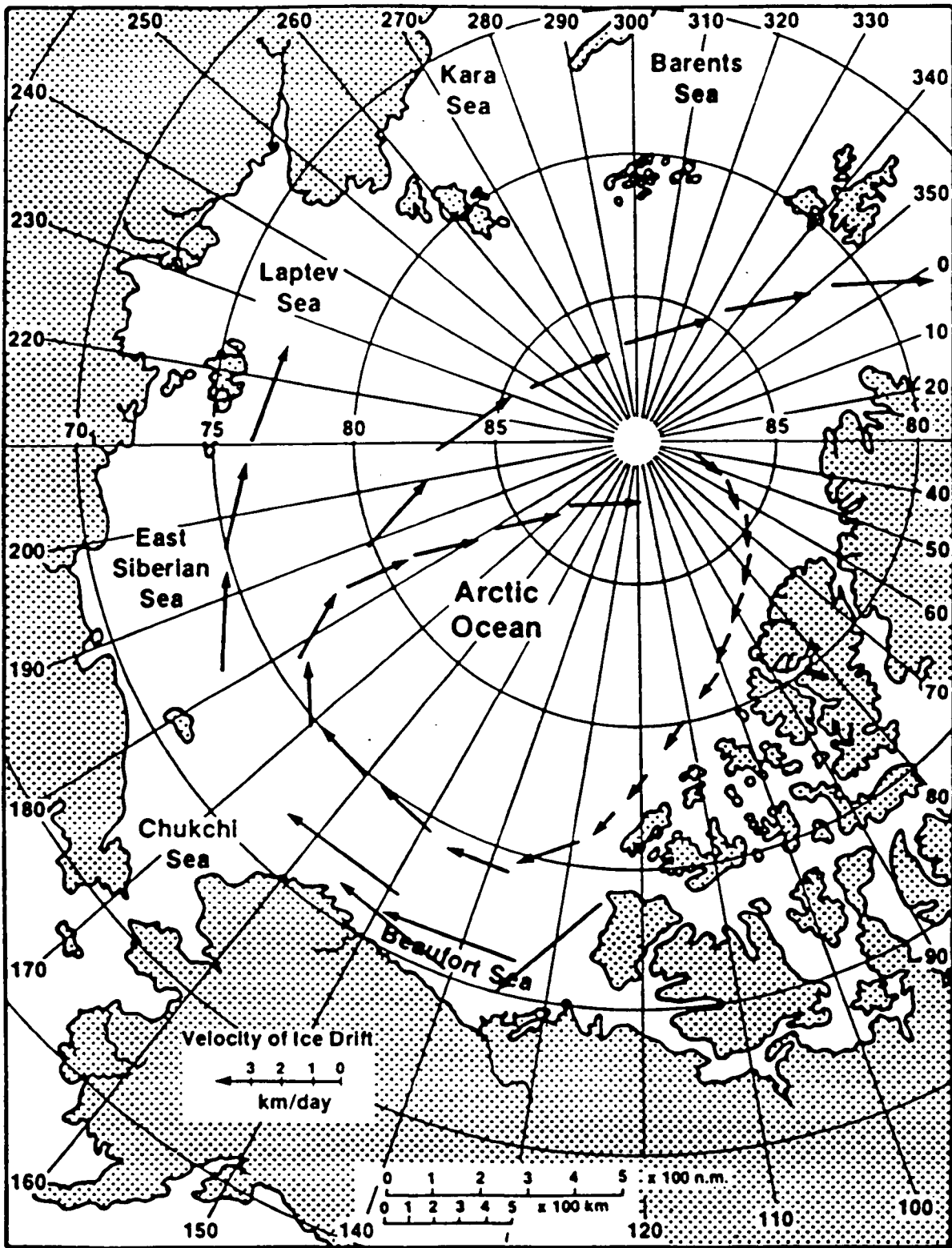


Figure 4.6: Mean Velocities of Ice Drift in the Arctic Ocean
 (Source: Cornett, 1986)



(photo courtesy of M. Metge, *CANATEC Consultants Ltd.*)



(from Hudson et al., 1980)

Figure 4.7: Aerial Views of a Multi-Year Hummock Field, Prince Patrick Island 1980.

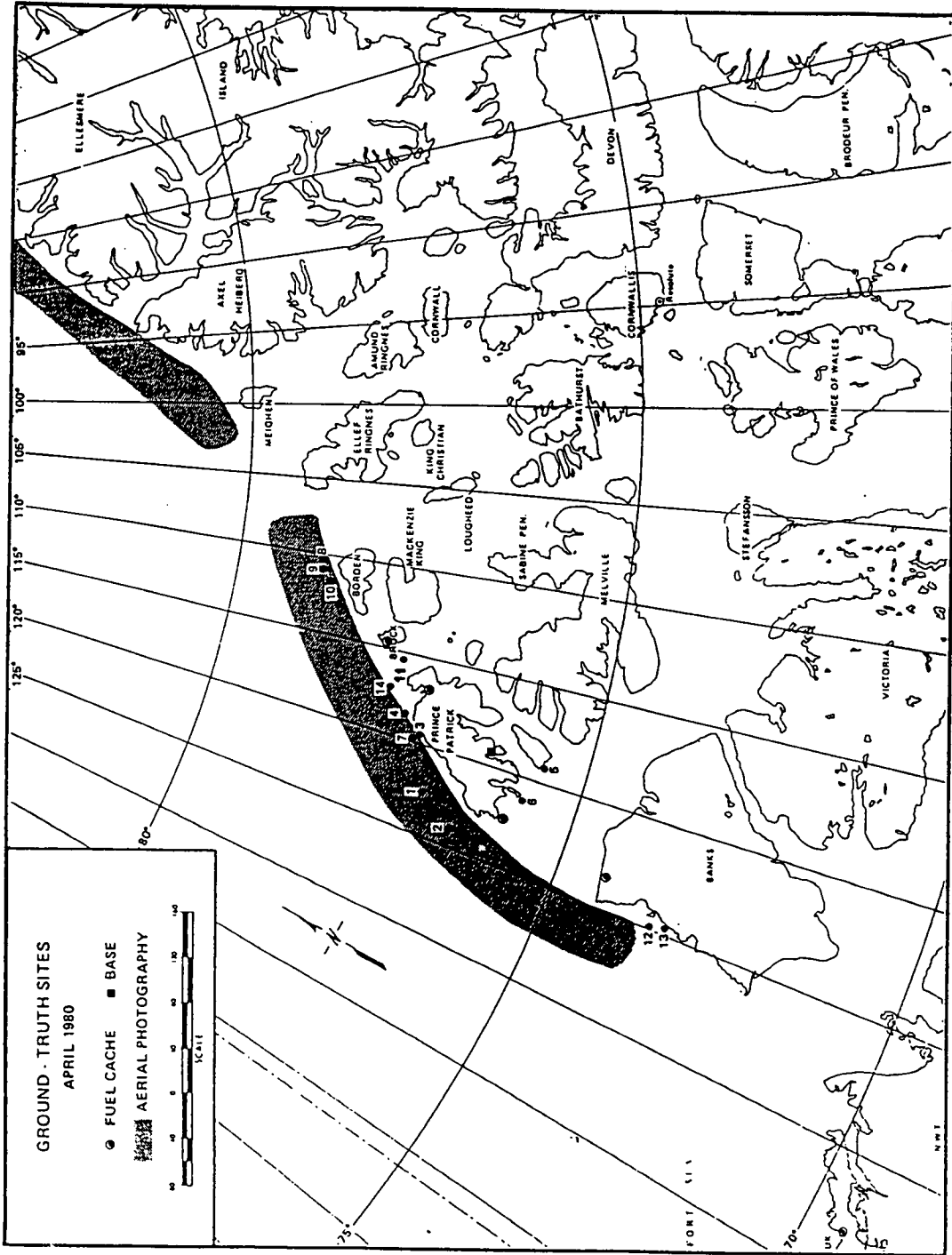


Figure 4.8: Ground Truthing Sites April 1980. (Source: Hudson et al., 1980)

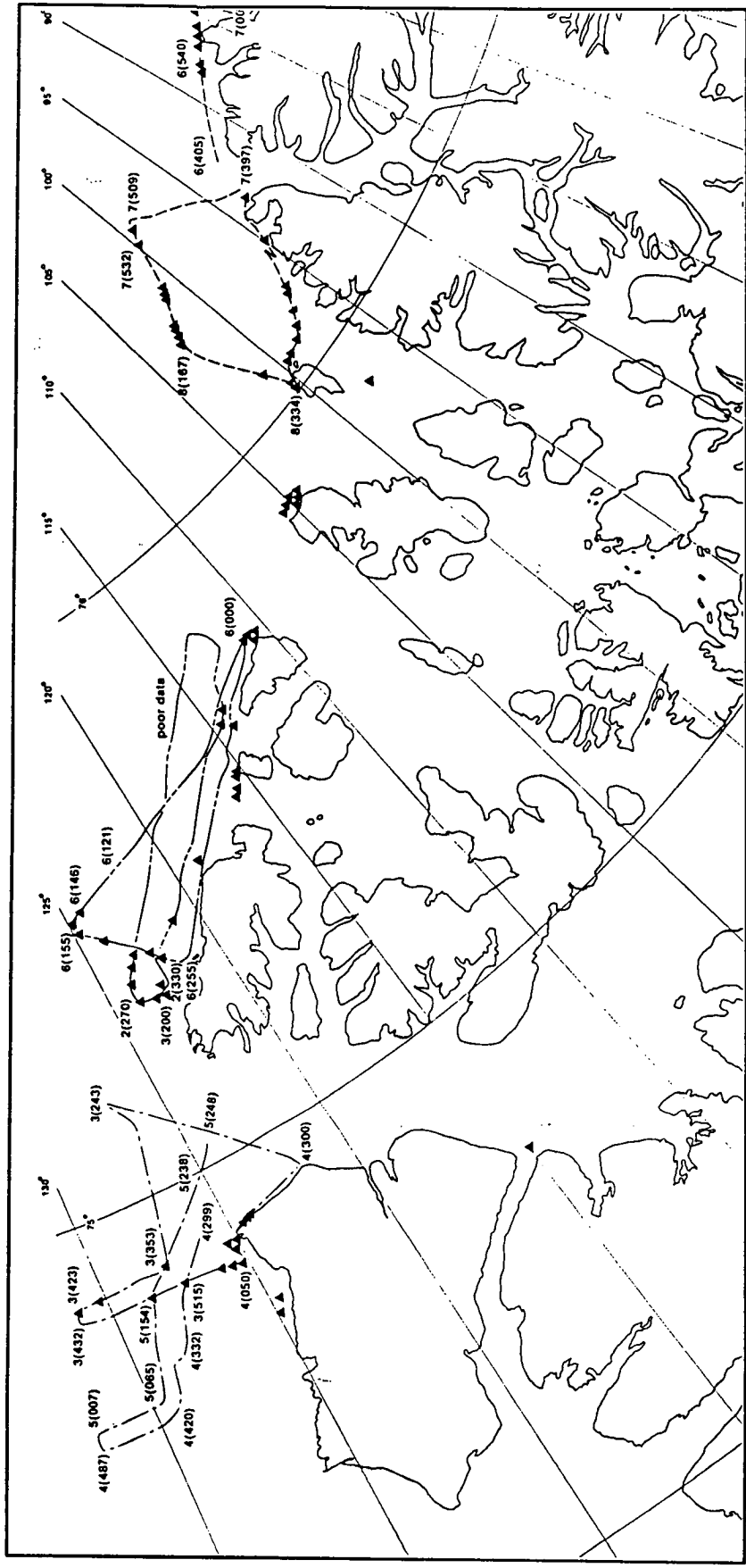


Figure 4.9: Aerial Photography Flight Lines April 1980. (Source: Hudson et al., 1980)

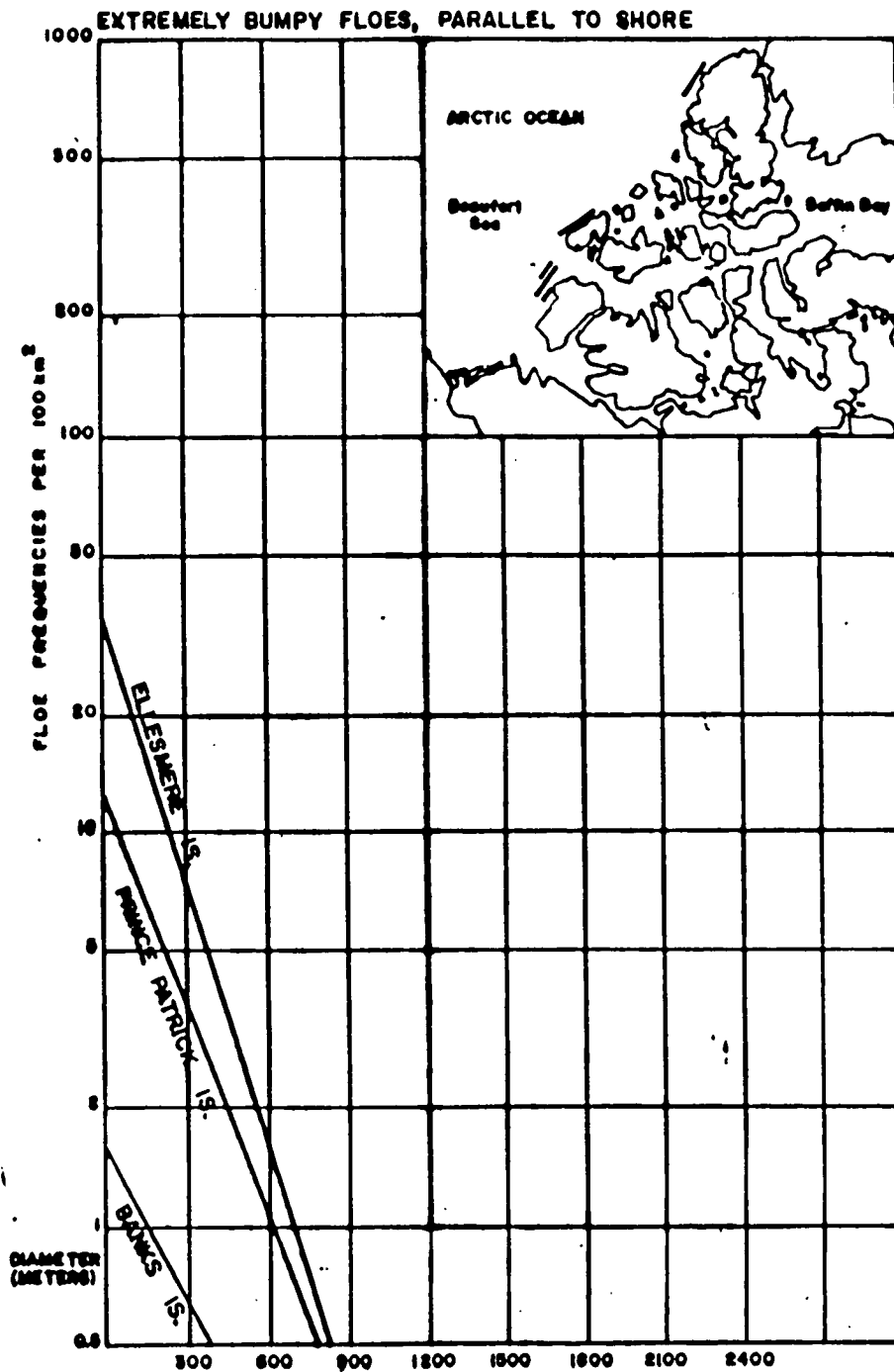


Figure 4.10: Floe Size Distributions of "Extremely Bumpy" Floes (MYHFs) April 1980.
 (Source: Hudson et al., 1980)



Figure 4.11: Aerial Photography of MYHF, March 1980 (Source: Wright et al., 1983)

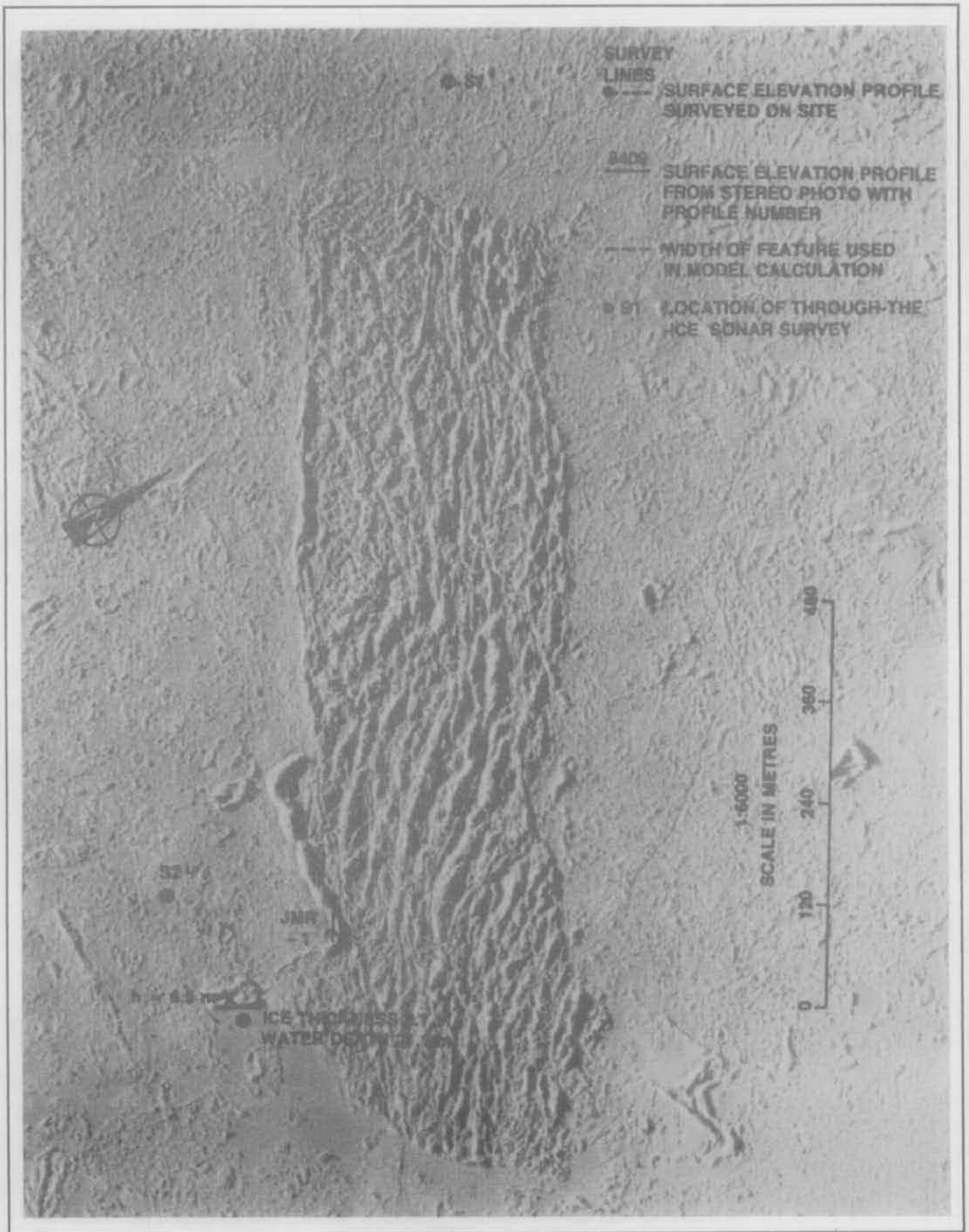


Figure 4.12: Aerial Photography of Second Year Hummock Field - April 1984.
(Source: McGonigal, 1984)

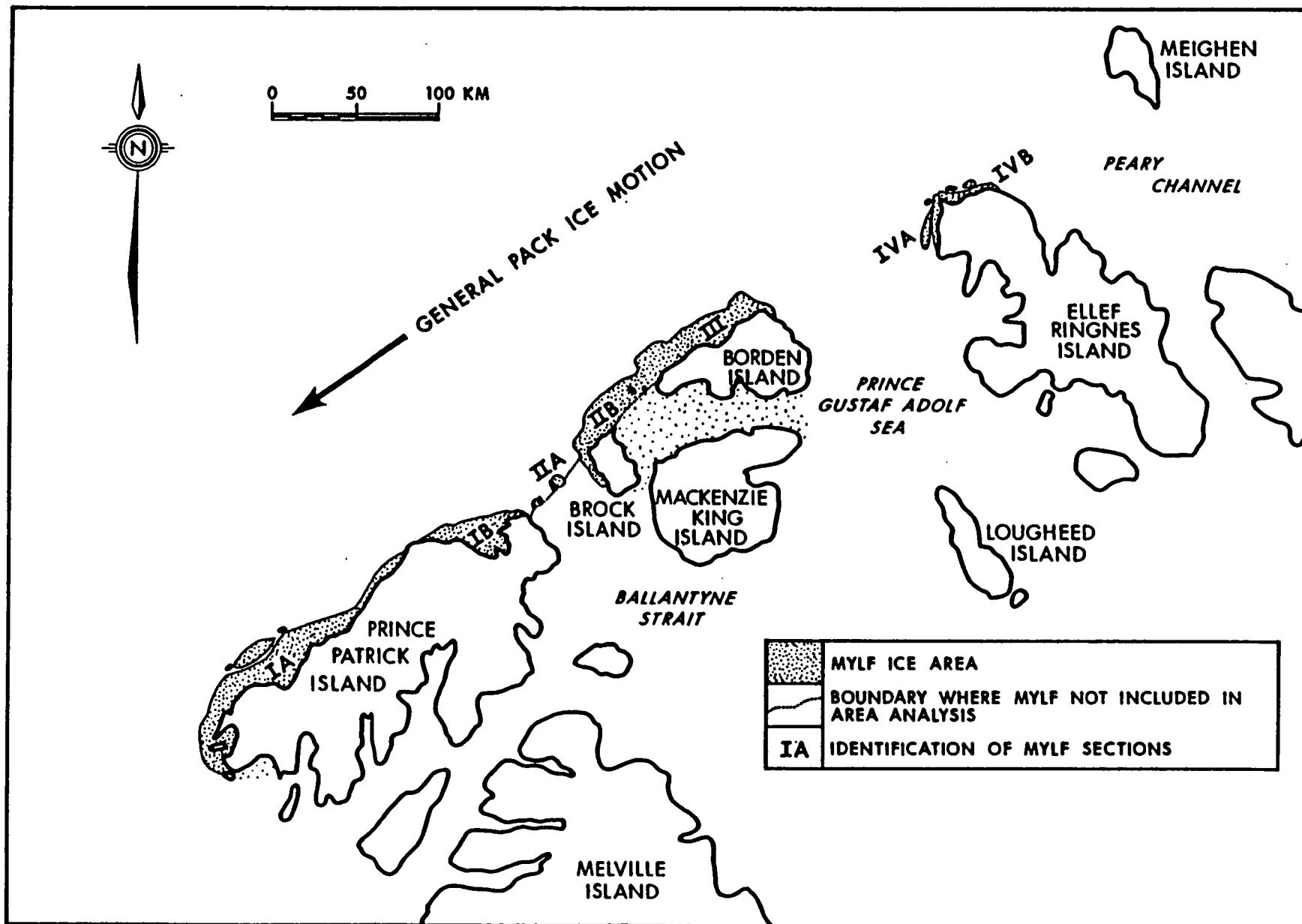


Figure 4.13: Areas of Multi-year landfast ice, Queen Elizabeth Islands

CHAPTER 5

PROPOSED STAR-2 FLIGHT PLAN AND GROUND TRUTHING

5.1 OBJECTIVES

Flight plan additions for the STAR-2 during the January 1991 AES Round Robin were designed to collect, with minimal extra flying, data which would permit the following:

i) Evaluation of the STAR-2 SAR's capability for the detection of extreme ice features. This resulted in the following requirements:

- The area flown had to contain various extreme ice features, i.e., ice islands, multi-year hummock fields, and multi-year landfast ice.
- Data had to be collected at 15 and 25 m resolutions.
- Data had to be collected at different flight line orientations relative to the same EIFs.
- There had to be extreme ice features close to and at some distance away from the aircraft flight path.

Peary Channel, between Ellef Ringnes and Meighen Islands, was known to contain large ice features (Hill 1990). In addition, Hudson et al. (1980) had indicated a large number of extreme features in the Arctic Ocean off the western shoreline of the Queen Elizabeth Islands (see Chapter 4).

- ii) Obtaining sufficient data set for calculation of extreme ice feature statistics.
- iii) Ground truthing of the SAR data by surface parties operating in the area.

5.2 PROPOSED FLIGHT PLAN

To meet the objectives of this project AES's 1991 Round Robin covered the Arctic Islands in a series of NS flight lines as shown in Figure 5.1, travelling from east to west. The double blocks in Figure 5.1 depict the two 100 km swaths imaged by the SAR system. It was proposed that three priority areas be flown, as described below:

- i) **Priority Area 1:** A test area flown over Peary Channel, as shown in Figure 5.2, at 15 m SAR resolution. Together with the 25 m data collected as part of the AES Round Robin Flight, Figure 5.1, this allowed investigation of the capabilities of the STAR-2 system for the detection of different types of ice features. STAR-2 data of this area were acquired on 14 January 1991, as part of this project.
- ii) **Priority Area 2:** It was proposed that the 25 m resolution north-south lines flown over the Queen Elizabeth Islands during the Round Robin be extended 100 km beyond the island coasts at 15 m resolution; Figure 5.3.

This, however, was not feasible due to the fact that the aircraft was already flying near to its maximum range of 3,360 km, as well as AES's budget restrictions.

- iii) **Priority Area 3:** It was also requested that the flight line along the coast of Banks Island normally flown at 25 resolution (Figure 5.1) be flown at 15 m resolution, for collection of extreme ice feature data, Figure 5.4. AES was unable to accommodate this request as they and other users required data directly comparable to the 25 m resolution data from the previous year's Round Robin flight.

5.3 GROUND TRUTHING

Fax messages were sent to 25 companies, institutes, and agencies (see Appendix A) to determine if any were planning spring season field operations in the area of interest. Seven replies were received.

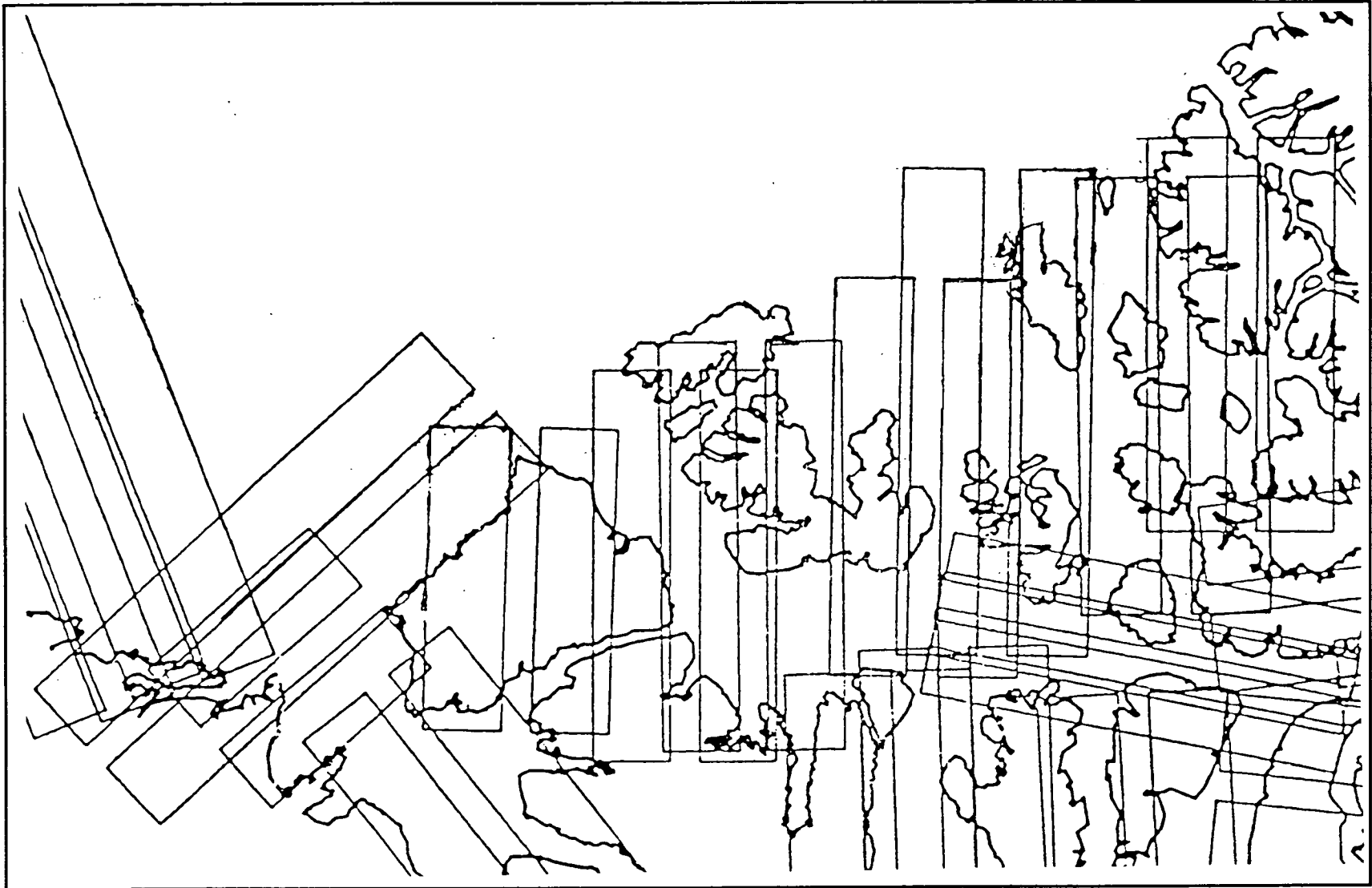


Figure 5.1: Flight paths for AES Round Robin
January 1991

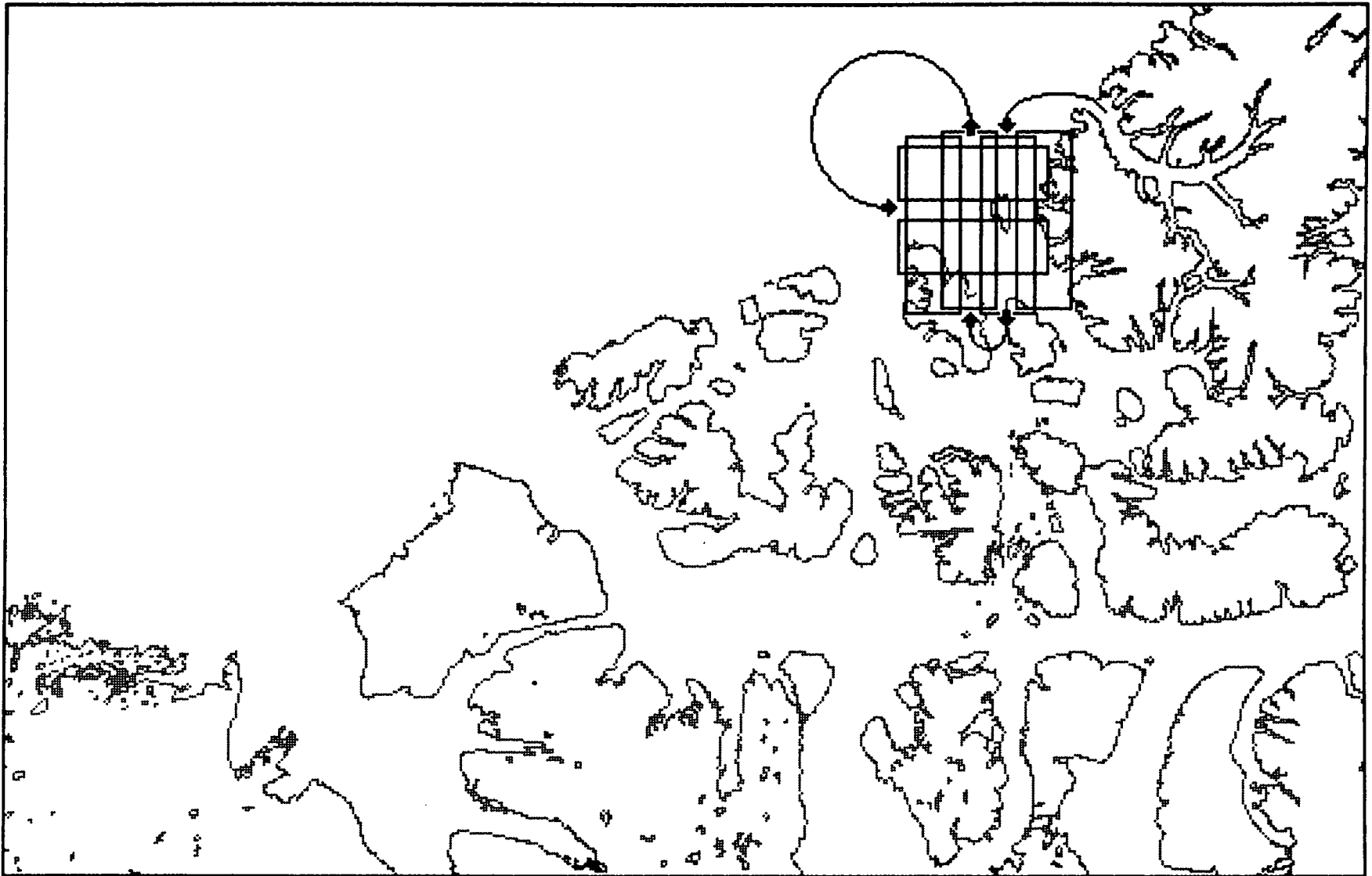


Figure 5.2: Detail of STAR-2 flight paths over test area, January 1991

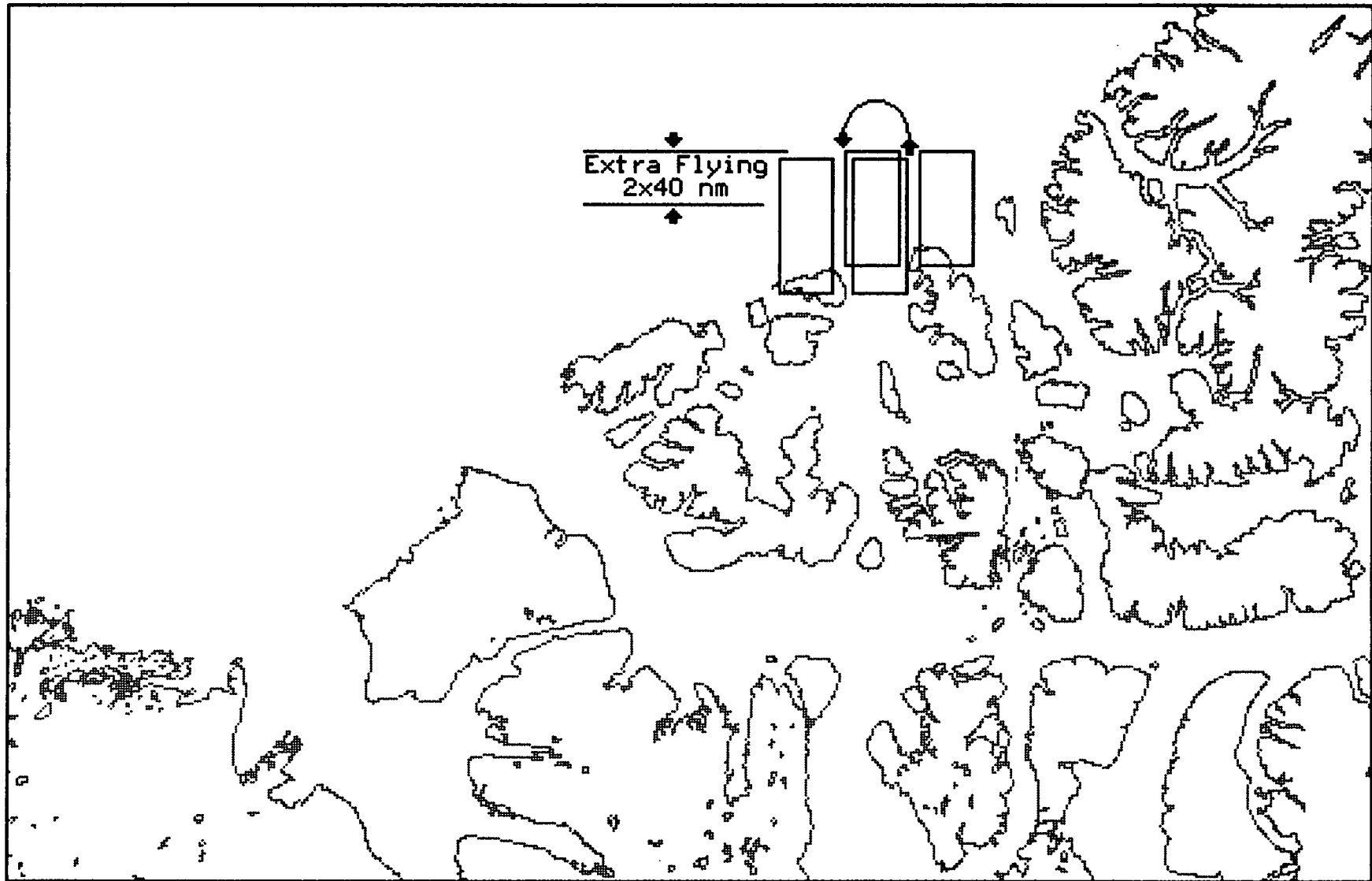


Figure 5.3: Extensions to regular STAR-2 flight lines, January 1991

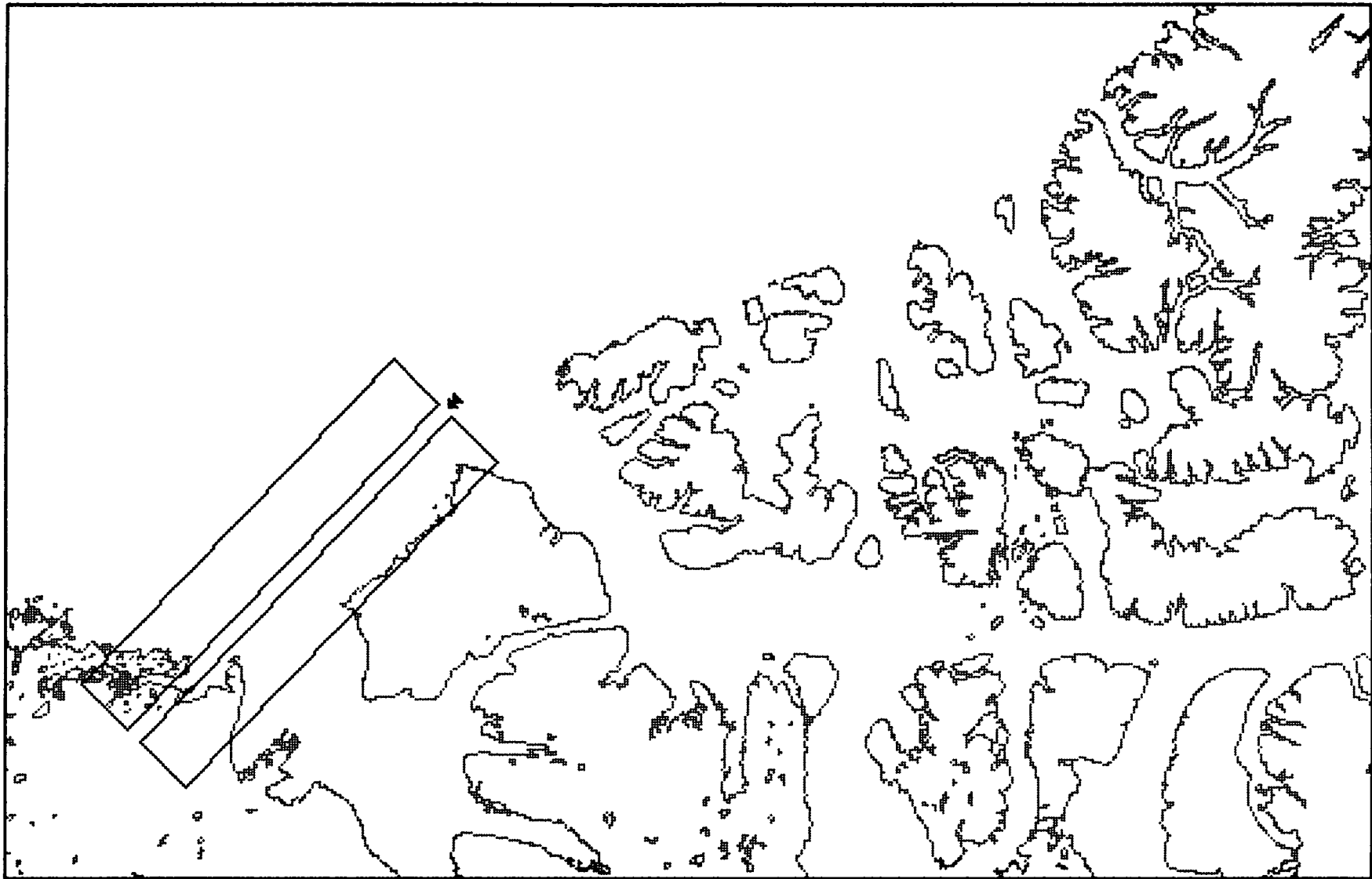


Figure 5.4: Proposed path of additional 15 m resolution STAR-2 flight line for collection of statistical data during January 1991 Round Robin

Only the Polar Continental Shelf Project (PCSP) office indicated that they would definitely be able to assist this project. The Hobson's Choice ice island camp manager, Dave Maloley, offered to ground truth ice features near the ice island following camp set-up in April. Ice features within 5 km were to be visited by snowmobile and observed. Features further afield were to be overflown and photographed if and when convenient. Plans were made to support this ground truth component with a "kit" consisting of a pre-printed reporting form (Figure 5.5), 35 mm colour film, and an enlargement print of the January STAR-2 image covering the immediate area of Hobson's Choice Ice Island (see Appendix A). However, PCSP's planned ground truth operations were not carried out due to cancellation of their 1991 field program at the ice island.

Other ground truth data sources of opportunity, linked to the PCSP ice island camp, were similarly not available. Tentative field projects by the National Research Council Canada, the Centre for Cold Ocean Resources Engineering, and the Institute of Ocean Sciences, had been scheduled in the area for the spring of 1991 but were also cancelled.

The Department of National Defence, whose camera-equipped surveillance aircraft frequently fly into the high Arctic, had expressed a willingness to acquire "ground truthing" air photos but was unable to direct a suitable flight over the area of interest (see section 6.2.1). Dr. T. Curtin of the U.S. Navy was also amenable to joint work. However, his field survey was carried out in the southern Beaufort Sea, too far removed from the area of interest for the EIF project.

Extreme Ice Features

Surface Truth Reporting Form

1. Date of observation: _____ Reported by: _____

2. Location (lat/long or bearing from known position): _____

3. Type of ice feature: ice island, hummock field, old ice floe,
 multi-year ridge, other (describe) _____

4. Observations

a) Ice Type (check): multi-yr; old ice; first-yr; young; new.

Comment: _____

b) Ice Thickness, metres (circle):

| | | | | | | | | | | | | |
|----|----|----|----|----|----|----|----|----|----|----|----|----|
| <1 | 1 | 2 | 3 | 4 | 5 | 6 | 8 | 10 | 12 | 14 | 16 | 18 |
| 20 | 22 | 24 | 26 | 28 | 30 | 32 | 34 | 36 | 38 | 40 | 42 | 44 |

estimated
 measured

c) Average Ridge Height, metres (circle):

| | | | | | | | | |
|------|-----|-----|-----|-----|-----|-----|-----|-----|
| <0.5 | 0.5 | 1.0 | 1.5 | 2.0 | 2.5 | 3.0 | 4.0 | 5.0 |
| 6 | 7 | 8 | 9 | 10 | 11 | 12 | 13 | 14 |

estimated
 measured

d) Maximum Ridge Height, metres (circle):

| | | | | | | | | |
|------|-----|-----|-----|-----|-----|-----|-----|-----|
| <0.5 | 0.5 | 1.0 | 1.5 | 2.0 | 2.5 | 3.0 | 4.0 | 5.0 |
| 6 | 7 | 8 | 9 | 10 | 11 | 12 | 13 | 14 |

estimated
 measured

e) Average Ridge or Other Surface Feature Spacing, metres (circle):

| | | | | | | | | | | | | |
|----|----|----|----|-----|-----|-----|-----|----|----|----|----|----|
| <2 | 4 | 6 | 8 | 10 | 12 | 14 | 16 | 18 | 20 | 30 | 40 | 50 |
| 60 | 70 | 80 | 90 | 100 | 150 | 200 | 250 | | | | | |

estimated
 measured

f) Other Dimensions (please state whether estimated or measured):

(Please complete the back of this page as well)

Figure 5.5

CHAPTER 6

OTHER SOURCES OF DATA

6.1 INTRODUCTION

As indicated in Chapter 5, only part of the additional AES STAR-2 requested during the round robin of January 1991 could be flown at a resolution of 15 m. As a result, it became evident that only a limited amount of these data would be available for analysis of EIFs. Because one of the primary project objectives involved improved statistics on EIFs, other SAR data, aerial photography, and satellite imagery acquired in recent years were sought in order to supplement the EIF data available from the 1991 SAR imagery. The additional data sources considered are outlined in the following sections.

6.2 AERIAL PHOTOGRAPHY

Aerial photography has proven to be an excellent source of EIF data. Two programs, Hudson et al. (1980) and Eley and Hudson (1982), provided a considerable quantity of data by this means. Aerial photography does, however, provide limited coverage - typically a 4-6 km (2.5 - 3.75 miles) swath at 3,000 - 3,100 m (10,000 feet) flying height. This contrasts with the 64 to 100 km (40 - 62 mi) swath obtained with the STAR-2 SAR. In some applications, stereo coverage is desirable and each photograph must overlap the next by 60% of its area. However, for the type of analyses where qualitative information or surface roughness of floes is sought, stereo analysis is not required. Thus, the survey aircraft can fly higher and provide a somewhat greater coverage without the need for photo overlap.

6.2.1 Department of National Defence (DND)

Mr. Tiit Romat of DND, indicated that Canadian Armed Forces aircraft regularly fly over the regions of interest to this project. He also suggested that, under suitable conditions of daylight and minimal cloud cover, DND aircraft could be directed to fly over the regions of interest to the EIF study at a specific altitude and take stereo mapping photographs.

Ultimately, DND was unable to provide aerial photography for the areas of interest. However, the following specific information was provided to DND and is repeated here as a guide to arranging access to future data sets of opportunity from DND.

Locations for photography:

The map from Hudson et al. (1980), Figure 6.1, was sent to Mr. Romat. The shaded areas are prime locations for ice islands and multi-year hummock field data acquisition and the lines are those flown in 1982 by Eley and Hudson (1982). The area between Axel Heiberg and Ellef Ringnes Islands should be considered the prime area as this is the area for which we have 15 m resolution STAR-2 data from the Round Robin flight in January, 1991 and the ice often remains more or less stationary in this location for a year or so. DND expressed assurance that the location of any relevant photography which they took could be made available.

Flight altitude:

An aircraft flight altitude of 3,000 m will permit detection of extreme ice features, provide a wide enough swath for obtaining adequate statistical sample, and allow a height resolution of at least 0.5 m from stereo analysis of the data, if required. Previous studies (Hudson et al., 1980, and Eley and Hudson, 1982) categorized the large floes as "smooth", "bumpy", and "extremely bumpy" (the "extremely bumpy" floes being considered as EIFs, by Hudson et al. and Eley and Hudson). Since stereo photography is not required for the type of subjective classification used here, the DND aircraft could fly at an altitude of 6,000 m (20,000 feet) without photo overlap, thus doubling the areal coverage for each photo, and still providing adequate resolution to detect the features of interest.

DND was requested to fly the priority lines (dotted) in Figure 6.1 at 3,000 m (10,000 ft) with 60% photo overlap for stereo analysis. Otherwise, photography was requested within the shaded areas, at 6,000 m (20,000 ft) with 10% overlap of images, for the subjective analysis of the ice surface features.

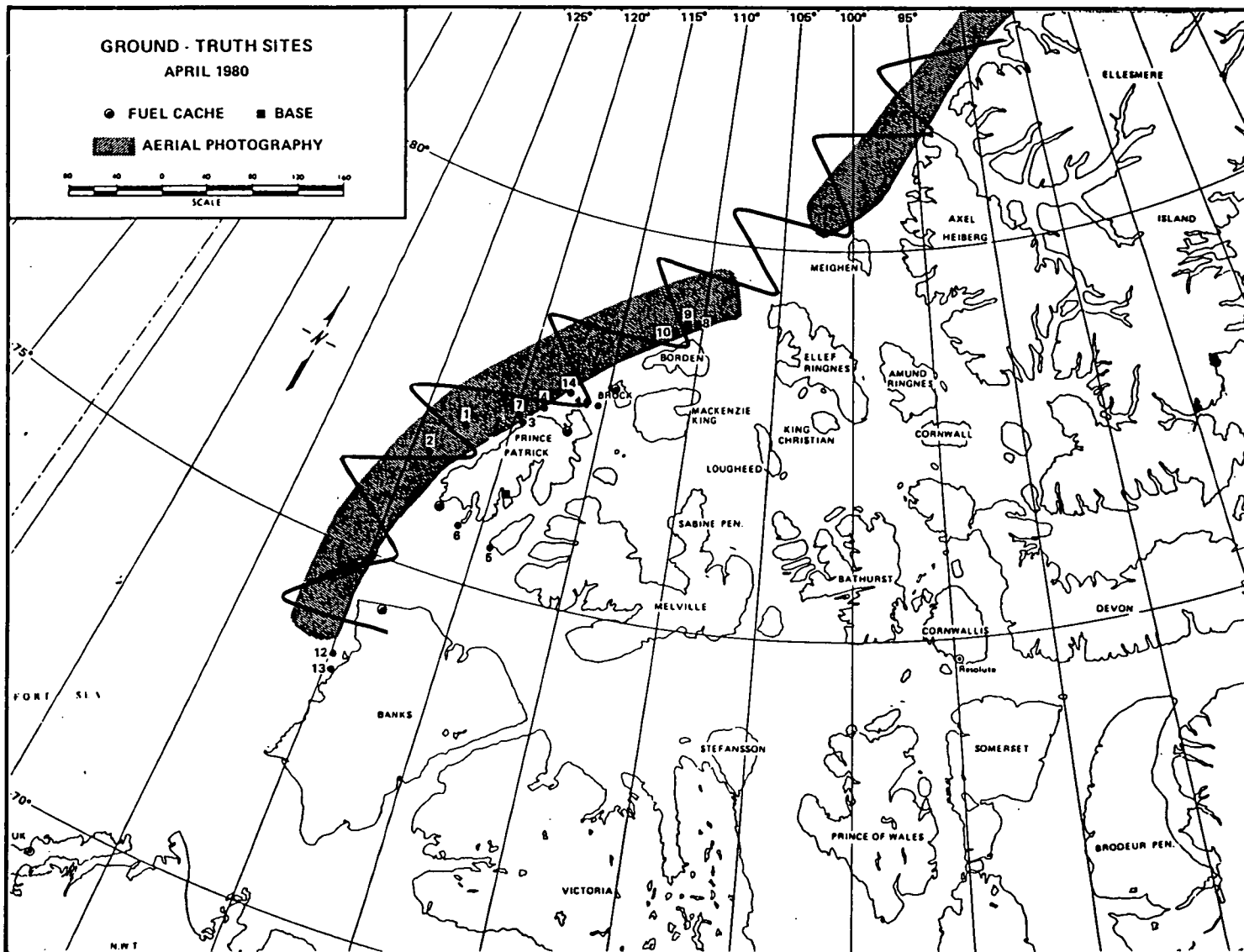


Figure 6.1: Areas of multi-year hummock fields (from Hudston et al. 1980) and suggested air photo flight lines: several of these flight lines overlap lines made by Hudson.

Date of Flights:

Due to the prolonged winter season darkness at high latitudes, normal panchromatic photography is not possible in the region of interest between the months of October and March. It was indicated to DND that the photography should be carried out on clear days after April 15, as close as possible to midday, when the sun angle is at its maximum of 20 to 21 degrees. Mid-summer flights during times of higher sun angles would be preferred, in order to minimize lost and ambiguous data due to excessive shadow.

Cost:

At the time of this project, DND was prepared to carry out the above work on an "as available" basis at no cost to the project.

Archived DND Data:

Mr. Romat indicated that it was unlikely DND would have any archived photographic data which would be useful to this project. He also indicated that it would be difficult to find this data in their archives.

Future:

It is recommended that Mr. Tiit Romat be contacted from time to time in the future, to see whether DND has obtained any useful data and/or is planning any flights over the northwest coast of the Queen Elizabeth Islands. Ongoing co-operation with DND in this regard would provide the opportunity for systematic, low cost, high quality data acquisition on EIFs in the future.

6.2.2 National Research Council (NRC)

The NRC occasionally fly aerial photo coverage in the southern Beaufort Sea. Their aircraft could carry out additional flights up the eastern edge of the Beaufort Sea to acquire EIF data. Ideally the aircraft should obtain aerial photography from the southern Beaufort Sea along the coast to the Peary Channel, but this would require a considerable budget. In future, with an adequate project budget, the NRC aircraft, or indeed any charter aircraft should fly the priority areas as shown in Figure 6.1. Such a flight, from Tuktoyaktuk to

Brock Island and return, would cost an estimated \$20,000 (1991 dollars), including mapping camera rental.

6.3 SAR DATA

6.3.1 Intera Technologies Ltd., Calgary

Intera developed the first commercial SAR system in 1983. This system, STAR-1, provides data with a swath width of 60 km and resolution (pixel size) of 12 m, or 30 km swath width and resolution of 6 m. In the fall of 1989 they commissioned a second SAR system, STAR-2, which is leased to AES for regular ice reconnaissance. As discussed in the Introduction, this sensor provides data in two 100 km swaths (one on each side of the flight line) with 25 m resolution, or in two 64 km swaths with 15 m resolution.

Over the past 8 years, Intera have flown STAR-1 and STAR-2 missions over the Arctic for clients and also have obtained data on their own account. Results of a review of Intera's data archive are summarized in Table 6.1. As shown in the table, no data of particular value to this study is available except for STAR data sets #3 and #8. These data have been analysed extensively within the scope of this project and are further described in Chapter 8.

A preliminary review of data set #7 indicated that it contained large rectangular floes in the Alaskan coastal regions. These may have been multi-year floes, but were more likely stamukhi zone rubble piles, as they lay near the Barrier Islands and in isolation from the polar pack to the north. Data set #9 was available at a substantial cost. However, a copy of the data could not be located for preliminary review and so it was not considered further. The remaining data sets did not extend far enough into the pack area to be of interest. In summary, it was not considered worthwhile directing resources from this study to review any of these data sets, except for #3 and #8.

Table 6.1: Archival SAR Data Available though Intera

| | SENSOR | RESOLUTION | DATA/REPORT | COMMENTS | USE FOR THIS STUDY |
|---|--------|------------|---|--|--------------------------------|
| 1 | STAR-2 | 25 m | 1990 Round Robin Arctic Atlas | Intera have imagery-atlas 1:2,000,000. No imagery into pack except end of 1 line. | none |
| 2 | STAR-1 | 12 m | 1986/87 Ice atlas | No data beyond edge of Arctic Islands. Data in M'Clure Strait. | none |
| 3 | STAR-1 | 12 m | Ice Atlases | Contact Bob Gorman - Canarctic | Yes, no cost |
| | STAR-2 | 25 m | | | |
| 4 | STAR-1 | 12 m | U.S. Beaufort & Chukchi Seas | Flight for Canarctic & K. Vaudrey. Good data, 2 Feb 89, No obvious features. | Nothing obvious |
| 5 | STAR-1 | 12 m | Nov/Dec/Feb 85-86 along Alaskan coast | Data to 150 km north. Appears to be all FY ice. | Unlikely |
| 6 | STAR-1 | 12 m | 1987 Chukchi Sea | No multi-year ice | none |
| 7 | STAR-1 | 12 m | Canadian & U.S. Beaufort Seas. 8 April 1989 Baillie Is. to Point Barrow | Some multi-year floes. Floes rectangular very bright reflectors, and 1-1.5 km across in Alaska area. | Yes, \$250 to review negatives |
| 8 | STAR-1 | 12 m | Canadian Ice Atlas | By CCG (Victor Santos Pedro) | Yes, no cost |
| 9 | STAR-1 | 12 m | 500 miles N from Tuk. and return. Date not known. | Obtained by Intera; sold to Vaudrey to study ice islands. Could not be located. | Likely cost? |

6.4 SPOT (SATELLITE POUR L'OBSERVATION DE LA TERRE)

This is visual imagery taken from the SPOT satellite with orbits in the region of interest as shown in Figure 6.2. The panchromatic linear array (PLA) imagery is of 10 m nominal resolution and the multi-spectral linear array (MLA) imagery is of 20 m nominal resolution. A SPOT image of Hobson's Choice (Jeffries and Sackinger, 1990) indicated extremely high quality imagery which clearly showed the ripples on the ice island surface. Unfortunately, no multi-year hummock fields could be identified in this published SPOT image.

Intera-Kenting, Polar Continental Shelf Project, AES, the Canada Centre for Remote Sensing, and the Geophysical Institute in Fairbanks, Alaska, were contacted to discuss the advantages and disadvantages of SPOT for the identification of old ice. Mr. Scott Paterson, of Intera-Kenting, indicated that one should choose SPOT imagery from the mid-summer period when the ice is wet, in order to obtain maximum contrast. In winter, the ice appears white and relatively featureless. SPOT retailer, Radarsat International (RSI), was provided with the location of the Hobson's Choice ice island for each summer from 1988 to 1990. RSI scanned the available data and produced a list of potentially useful images for the location required. Tables 6.3 and 6.4 list potential images identified by RSI for the latitude/longitude ranges requested (Table 6.2). These summer images were then examined on microfiche but showed essentially a blank "picture" of the ice, despite the fact that coastlines and islands showed up clearly and in considerable detail. This indicated that SPOT imagery requires special exposure to adequately show EIFs in summer.

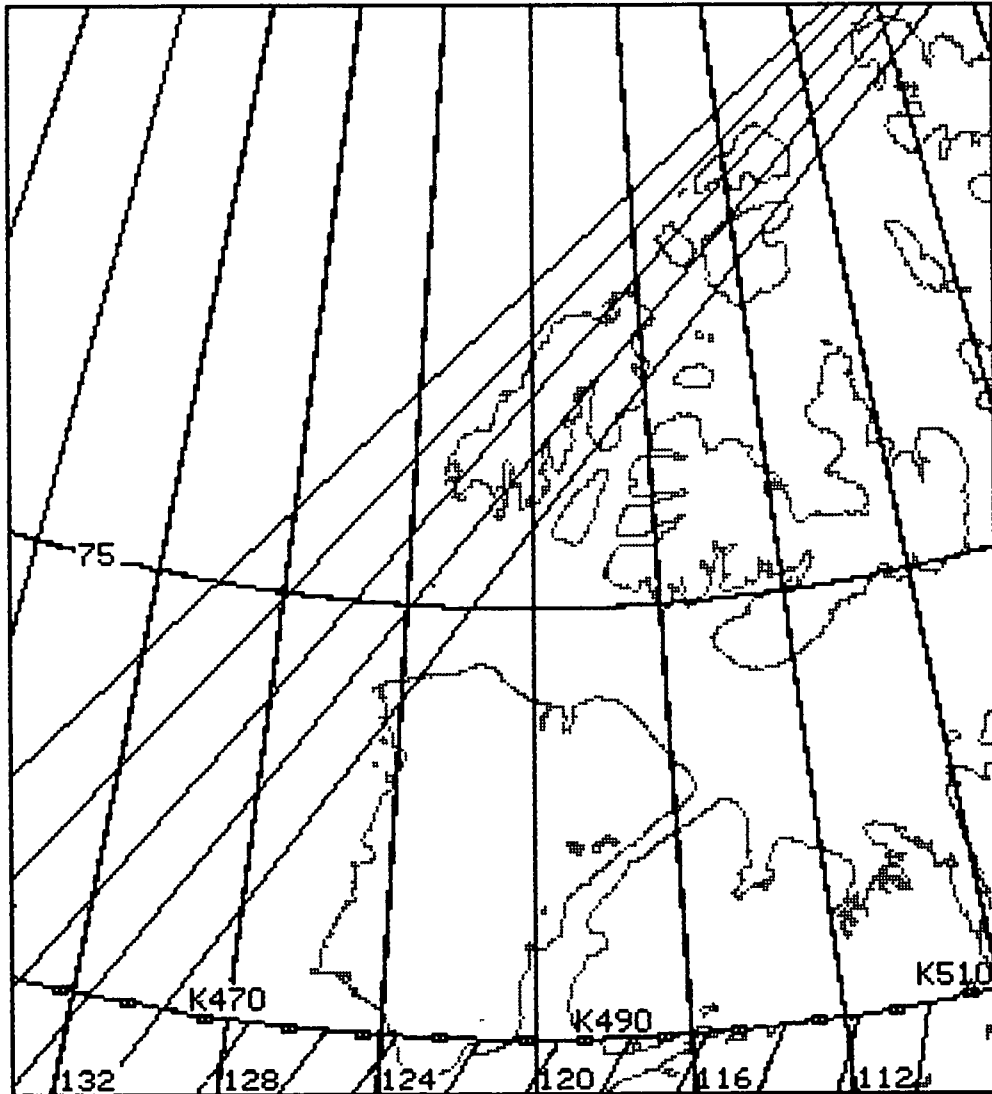


Figure 6.2: SPOT satellite orbit paths over the study area
(Modified after SPOT Image, 1986)

Table 6.2: Latitude and Longitude ranges of Hobson's Choice ice island positions, 1988-1990

| Year | Latitude Range | Median | Longitude Range | Median |
|------|----------------------|----------|------------------------|-----------|
| 1988 | 79° 05'N to 80° 09'N | 79° 37'N | 101° 12'W to 106° 48'W | 104° 00'W |
| 1989 | 78° 28'N to 79° 32'N | 79° 00'N | 98° 12'W to 103° 48'W | 101° 00'W |
| 1990 | 78° 14'N to 79° 46'N | 78° 46'N | 96° 42'W to 102° 18'W | 99° 30'W |

Only one image, from 27 July 1988, was located which was suitable for this study. In the other images reviewed, the ice island was either off the frame, too close to the edge of the image, or obscured by cloud cover. In 1989, there was no suitable image and in 1990 there were four potentially useable images. The 1988 image presented by Jeffries and Sackinger (1990b) - ID# 061108880725205539 - was not located in the initial RDI search.

RSI were requested to conduct a search in the region between 78 - 79° N and 96 - 102° W from 1986 to 1990, July to September inclusive, to locate potential images of EIFs over the past five years. The results of this search are shown in Tables A.1 to A.4 in Appendix A. It is seen that there is no data for 1986 but, otherwise, there are a number of images for the other four years, where cloud cover is low. (The "CLOUD" number is the cloud cover in tenths in the 4 quarters of the image).

The 1988 SPOT image shown by Jeffries and Sackinger (1990), and referenced above, was located by RSI and purchased for this project as it was known to contain many EIFs. This image clearly shows the Hobson's Choice ice island and various ice island fragments plus, on closer examination, features which are interpreted as MYHFs. More details of this image are provided in Chapters 7 and 8. A comparison of ice features on this 1988 SPOT image with those on a 1988 STAR-1 image for the same season proved extremely valuable in establishing guidelines or keys for the interpretation of EIFs on SAR.

SUMMARY OF SEARCH PARAMETERS

Data base selected: SPOT 1 & 2
 Spectral mode selected: Panchromatic
 Date range: From 01 08 88 to 30 08 88
 LATITUDE range: From 78 20 to 80 20 NORTH
 LONGITUDE range: From 099 30 to 102 30 WEST

QUERY STATISTICS

Number of images found: 6

| NO | HRV | SPOT MODE | ANGLE | SCENE CENTRE | | ORB | DATE RECORDED | | | CLOUD | QUAL | S | HDTID |
|----|-----|-----------|-------|--------------|--------------|-----|---------------|----|----|-------|------|---|----------|
| | | | | K/J | LAT/LONG | | DD | MM | YY | | | | |
| 1 | 2 | XS | 2.3 | 065/116 | 79 23/102 19 | 276 | 09 | 08 | 88 | 0000 | | P | P0700783 |
| 1 | 2 | XS | 2.3 | 067/118 | 79 39/099 54 | 276 | 09 | 08 | 88 | 0000 | | P | P0700783 |
| 1 | 1 | XS | -2.3 | 069/116 | 80 12/100 15 | 276 | 09 | 08 | 88 | 0000 | | P | P0700783 |
| 1 | 2 | XS | 2.3 | 068/116 | 80 07/100 35 | 333 | 13 | 08 | 88 | 8389 | S | P | P0700791 |
| 1 | 1 | PD | -31.1 | 062/118 | 78 32/101 43 | 005 | 16 | 08 | 88 | 9999 | | P | P0700797 |
| 1 | 1 | PD | -31.1 | 065/118 | 78 59/100 34 | 005 | 16 | 08 | 88 | 9999 | | P | P0700797 |

Table 6.3: Results of SPOT imagery 1988 search (Source: Radarsat International)

(See page B-9 for abbreviations)

SUMMARY OF SEARCH PARAMETERS

Data base selected: SPOT 1 & 2
 Spectral mode selected: Panchromatic
 Date range: From 01 07 90 to 30 09 90
 LATITUDE range: From 78 14 to 79 10 NORTH
 LONGITUDE range: From 096 42 to 102 18 WEST

QUERY STATISTICS

Number of images found: 4

| NO | HRV | SPOT MODE | ANGLE | SCENE CENTRE | | ORB | DATE RECORDED | | | CLOUD | QUAL | S | HDTID |
|----|-----|-----------|-------|--------------|--------------|-----|---------------|----|----|-------|------|---|----------|
| | | | | K/J | LAT/LONG | | DD | MM | YY | | | | |
| 2 | 2 | PD | -26.5 | 061/118 | 78 25/102 13 | 289 | 21 | 08 | 90 | 1020 | | P | P0701375 |
| 2 | 2 | PD | -26.5 | 064/118 | 78 51/100 56 | 289 | 21 | 08 | 90 | 0000 | | P | P0701414 |
| 2 | 2 | PD | -26.5 | 065/120 | 78 44/098 56 | 360 | 21 | 09 | 90 | 0066 | | P | P0701414 |
| 2 | 2 | PD | -26.5 | 067/121 | 79 09/097 28 | 360 | 21 | 09 | 90 | 0000 | | P | P0701414 |

Table 6.4: Results of SPOT imagery 1990 search (Source: Radarsat International)

(See page B-9 for abbreviations)

CHAPTER 7

INTERPRETATION OF EXTREME ICE FEATURES FROM SAR, 1988 - 1991

7.1 INTRODUCTION

The original plan was to develop EIF interpretation keys from the 1991 STAR-2 imagery and verify them with simultaneous ground truth information. Since ground truth acquisition proved impractical, interpretation keys were developed through a comparison of 1988 STAR-2 imagery with a high resolution visible spectrum SPOT image of identical ice features. The results of this intercomparison, detailed below, were applied to other SAR images available in public archives in order to extend the existing data base and obtain improved statistics on EIFs.

7.2 METHODOLOGY

The SAR image of February 19, 1988, was compared with a SPOT image of August, 1988. The objective of this comparison was to use the visible spectrum ice surface patterns on the SPOT image to confirm or reject, suspected EIF targets identified on the SAR. The five-month gap between image dates is attributable to the limitations of the SPOT system but was inconsequential, since little relative movement in the ice area occurred over this period. The panchromatic linear array (PLA) of the SPOT satellite is sensitive only to reflected visible wavelengths and could not receive satisfactory data during the winter period of polar darkness. The limited satellite revisit schedule, frequent cloud cover, and lack of user interest in the Queen Elizabeth Islands region resulted in the five-month hiatus before a satisfactory image was acquired. Also, as mentioned earlier, late fall, winter, or spring SPOT imagery show none of the contrast seen in the August imagery when the ice is melting.

In spite of the difference in image dates, the SAR and SPOT imagery covered a common area which contained several well-documented EIFs. These features included the Hobson's Choice ice island, several other distinctively-shaped ice island fragments and extreme multi-year ice floes. Because the five-month time gap occurred during winter and spring, there was minimal regional ice movement with major identifiable ice distribution patterns

remaining clearly evident (Figure 7.1). The two images offered comparable spatial resolution; the SPOT PLA image had a nominal 10 m pixel size and the STAR-2 had a nominal 12 m pixel size. The 1988 STAR-2 was an earlier configuration of the sensor used operationally in 1991 and operated with a 12 m as opposed to the current 15 m pixel size.

The SAR image was interpreted first. Targets of interest were marked on a transparent overlay sheet on the image. Next, as many of these targets as possible were located on the SPOT image of the same area. Finally, additional targets of interest, not apparent on the SAR, were identified on the SPOT.

7.2.1 Notes on the 1988 STAR-2/SPOT Imagery Interpretation

Ice island fragments and other EIFs of interest were identified on the imagery. The ice islands were easily identifiable due to their very distinctive surface patterns, tonal difference, and the radar shadows cast by the smaller fragments. Previous experience in interpreting ice islands on SAR (Hill, 1990) was particularly useful.

The other features of interest were the following:

- old ice floes surrounding hummocked ice areas,
- areas of dense linear texture
- areas of dense mottling and "pock-marks" as described by AES in the SAR Ice Interpretation Guide (AES, no date).

A total of 47 extreme ice feature targets were identified on the area of SAR imagery common to the SPOT coverage. Of these, 23 were re-located on the SPOT image but six common features were rejected from the "extreme" category upon closer examination of the SPOT image.

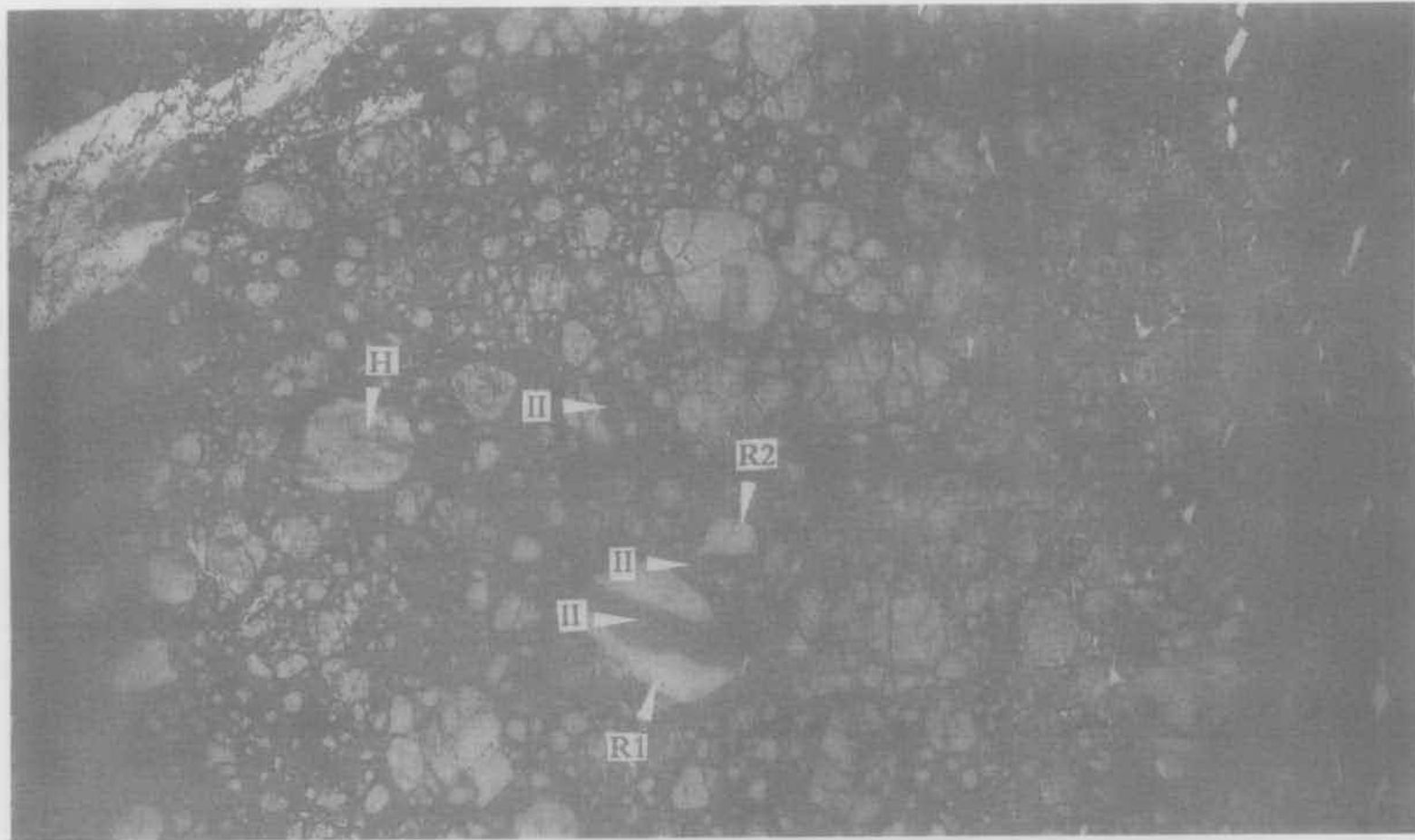


Figure 7.1: Detail of STAR-2 image of 19 February 1988, used during intercomparison with SPOT imagery. Scale is 1:250,000. (Imagery courtesy of Polar Continental Shelf Project office).

The SPOT was the superior image type as it permitted easier identification of unique ice surfaces such as those of ice islands, re-entrant ice fragments, and the closely spaced ridges of MYHFs. The STAR-2 imagery on the other hand, provided far better distinction of individual floes within very close pack concentrations. In the SPOT imagery, all ice is white, whereas in the SAR imagery, old ice is a light grey and first year ice is a dark grey.

7.2.2 SAR Interpretation Key

Three types of SAR image, each of a different pixel size, were analyzed together with a 1988 SPOT satellite image. The SAR imagery pixel sizes were 12 m (representative of pre-1991 archive SAR), 15 m (from January 1991 flight), and 25 m (from January 1991 flight). The interpretive keys are described individually for each SAR, since a difference in overall image appearance among the SARs suggested that there would be differences in the appearance of details. This qualitative difference in appearance applies to the 12 m and 15 m SAR images. The 15 m images from the 1991 flight displayed a marked graininess in overall image texture relative to the finer textural appearance of the 12 m imagery. The graininess description applies equally to the 25 m imagery of 1991. This particular change in overall textural appearance was noted in imagery of a single SAR mission involving a newly commissioned sensor. It is possible that less-than-optimum system settings had been applied and consequently, could be adjusted on future missions. It is suggested that a controlled comparison of STAR-2 images from separate missions be considered.

Three types of EIF were interpreted from the data sources at hand. Their features were:

- Ice Island Fragments
- Multi-Year Hummock Fields (MYHF)
- Multi-Year Landfast Ice (MYLI) or Re-Entrant Ice

The latter term, Re-Entrant Ice, is used to describe the sea ice which adheres to the outer edge of shelf ice, remaining in place and developing in thickness over a period of years.

The ice island fragments identified have been described and illustrated in previous literature

and so were easily confirmed. The other EIFs are qualified as "probable" in the absence of any supporting data, either surface truthing or in the literature.

The following keys were developed for the three EIF types identified during the imagery analysis and should be considered in conjunction with Figures 7.2, 7.3, 7.4, and 7.5.

7.2.2.1 Ice Islands

Identified as II in Figures 7.2 to 7.5

SPOT Panchromatic Image (Figure 7.2)

- a) **Tone** is light grey, darker than surrounding ice floes.
- b) **Pattern** is distinct longitudinal banding due to the rolls of the ice surface, especially in July when the troughs of the rolls fill with meltwater. Each roll is distinctly visible, measuring approximately 350 m wide.
- c) **Shape** is elongate due to tendency to fracture parallel to the surface roll pattern.
- d) **Shadow** is an important diagnostic in identifying very small fragments of single rolls. The rounded fragment surface changes tone gradually as it rolls away from (or towards) incident light. The high freeboard of the fragment may also cast a thin black shadow on an adjacent floe surface.

STAR-1, 12 m pixel (Figure 7.3)

- a) **Tone** is lighter than surrounding floes (darker in negative) and darker than ridged deformed ice at floe boundaries (lighter in negative).
- b) **Pattern** is distinct longitudinal banding. Each roll of the fragment surface shows up distinctly.
- c) **Shape** is elongate.
- d) **Shadow** effect on the surface rolls is very distinct with the portion of the roll in the shadow of the incident radar beam showing as black (white in negative).
- e) **Size** of the smallest identifiable ice island fragment is approximately 2 km. Smaller fragments, had they been present, could also have been identified, especially if surrounded by relatively featureless ice. Experience with coarser resolution sources (see below) suggest that fragments measuring 500m can be identified.

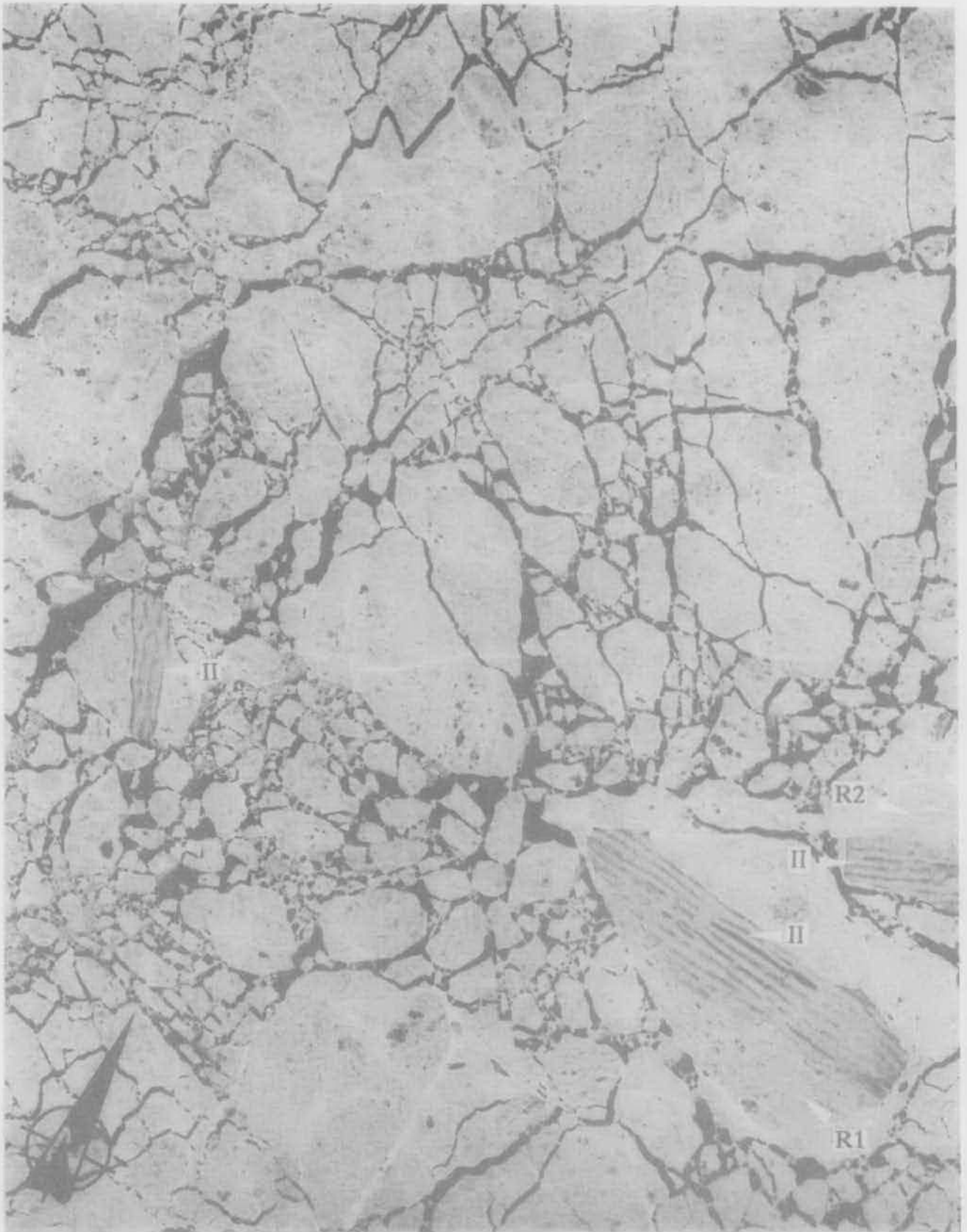


Figure 7.2: Detail of SPOT image of 27 July 1988. Scale is 1:225,000.

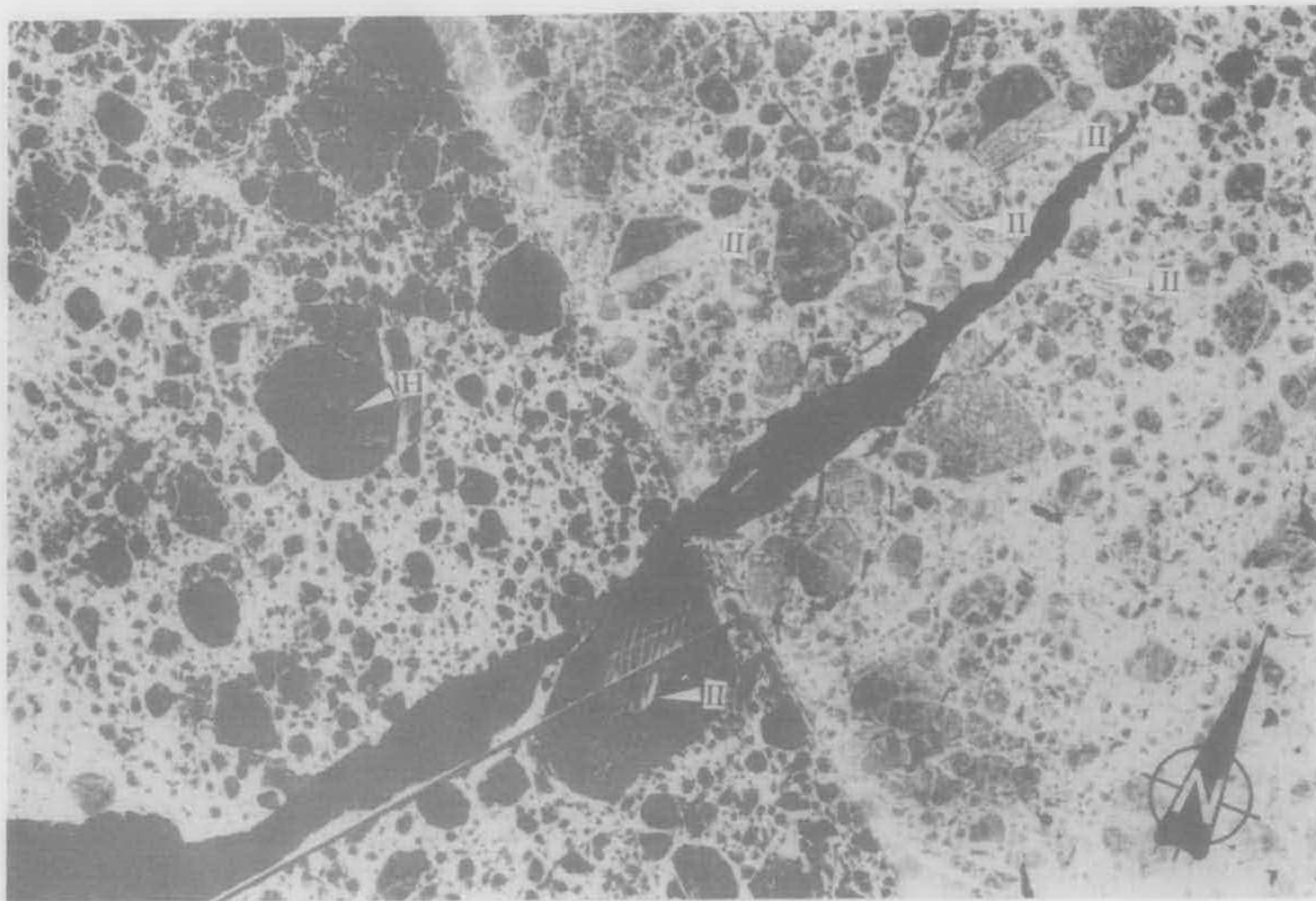


Figure 7.3: Detail of STAR-1, 12 m pixel image of 24 March 1989. Scale is 1:250,000.



Figure 7.4: Detail of STAR-2, 15 m pixel image of January 1991. Scale is 1:250,000.

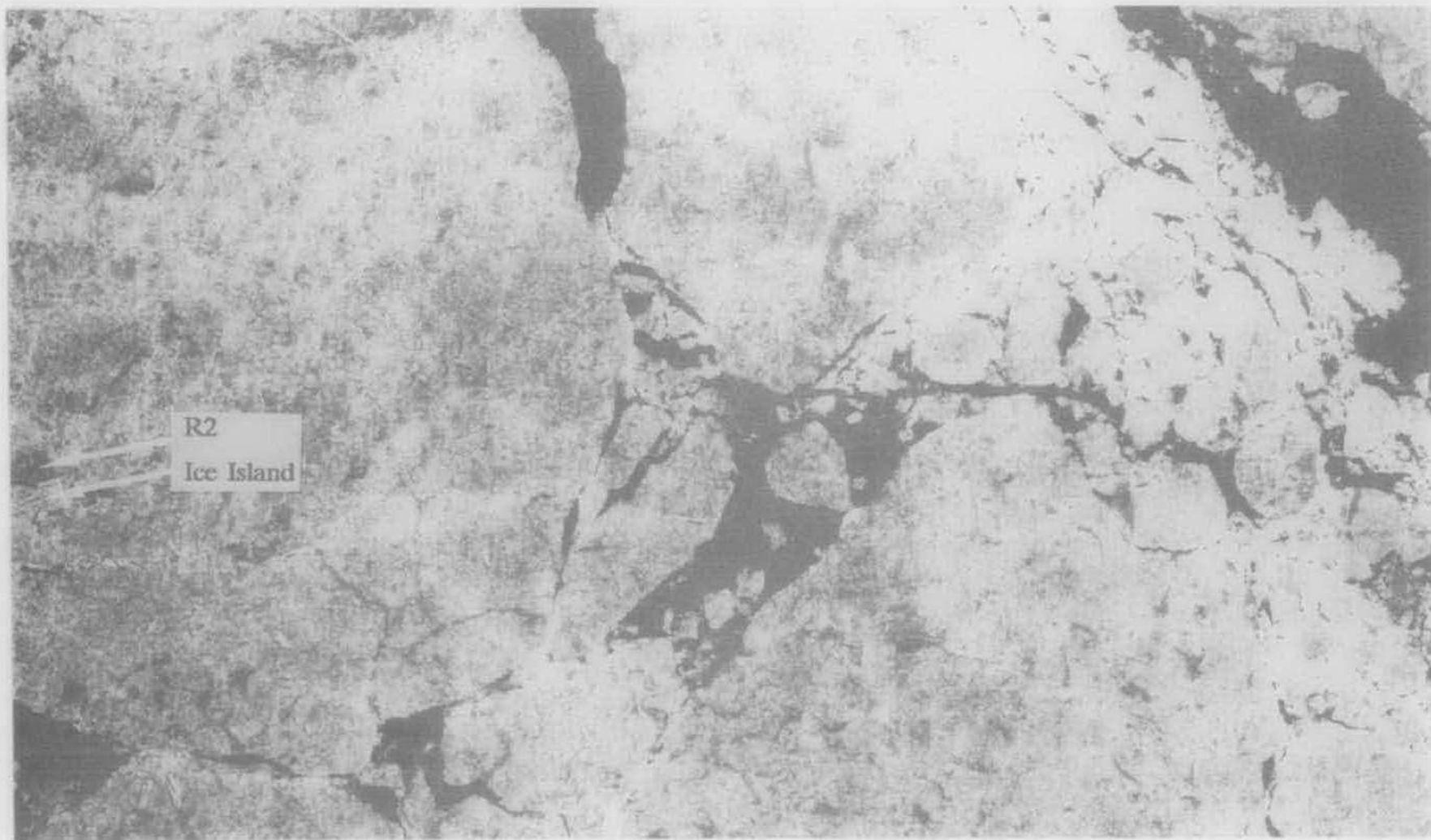


Figure 7.5: Detail of STAR-2, 25 m pixel image of January 1991. Scale is 1:250,000.

STAR-2, 15 m pixel (Figure 7.4)

- a) **Tone** is much lighter than surrounding floes (much darker in negative) and darker than ridged and deformed ice at floe boundaries (lighter in negative).
- b) **Pattern** is distinct longitudinal banding with individual surface features discernible.
- c) **Shape** is elongate.
- d) **Shadow** effect on surface rolls is distinct, with the portion of the roll in the shadow of the incident radar beam showing as very dark (very light in negative).
- e) **Size** limit (long dimension) of approximately 500 m (i.e. 2 mm at 1:250,000 scale).

STAR-2, 25 m pixel (Figure 7.5)

- a) **Tone** is much lighter than surrounding floes and darker than ridged and deformed ice at floe boundaries.
- b) **Pattern** is longitudinal banding with individual surface features discernible.
- c) **Shape** is elongate.
- d) **Size** limit (long dimension) likely to be in the 500 m range (i.e. 2 mm at 1:250,000 scale). Smallest fragment actually located measured 1500 x 300 m.

7.2.2.2 Multi-year Hummock Fields

Identified as target "H" in Figures 7.3 and 7.4.

SPOT Panchromatic Image (Figure 7.2)

- a) **Tone**, overall, is similar to that of surrounding floes and hence is not a diagnostic element.
- b) **Texture** is linear and especially evident in July when meltwater collects in dark-toned puddles on feature surface. No single linear element distinguishes itself.
- c) **Shape** can be rounded or straight-sided.
- d) **Associated** with surrounding rounded floes of old ice which form part of the overall EIF.

STAR-1, 12 m pixel (Figure 7.3)

- a) **Tone** is similar to that of surrounding floes, with addition of higher intensity spots

(white in positive, black in negative) distributed through the feature.

- b) **Texture** is linear with no single linear element distinguishing itself; overall appearance may be described as "fibrous" (see target "H" in Figure 7.3).
- c) **Shape** of individual feature not consistent. Often associated with round floes (see next key element, **Association**).
- d) **Associated** with surrounding old floes. Feature appears as inclusion within or attachment to such floes which, in turn, are usually rounded.

STAR-2, 15 m pixel (Figure 7.4)

- a) **Tone** is identical to that of surrounding floes, with sometimes perceptible higher intensity spots which contribute to texture.
- b) **Texture** is linear but not always discernible. Feature "H" on Figure 7.4 is the same target as feature "H" on Figure 7.3 yet does not display the characteristic linear texture as clearly. Nor does it display the ridges around the floe as clearly.
- c) **Shape** of individual feature not definable. Associated with rounded old floes.
- d) **Associated** with rounded old floes. Features are inclusions within or attachments to the floes.

STAR-2, 25 m pixel (Figure 7.5)

No multi-year hummock fields could be distinguished on the sample imagery available.

7.2.2.3 Multi-year Re-entrant Ice Fragments

Identified as targets "R" in imagery.

SPOT Panchromatic Image (Figure 7.2)

- a) **Tone** is identical to that of surrounding ice floes.
- b) **Texture** is coarse linear, approaching pattern; enhanced by dark areas of meltwater in July image.
- c) **Shape** includes one or more straight sides where fragment might previously have been attached to ice shelf (Targets "R1" and "R2" on Figure 7.2).

- d) **Associated** with ice island fragments which originated in the same area, i.e. Ellesmere Island ice shelves.

STAR-1, 12 m pixel (Figure 7.3)

- a) **Tone** is similar to that of surrounding ice, with spots of higher return picking out the feature texture.
- b) **Texture** is coarse linear, approaching pattern.
- c) **Shape** includes one or more straight sides where fragment might previously have been attached to ice shelf.
- d) **Associated** with ice island fragments which originated in the same area, i.e. Ellesmere Island ice shelves. Also associated with the area immediately offshore of the ice shelves and multi-year landfast ice of northern Ellesmere Island.

STAR-2, 15 m pixel (Figure 7.4)

Known re-entrant ice fragment (Target "R" on Figure 7.4) identified as such solely by association with large ice island fragment.

STAR-2, 25 m pixel (Figure 7.5)

Known re-entrant ice fragment (Target "R" on Figure 7.5) identified as such solely by association with large ice island fragment.

7.2.3 General Observations On SAR Interpretation

Basic Interpretation Keys

The most important element for interpreting EIFs on SAR is deemed to be "linearity". Both ice islands and re-entrant ice fragments develop a distinct pattern of waves and troughs on their respective surfaces. This pattern is shown up by reflected radar energy, particularly if it strikes perpendicular to the pattern. Densely packed, parallel hummocks will exhibit a linear radar "texture" in which individual, continuous, linear elements cannot be distinguished. This area of linear texture will be of a brighter tone than surrounding ice and adjacent features.

Features Orientation to Flight Line

In examining SAR for areas of linear pattern and texture, caution must be exercised regarding the line scanning pattern of the radar imaging system. In building of the SAR image, the reproduction equipment produces a faint system of regular lineations in the range direction of the image. A secondary background lineation also appears at right angles to the image scan. Possible EIFs which exhibit lineations parallel to the image edges thus become strongly suspect and may have to be rejected from further consideration. Apart from this problem, no difference in EIF recognition was noted between North-South and East-West SAR flight lines over the same area of ice.

Features in Near and Far Range

The near-range and far-range fringes of a SAR image should normally be removed from any study "interpretation" area. This is due to loss of floe detail related to excessive backscatter (near range) and insufficient radar returns (far range).

7.3 INTERPRETATION OF ARCHIVE SAR, 1988-1989

Prior to developing the SAR interpretation keys, a visit was made to the Ice Forecasting Centre, Ottawa, during which a search of the Centre's SAR archive was made. All segments of high resolution 12 m pixel SAR from the outer coasts of the Queen Elizabeth Islands were identified and examined for EIFs. The data acquired were those used in the Coast Guard Arctic Ice Atlases (De Bastiani, 1990) - items 3 and 8 in Table 6.1.

Initial interpretation carried out in Ottawa suggested numerous EIFs and in retrospect, overestimated the EIF population. Permission was obtained to procure copies of the relevant SAR negatives from Ice Centre and subject them to a more structured interpretation according to the keys. (The CCGS atlas (De Bastiani, 1990) could not be used for interpretation due to its small scale; the original larger scale data were required).

Twenty-three SAR segments were studied. The data had been acquired during the winter

months of 1988 and 1989 over coastal areas from Ellesmere Island to Prince Patrick Island. An additional STAR-1 mosaic from March 1989 was supplied from *CANATEC's* research files from a recent NRC project (Hill, 1990).

The interpretation keys, developed during the SPOT/STAR-2 intercomparison, were strictly applied to analyze the 1988 and 1989 data. An attempt was made to reduce interpreter bias by interpreting the segments in a random order. The idea was to confront the interpreter with succeeding images from different geographical areas and different time periods rather than allow him to group imagery according to where and when he felt extreme features should be found. The entire area covered by each SAR segment was examined.

A two-step interpretation process evolved. A SAR segment would be scanned visually for features distinctly different from their surroundings. Targets identified on the visual scan would be confirmed or rejected following examination at ten times magnification. A full SAR image was never subjected to a scan under magnification. Such an over-use of magnification would reduce the field of view needed to see the overall ice cover context against which a feature would be judged. It would also bring out too much lineation due to the SAR system's line scan which, in turn, risked obscuring actual feature texture.

In total, 155 possible EIFs were identified and noted on clear overlay sheets. The information noted on the overlays included the following:

- image date
- image identification number
- coastlines
- feature outline
- surrounding floe outline (if any)

Geographical locations of ice features were approximated by measuring distances from coastal headlands of known latitude and longitude. The long and short axes of these discrete

EIFs were also measured and noted. These axis measurements were input to a Quattro Pro spreadsheet file and scale factors applied to convert the on-image measurements to kilometres. Scales were determined for each SAR image by dividing the on-image distance between known geographical points into the calculated great circle distance between these points.

7.4 INTERPRETATION OF JANUARY 1991 STAR-2

The exabyte tape cartridge of the four high resolution (15 m pixel) lines of the 1991 AES STAR-2 round robin flight (see Fig. 5.1) was obtained and subjected to digital enhancement. Using facilities of Intera Technologies Ltd., optimum contrast data sets were generated, converted to photographic negative, and printed to 1:250,000 scale.

Unlike the 1988 and 1989 images, the preferred medium for interpretation was the positive print. Both negative and print, however, were of inferior quality to the 12 m imagery acquired with STAR 1 or STAR 2 in 1985 and 1988. Identification of extreme features in the 1991 STAR 2 data proved more difficult and less certain than with the earlier data, although the large ice island fragments present in both the 1988 and 1989 imagery were easily re-identified. (These fragments moved from 76 km due north of Ellef Ringnes island in 1988 to 18 km east of the northern tip of the island in 1989, then a further 3 km to the east in 1991. Floes containing dense hummocks, however, were identified only by previously gained knowledge of where they should be found. Floe definition within the consolidated ice cover of Peary Channel was not obvious in the 15 m resolution imagery (Figure 7.4). MYHFs known to surround identified ice island fragments could no longer be clearly identified.

Magnified examination of ice features was not beneficial because of the coarser photographic texture. At ten times magnification, the graininess of the photo image overwhelmed any texture or pattern that may have been present. Instances of linearity could only be located through an unmagnified visual scan of the image.

The 25 m STAR-2 (Figure 7.5) showed the general regions of old (generally light) and new (generally dark) ice, but permitted no detailed identification of ice surface features. Knowing the locations of the ice islands, the larger fragments could be seen, but it is questionable whether they would have been identified without this a priori knowledge. Identification of EIFs was not possible with the 25 m STAR 2 imagery.

CHAPTER 8

DATA SUMMARY AND ANALYSIS

8.1 INTRODUCTION

The EIF data obtained from the SAR and SPOT satellite imagery of 1988, 1989, and 1991 were subjected to statistical analysis of a descriptive and preliminary nature. The objectives of these analyses were to compare the new data (that from 1988, 1989 and 1991 imageries) with previously obtained data (presented in Section 4), and to expand the original data base given in Sections 4.

8.2 DATA TABLES AND MAPS

8.2.1 Tables

The EIFs data extracted from SAR and SPOT images of 1988, 1989, and 1991 were input to a micro-computer spreadsheet file. The sample shown in Table 8.1 represents the format used for the new EIFs database. The values for latitude, longitude, X and Y axis dimensions, and scale were derived from intermediate measurements and calculations. The entire "old" and "new" EIF data base listing is provided in Appendix C.

A spreadsheet application was selected over a full-scale relational database program because the amount of EIF data obtained is not extensive, the number of feature parameters measured from SAR sources is limited, spreadsheet application packages are more widely used and require a shorter training period to arrive at an acceptable level of user competence. In addition, the database handling functions, programming language, and plotting attributes of spreadsheet are sufficient to handle the type and volume of data in the EIFs database.

A brief description of each field of the EIFs database is given as follows: (refer to Table 8.1):

- a) Latitude, expressed in degrees.
- b) Longitude, expressed in degrees. Values in this particular database are

| Latitude | Longitude | Date | X-floe (km) | Y-floe (km) | X (km) | Y (km) | 1 cm= | Type | Comment |
|----------|-----------|--------|----------------|----------------|-----------|-----------|-------|------|---------|
| 78.2874 | -116.9787 | 880219 | 1.14 | 1.14 | 999.00 | 999.00 | 2.85 | HUM | |
| 78.4362 | -115.9755 | 880219 | 1.14 | 1.14 | 999.00 | 999.00 | 2.85 | HUM | |
| 78.4362 | -115.2043 | 880219 | 2.85 | 2.28 | 2.00 | 1.71 | 2.85 | HUM | |
| 78.6129 | -114.6221 | 880215 | 1.33 | 1.04 | 999.00 | 999.00 | 2.96 | HUM | |
| 78.7232 | -113.2614 | 880215 | 2.41 | 1.35 | 999.00 | 999.00 | 3.01 | HUM | |
| 78.8641 | -108.8044 | 880215 | 0.75 | 0.75 | 999.00 | 999.00 | 3.01 | HUM | |
| 78.8316 | -108.5784 | 880215 | 2.11 | 2.11 | 999.00 | 999.00 | 3.01 | HUM | |
| 77.8140 | -117.0401 | 890406 | 2.00 | 1.25 | 999.00 | 999.00 | 2.50 | HUM | |
| 77.6655 | -115.8592 | 890406 | 1.25 | 1.25 | 999.00 | 999.00 | 2.50 | HUM | |
| 77.7353 | -116.3526 | 890406 | 1.63 | 1.00 | 999.00 | 999.00 | 2.50 | HUM | |
| 77.8568 | -115.8755 | 890406 | 1.50 | 1.00 | 999.00 | 999.00 | 2.50 | HUM | |
| 77.7758 | -114.7824 | 890406 | 1.00 | 1.00 | 999.00 | 999.00 | 2.50 | HUM | |
| 77.7983 | -114.2442 | 890406 | 0.75 | 0.63 | 999.00 | 999.00 | 2.50 | HUM | |
| 77.7780 | -114.0684 | 890406 | 1.00 | 0.88 | 999.00 | 999.00 | 2.50 | HUM | |
| 77.6903 | -111.2278 | 890406 | 1.25 | 0.75 | 999.00 | 999.00 | 2.50 | HUM | |
| 77.6250 | -110.7063 | 890406 | 0.75 | 0.50 | 999.00 | 999.00 | 2.50 | HUM | |
| 78.2262 | -117.5713 | 890406 | 1.45 | 1.08 | 999.00 | 999.00 | 2.41 | HUM | |
| 78.2978 | -117.4140 | 890406 | 0.96 | 0.72 | 999.00 | 999.00 | 2.41 | HUM | |
| 78.2414 | -117.4068 | 890406 | 0.72 | 0.48 | 999.00 | 999.00 | 2.41 | HUM | |
| 78.3130 | -117.2243 | 890406 | 1.21 | 0.96 | 999.00 | 999.00 | 2.41 | HUM | |
| 78.1959 | -116.9431 | 890406 | 1.21 | 0.24 | 999.00 | 999.00 | 2.41 | HUM | |
| 78.2349 | -116.9845 | 890406 | 1.08 | 0.60 | 999.00 | 999.00 | 2.41 | HUM | |
| 77.5096 | -119.8409 | 890406 | 1.82 | 1.56 | 999.00 | 999.00 | 2.60 | HUM | |
| 77.5377 | -116.7443 | 890406 | 1.56 | 1.04 | 999.00 | 999.00 | 2.60 | HUM | |

Table 8.1: Sample of the extreme ice features data extracted from SAR imagery.
(Note: the entry "999.00" indicates "no data")

negative, being west of the 200 meridian.

- c) Date, expressed as a six-digit value, the digits standing for year, year, month, month, day, day.
- d) "X-floe", expressed in kilometres. This is the long dimension of an old ice floe surrounding, or attached to, the EIF. If such a surrounding floe was not detectable, the dimensions refer to the extreme feature itself.
- e) "Y-floe", expressed in kilometres. This is the short dimension with the same qualifications as d), above.
- f) X, expressed in kilometres, is the long dimension of an EIF inclusion in an old floe. The entry "999" was substituted when no data were found.
- g) Y, expressed in kilometres, is the short dimension of an EIF inclusion in an old floe. The entry "999" was substituted when no data were found.
- h) "1 cm=" is a scaling factor. The values in this field are expressed in kilometres and refer to the distance represented by 1 cm on the original source imagery. ("2.5 km" corresponds to a scale of 1:250,000).
- i) "Type" is a text string describing the EIF. Multi-year hummock fields are designated HUM, ice islands ISL, and re-entrant shelf ice REI. MYLF ice and ice plugs are not included as they are, after further consideration, not considered EIFs on their own.
- j) "Comments" is a field reserved for text which might be required to clarify some aspect of the data record.

With the possible exception of "Comments", any of the above fields may be keyed on by a database sort command in order to group records of a common feature type, time period, size, etc. The full table of 1988, 1989, and 1991 EIF data appears in Appendix C.

The database gathered from previous literature and described in Chapter 4 was entered into a similar, but separate, spreadsheet file for subsequent statistical analysis, and is also provided in Appendix C.

As discussed in Chapter 3, an EIF is an ice feature which causes a load of 300,000 tonnes on a 200 m diameter production structure. Such a feature is estimated to consist of a "thick ice floe" at least 500 m diameter, frozen into a "multiyear floe" with a diameter of at least 2 km. In this analysis both the "thick ice floe" and the "multiyear floe" were identified where possible; however, as noted in the Tables in Appendix B, this was generally not possible as indicated by the "999" (no data) notation in columns 5 and 6 of the Tables.

In the case of ice islands, one could readily identify the ice island or ice island fragment and, where applicable, the re-entrant or multiyear floe into which it was frozen.

In the case of MYHFs or extremely rough floes, the features were generally surrounded by first year ice or open water, and not frozen into a multiyear floe. Hence, the only "MYHFs" or "extremely rough floes" generally appeared as identifiable floes, but with no easily discernible multiyear floe surrounding them. Thus only the X-floe/Y-floe dimensions are quoted. In these cases, the EIF has the same dimensions as the "multiyear floe". In all subsequent analyses, the X-floe/Y-floe dimensions are used. Note that the "thick ice floe" dimensions (X/Y) are, in general, greater than 500 m, as this is about the limit of EIF detectability in the SAR imagery. It is noted that in no case was the "multiyear floe" size quoted without a corresponding "thick ice piece".

8.2.2 Maps

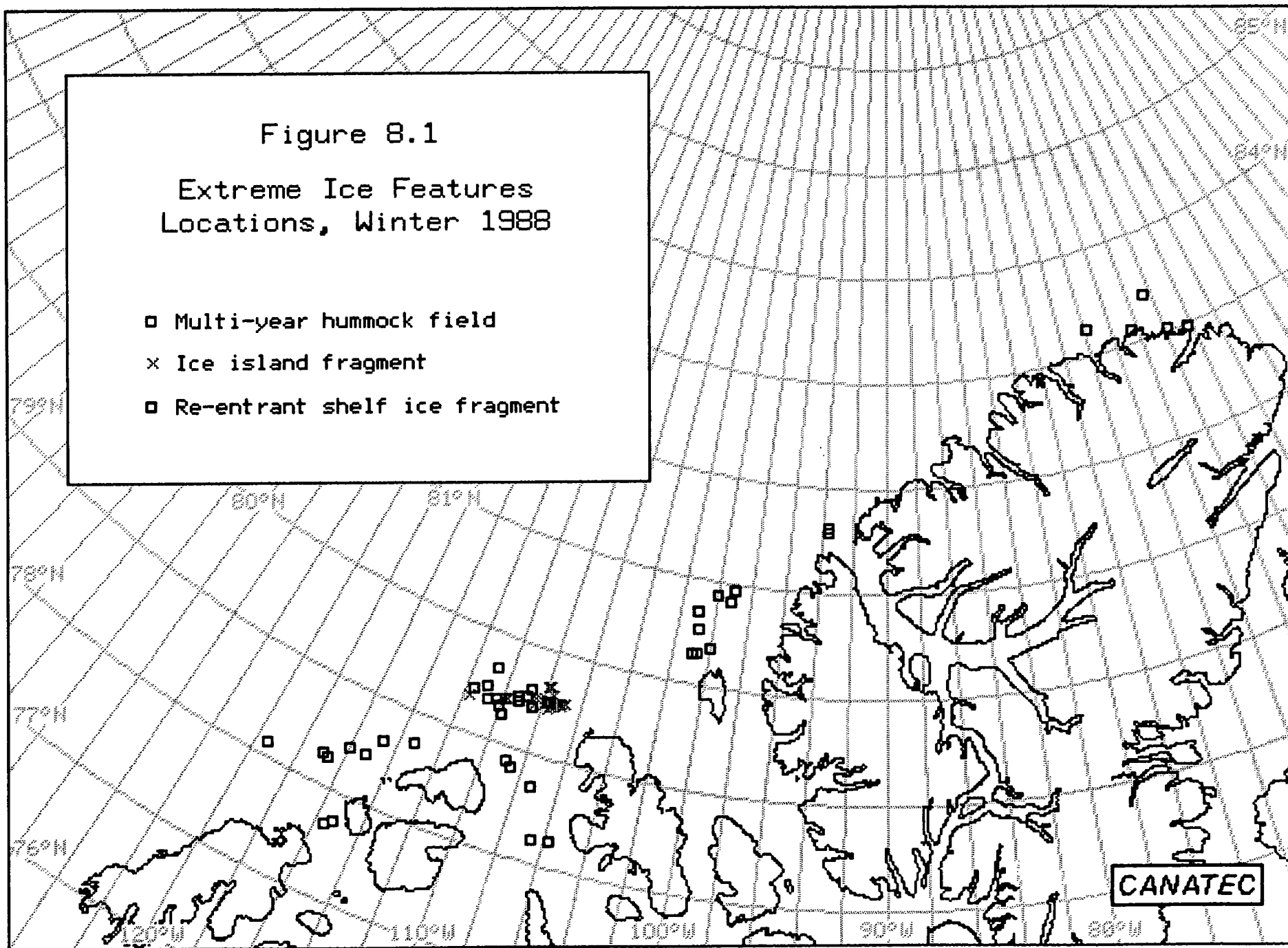
The 1988, 1989, and 1991 spreadsheet data file was converted to an ASCII file for import to a geographical information display system. Locations of the various EIFs were then plotted, by year, on base maps of the Queen Elizabeth Islands (Figures 8.1, 8.2, 8.3) to indicate the pattern of geographical distribution. A fourth map, combining all known feature locations for all years, was also generated (Figure 8.4).

Features identified as MYHFs were most plentiful along the southern half of the area covered, from the coast out to about 100 km offshore. Re-entrant shelf ice and old landfast ice fragments appeared more plentiful off the coasts of Ellesmere and Axel Heiberg Islands.

Figure 8.1

Extreme Ice Features
Locations, Winter 1988

- Multi-year hummock field
- × Ice island fragment
- ▣ Re-entrant shelf ice fragment



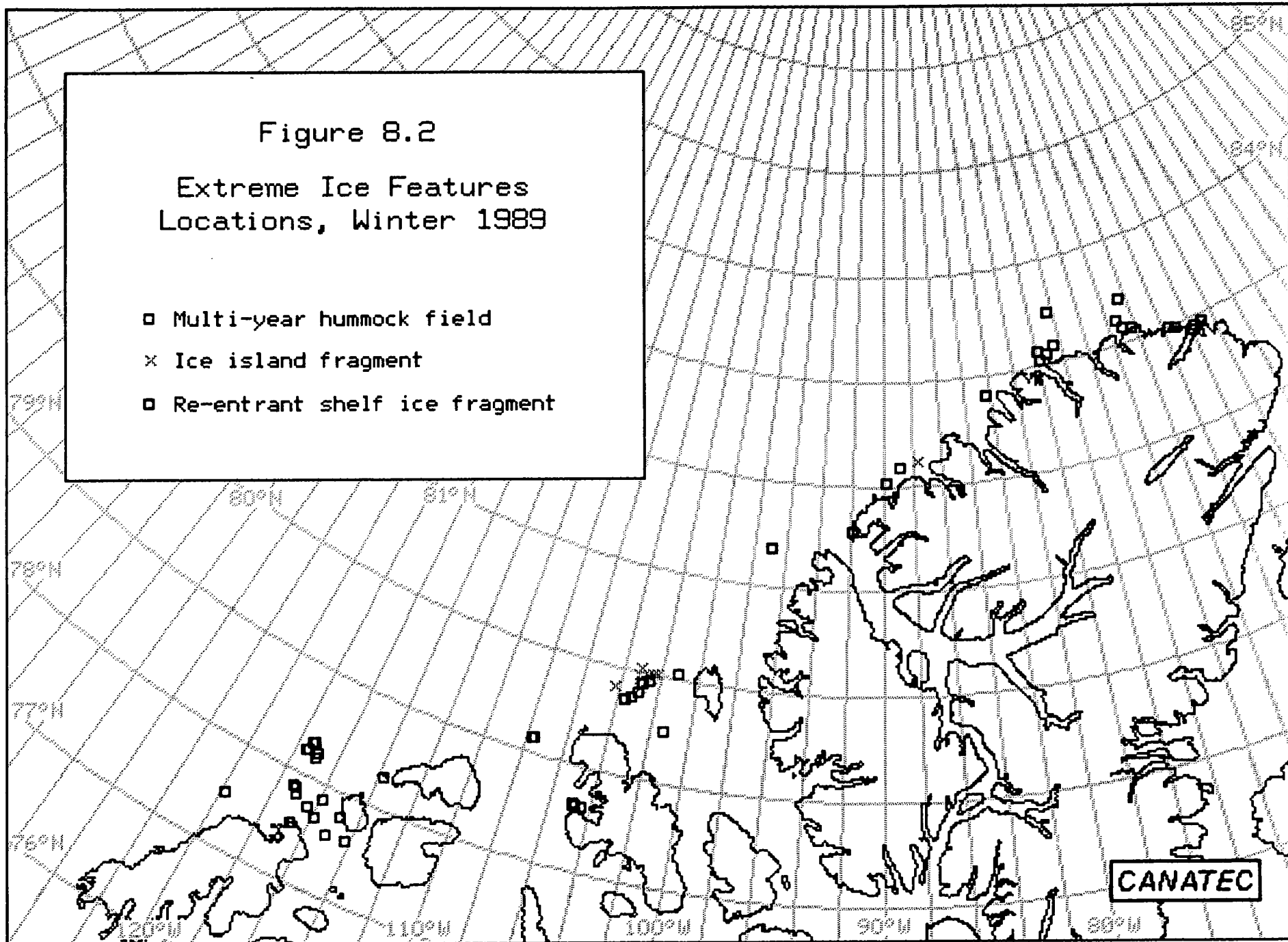


Figure 8.3
Extreme Ice Features
Locations, Winter 1991

- Multi-year hummock field
- × Ice island fragment
- ▣ Re-entrant shelf ice fragment

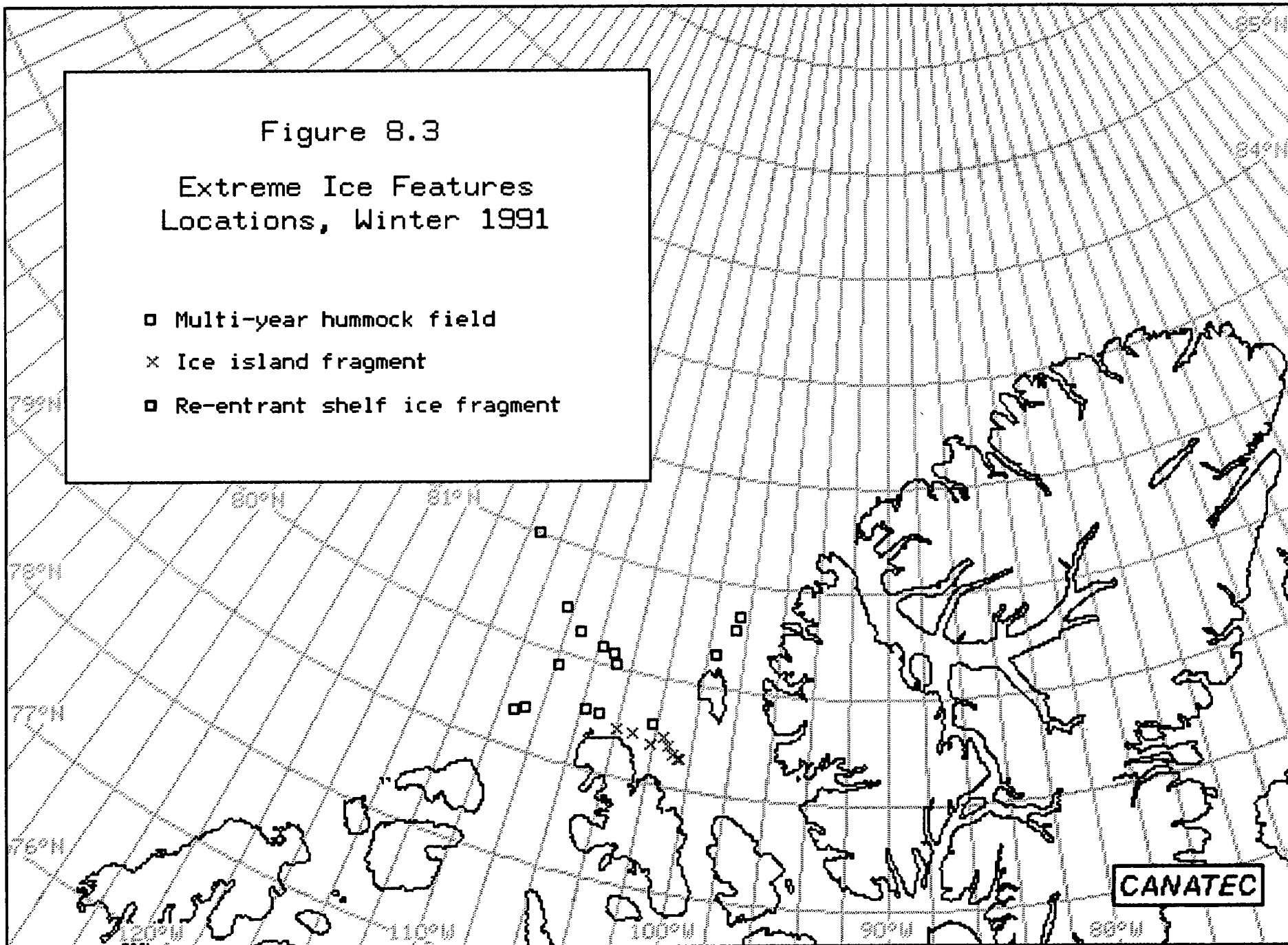
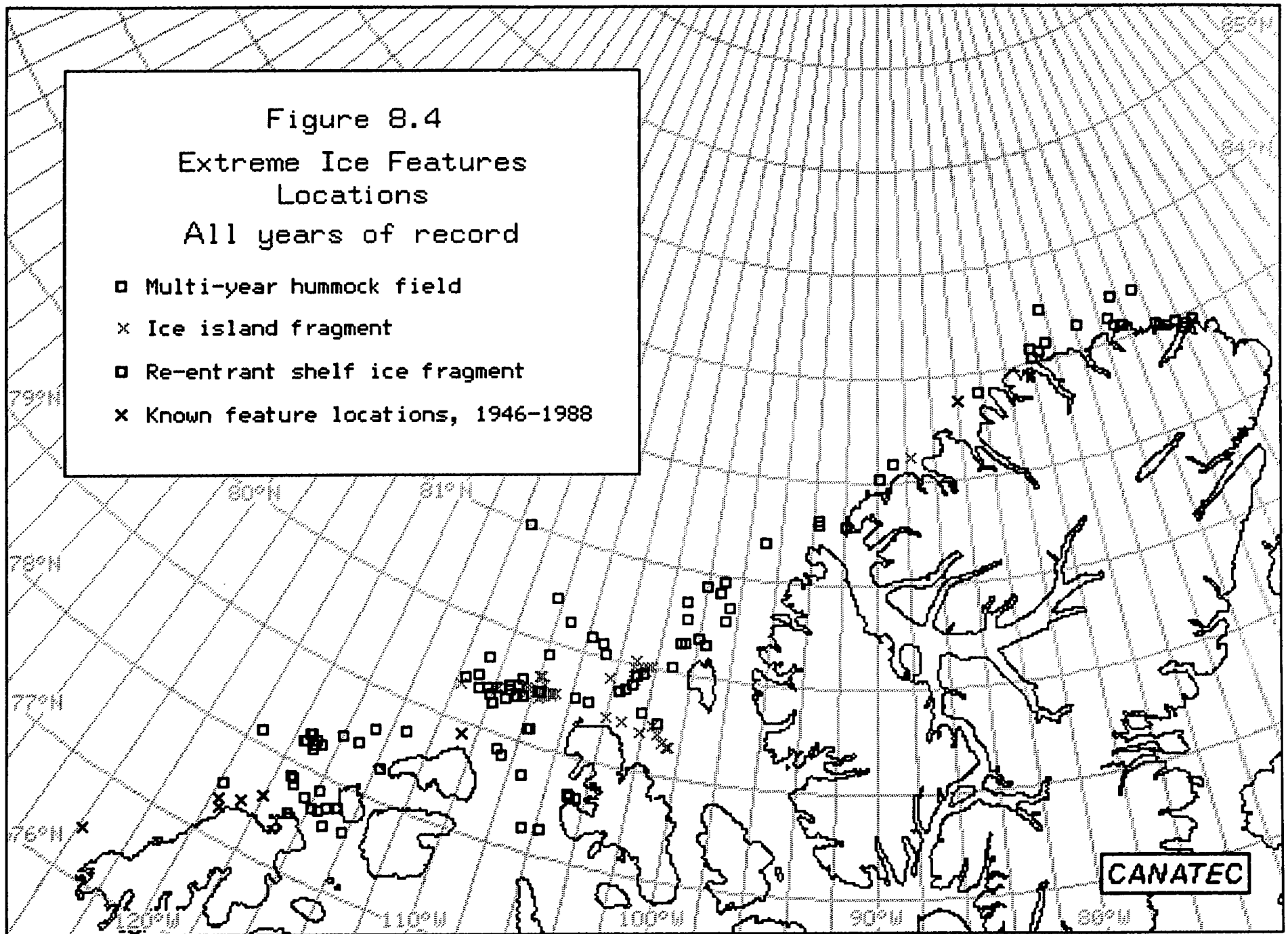


Figure 8.4
Extreme Ice Features
Locations
All years of record

- ▣ Multi-year hummock field
- × Ice island fragment
- ▣ Re-entrant shelf ice fragment
- × Known feature locations, 1946-1988



Ice island fragments representing the Hobson's Choice group, were concentrated off the north coast of Ellef Ringnes Island. There appeared to be a strong tendency for the MYHFs and re-entrant ice fragments to group near to their known areas of origin. The ice islands, results of episodic calving from the ice shelves of Ellesmere Island, are known to be transiting through the area of Ellef Ringnes Island at present and into the Sverdrup Basin, and as a result they will not be found in the same areas nor in the same concentrations in future years.

Towards the southern end of the Queen Elizabeth Islands, the offshore range of EIF locations appears to widen. It was noted during SAR analysis that there was a strong shearing pattern off Axel Heiberg Island, where the Beaufort Gyre makes a southward turn. Predominant ice movement would be towards the coasts in this region and so ice islands and re-entrant ice fragments would not drift far from the Ellesmere and Axel Heiberg coasts. The majority of MYHFs appear to be formed adjacent to the small island between Prince Patrick Island and Ellesmere Island. This would suggest that the peak shearing pressure is in this region presumably due to the dynamics of the pack.

Figure 8.4 also illustrated that EIFs can exit the southward movement of the Beaufort Gyre via Peary Channel, Prince Gustaf Adolf Sea, and Ballantyne Strait (Figure 1.1). However, escape via Sverdrup Channel and Nansen Sound is episodic since ice plugs in these waterways often persist for several years and prevent ice movement through the area.

8.3 ANALYSES

The EIF data sets obtained from the SAR imagery and from previous information were subjected to the following analyses:

- a) Feature size distribution
- b) Areal density
- c) Plot of major/minor axis ratio against feature size

In addition, a study of historical ice charts was carried out in order to ascertain the

likelihood of development and break-off of the multi-year landfast ice edge, which is the origin for many of these features.

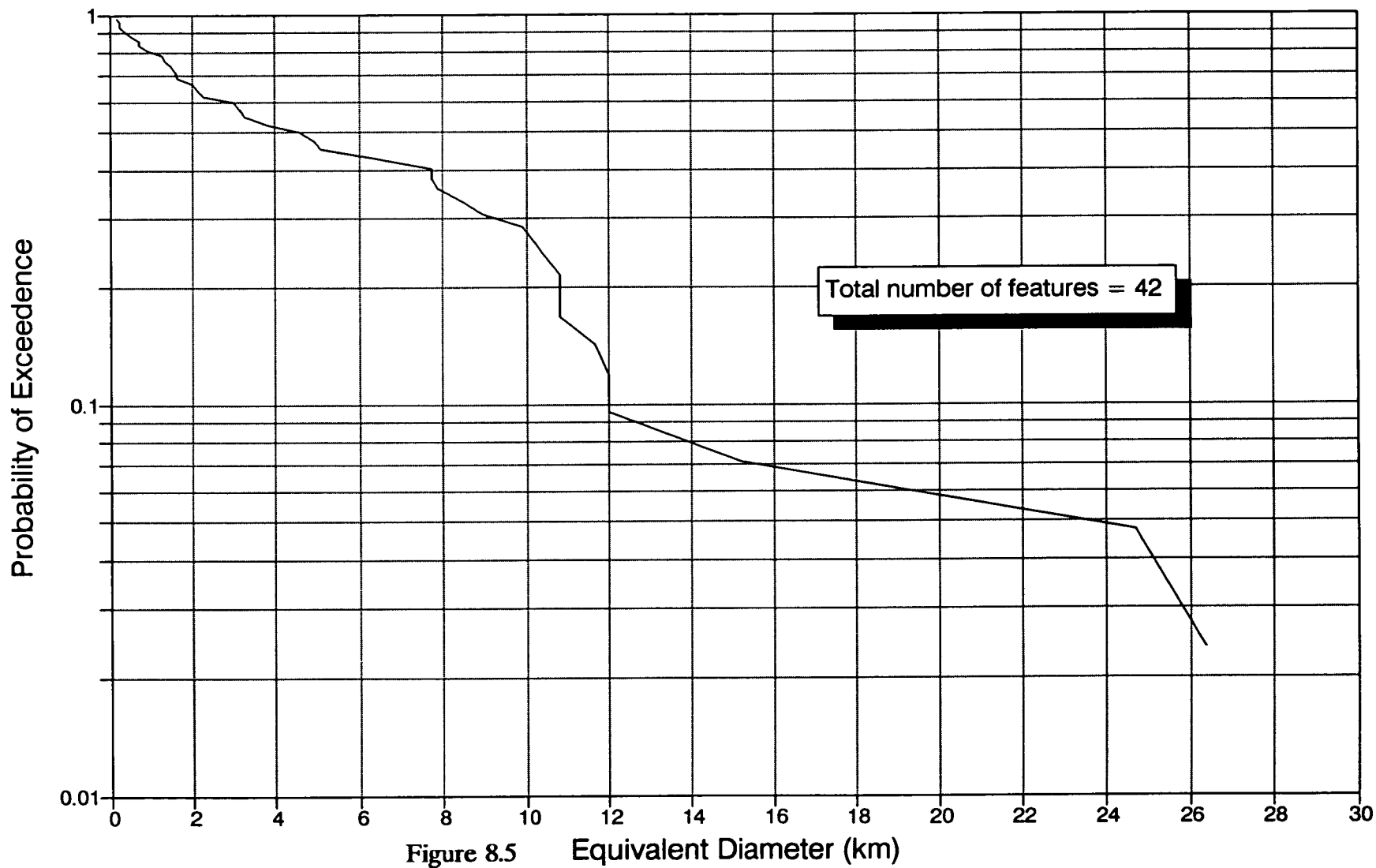
8.3.1 Feature Size Distribution

Probability exceedence plots were generated separately for the feature sizes measured during the current study and for feature sizes taken from previous literature (see Chapter 4). All EIFs, without distinction as to type, were plotted as shown in Figures 8.5 and 8.6. Feature size exceedence probabilities for multi-year hummock fields, ice islands, and re-entrant ice fragments are plotted separately in Figures 8.7, 8.8, and 8.9, respectively.

The feature size parameter used was the "equivalent diameter", which is the calculated square root of the product of a feature's major and minor axes. This basically assumes that the feature is elliptical; "equivalent diameter" being the diameter of a circle of equal area.

A comparison of the "all features" plots in Figures 8.5 and 8.6 brings out obvious differences between distributions of the 1988-1991 ("new") and the 1946-1988 ("historical") data sets. The historical data shows a wider range of feature sizes, with the largest exceeding 25 km equivalent diameter. The largest features in the new data did not exceed 8 km equivalent diameter. Large feature sizes in the historical data (essentially all of which are ice islands) also accounted for a greater proportion of the total sample. For example, ten percent of the historical data set (4 features only) exceed 12 km equivalent diameter, whereas the "top" ten percent of ice feature sizes from the new data set (15 features) exceeds 3 km equivalent diameter. Also, approximately 50% of the features in the historic data set are larger than the largest feature identified in the new data sets.

Exceedence Probability Plot Extreme Ice Features, 1946-1988



Extreme Ice Features New Data Sources

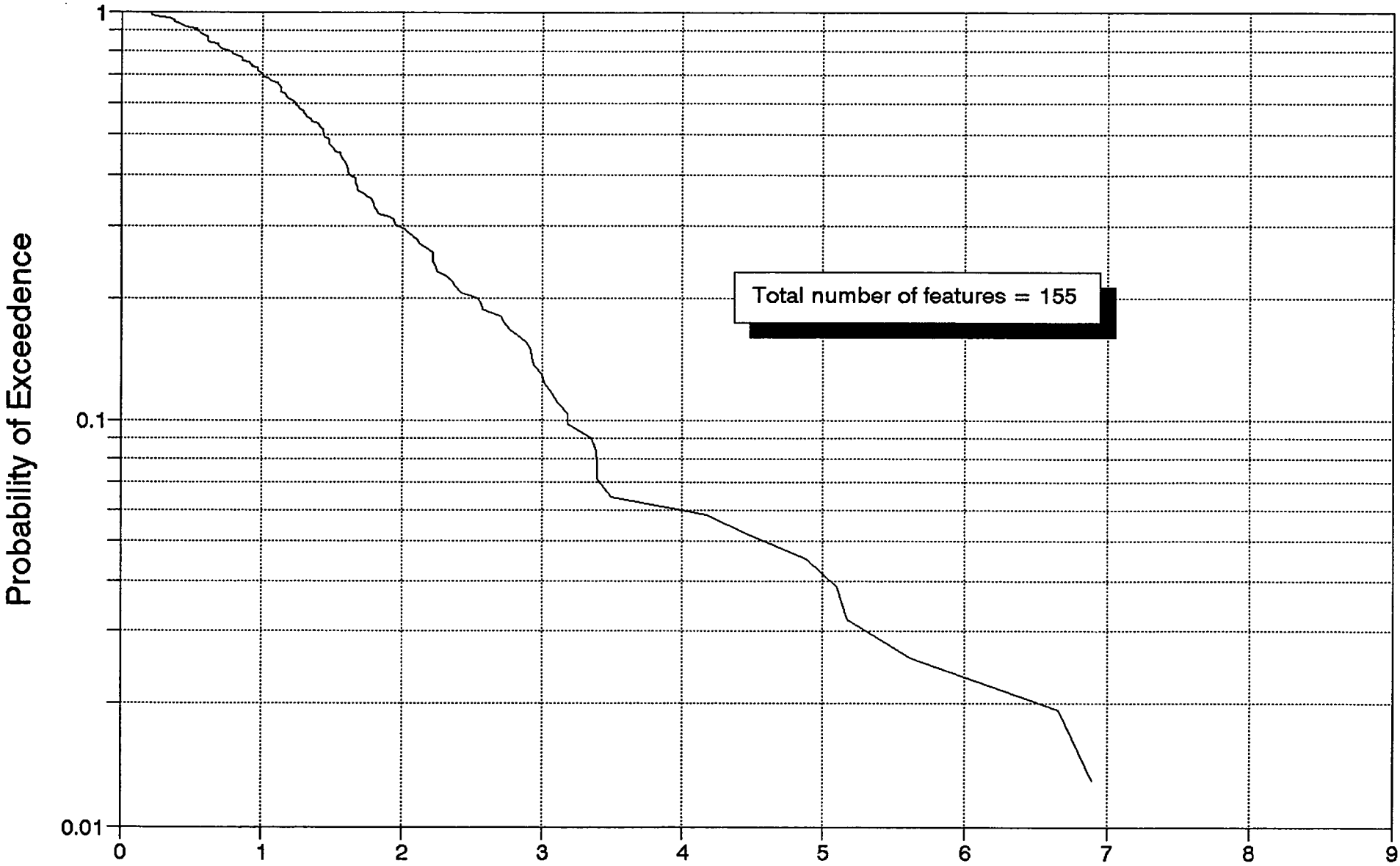


Figure 8.6

Equivalent Diameter (km)

Exceedence Probability, 1988-1991
MY Hummock Fields greater than 2 km

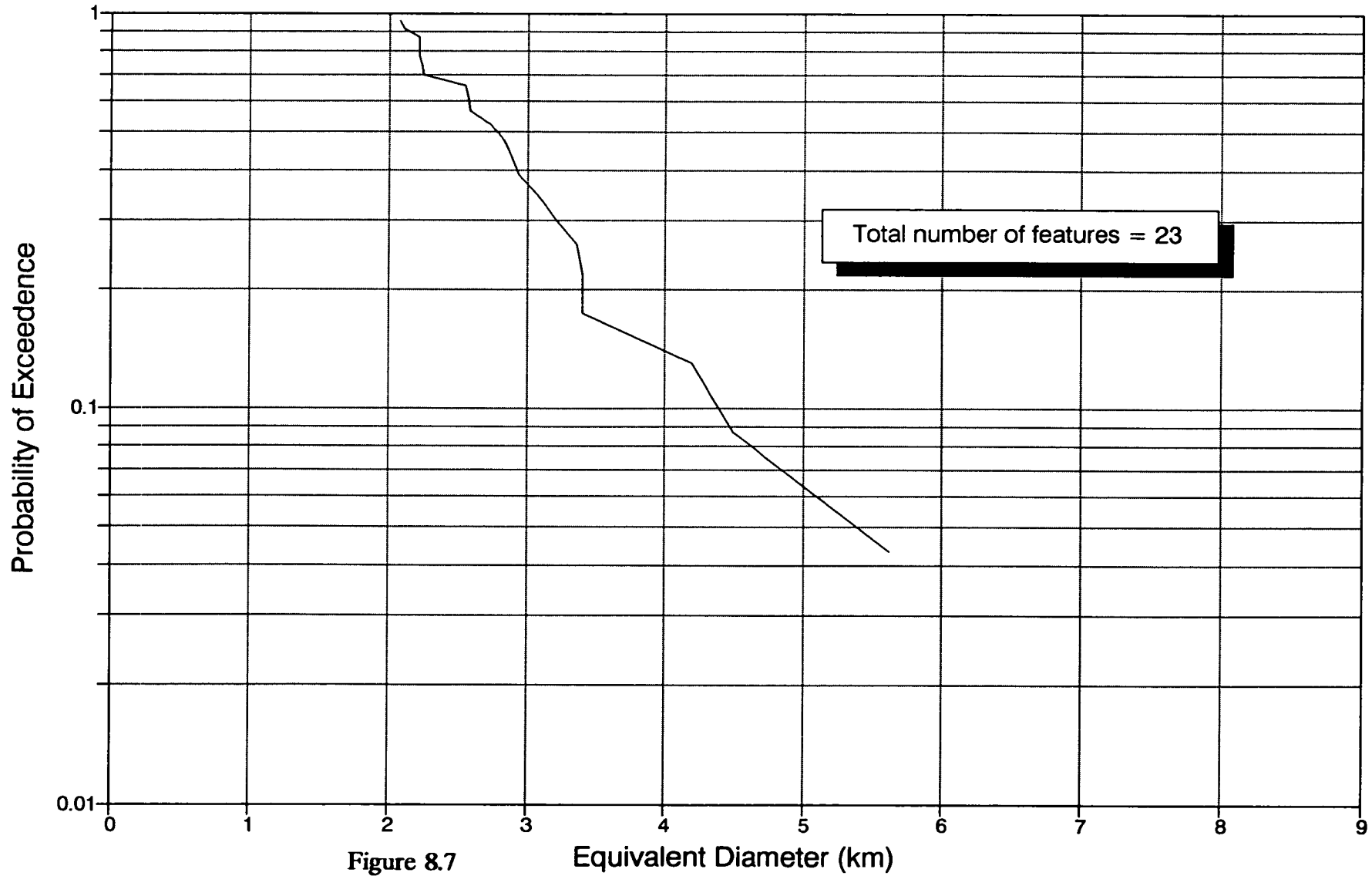


Figure 8.7

Exceedence Probability, 1988-1991
Ice Islands greater than 2 km

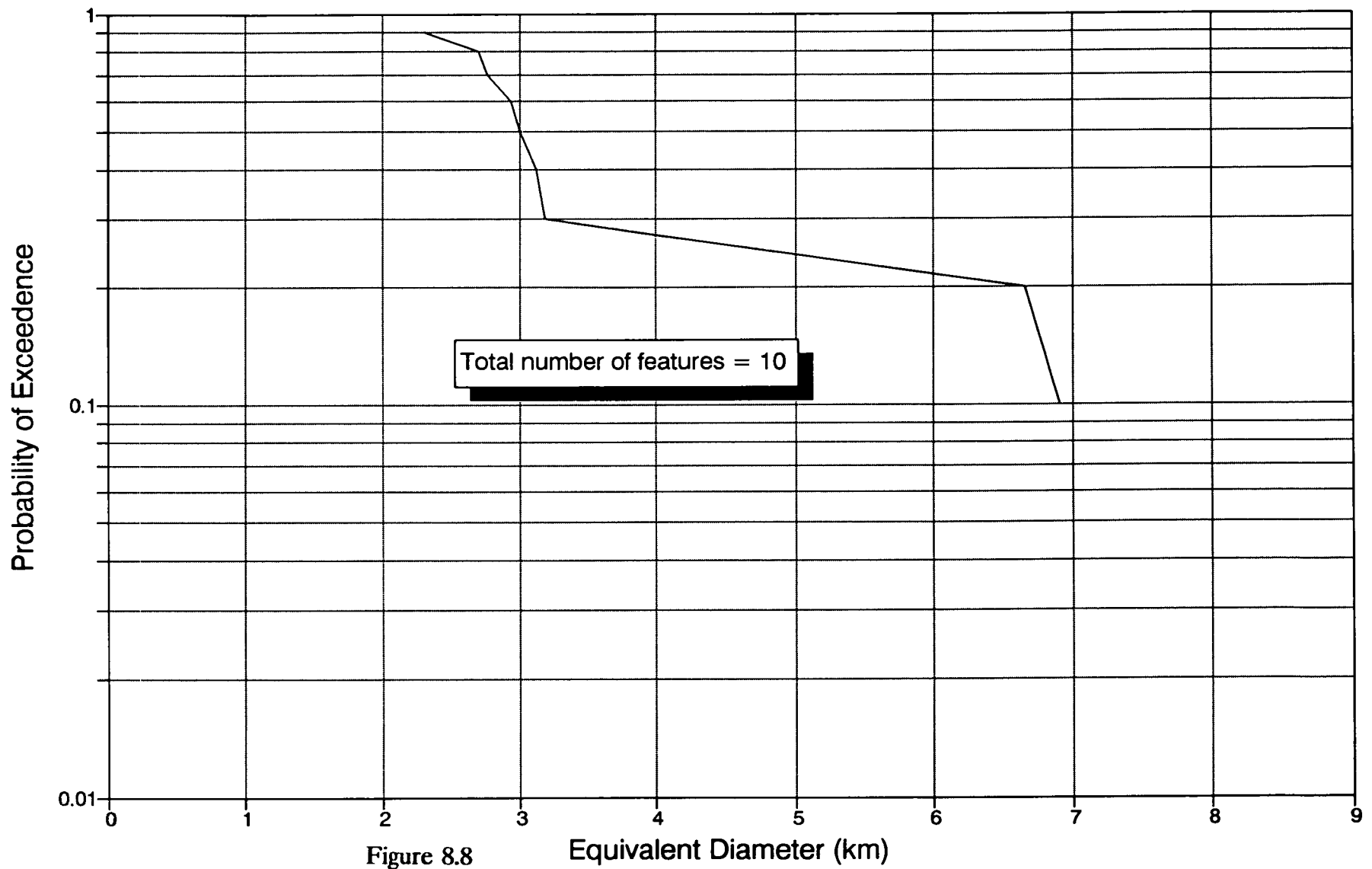


Figure 8.8

Equivalent Diameter (km)

Exceedence Probability, 1988-1991
Re-entrant Ice greater than 2 km

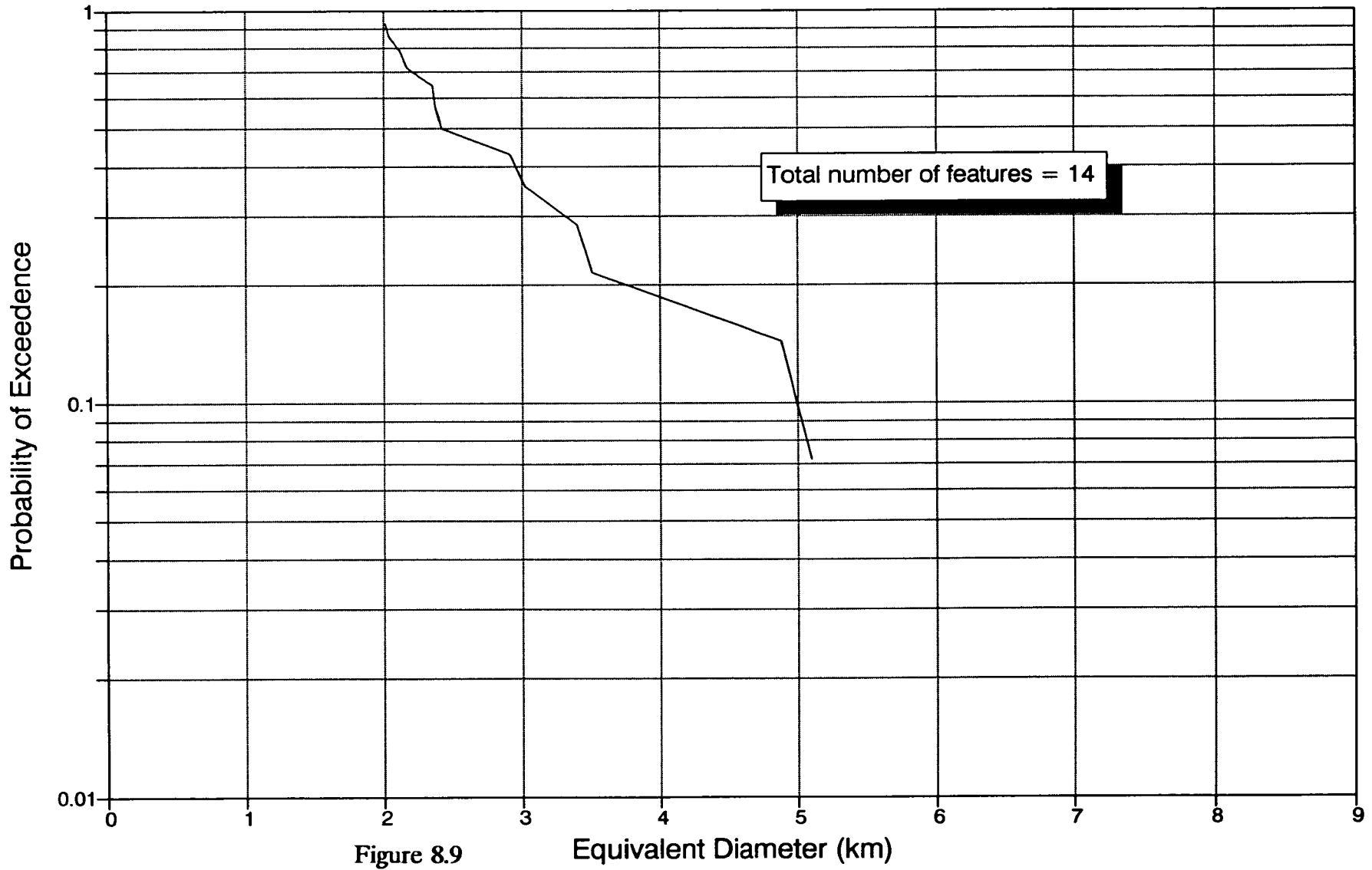


Figure 8.9

Equivalent Diameter (km)

Three factors explain the apparent discrepancies in what might otherwise have been expected to be comparable data sets.

- 1) The historical data were obtained from several sources of opportunity which span four decades. The sources were often concerned with a single type of feature, e.g., ice island or multi-year hummock field. The new data set is the result of a focused study of more regular regional-scale data sets spanning four years. All types of EIFs were specifically sought.
- 2) Following on from this factor of data collection methods is the second factor, which may be termed "selective data inclusion". The historical data set contains a high proportion of macro-scale features (10 km and greater equivalent diameter), especially ice islands. Several of the individual research initiatives from which the historical data were extracted were specifically directed to large size features stable enough to support on-ice research camps. Plus, the historical data were based to a large extent on relatively low resolution observations which generally permit identification of large ice islands and, possibly, very large MYHFs, plus field studies which deliberately selected the larger features.
- 3) Ice island history: The historical data contain information on the most prominent ice islands which appeared in the region over 40 years (e.g. the "WH" and "T" series). The new data, from a four-year period, cover a time of reduced ice island presence, does not include any of the "WH" or "T" ice islands, and in fact only Hobson's Choice ice island and its fragments were within the available data coverage.

Different data collection methods (e.g. visual from aircraft and low resolution SLAR), selective data inclusion, and a bias toward episodic event data in the historical data set suggest that it is not directly compatible with the newly acquired data set. Hence, these two data sets will be maintained as separate files.

8.3.2 Areal Density

Figures 8.1 to 8.4 show the distribution of the EIFs along the coast from Banks Island to the northern tip of Ellesmere Island. As is evident in Figure 8.4, the majority of EIFs are in the coastal waters off the Queen Elizabeth Islands. The ice islands and re-entrant shelf ice are in the region of the Peary Channel, which is where the Hobson's Choice ice island is located at this time. Over the next few years, the ice island and fragments will either move down through the Arctic Island's channels, and/or be driven back into the Beaufort Gyre and continue their passage south. Hummock fields appear to be more or less uniformly distributed in the coastal region from Prince Patrick Island to Ellef Ringnes Island. Adjacent to Ellesmere Island, the concentration of EIFs of all types is much less than further south. This is a result of the MYHFs forming predominantly in the coastal regions of the Queen Elizabeth Islands. Hobson's Choice, the largest ice island in the vicinity, its associated fragments and re-entrant ice happens to be in Peary Channel at present. The density of EIFs in this region is detailed in the following table:

Table 8.2: Areal Density of EIFs

| Year | Approx. Total Area of Imagery (km ²) | Approx. Area Off Prince Patrick I (km ²) | Number of EIFs | | Yearly Density of EIF off PPI 10 ³ km ² |
|--------|--|--|----------------|---------|---|
| | | | Total | Off PPI | |
| 1988 | 98,884 | 66,924 | 68 | 50 | .75 |
| 1989 | 92,600 | 42,506 | 64 | 41 | .99 |
| 441991 | 68,813 | 68,813 | 23 | 23 | .33 |

This table shows 114 EIFs off Prince Patrick Island (PPI) and a total area of 178,243 km². Hence, the density of EIFs is $6.4 \times 10^{-4}/\text{km}^2$. Note that many of the EIF may be the same ones from one year to the next.

Of these, 46 are greater than 2 km (Figure 8.7).

Hence, the density of EIFs greater than 2 km in size is $2.6 \times 10^{-4}/\text{km}^2$.

8.3.3 Major/minor axis ratio

Figures 8.10 through 8.12 show the ratio of long and short axes for the three EIF types plotted against equivalent diameters. It is evident that the larger features are essentially circular (i.e., X/Y axis ratio equal to 1), whereas the smaller features can be quite elongated.

8.3.4 Landfast Ice

Environment Canada weekly Composite series ice charts from the period 1974 - 1991 were examined (Figure 8.13) in order to assess the frequency with which old landfast ice breaks up and is released into the dynamic ice of the Arctic Basin. The geographical area presented on the Beaufort Sea charts did not extend north of Meighen Island. Thus, ice boundary break up off the outer coasts of Axel Heiberg and Ellesmere islands could not be assessed. By recording variations in the fast ice boundary, periods of significant fast ice release can be estimated. However, the very approximate positioning of the fast ice edge by AES is recognized and the results considered qualitative at best.

For each season of charts studied, two ice boundaries were recorded on separate base maps. The first boundary was the fast ice edge displayed on the first chart of a given season, usually in mid-June. The second boundary represented the minimum extent of landfast ice for the given season. It was determined by reviewing all of the charts for the season. In some years, it was a composite line since minimum fast ice extent in one area may have been preceded or succeeded by minimum fast ice elsewhere. From the resulting series of season boundaries, it was possible to roughly identify areas of fast ice which persisted throughout a given season and through consecutive seasons.

Trends in fast ice extent were inferred from the pattern of line-drawing used by the Environment Canada ice interpreters. A line of demarcation was always drawn along the outer coasts of the Queen Elizabeth Islands during the weeks of spring and early summer. Seaward of this line, over the Arctic Basin, ice concentration was, at most, 9+/10ths indicative of the polar pack ice regime and movement. Shoreward of this line, ice concentration was 10/10ths characteristic of the fast ice anchored by its grounded outer edge and the islands of the western Sverdrup Basin.

Shape vs Size, 1988-1991
MY Hummock Fields

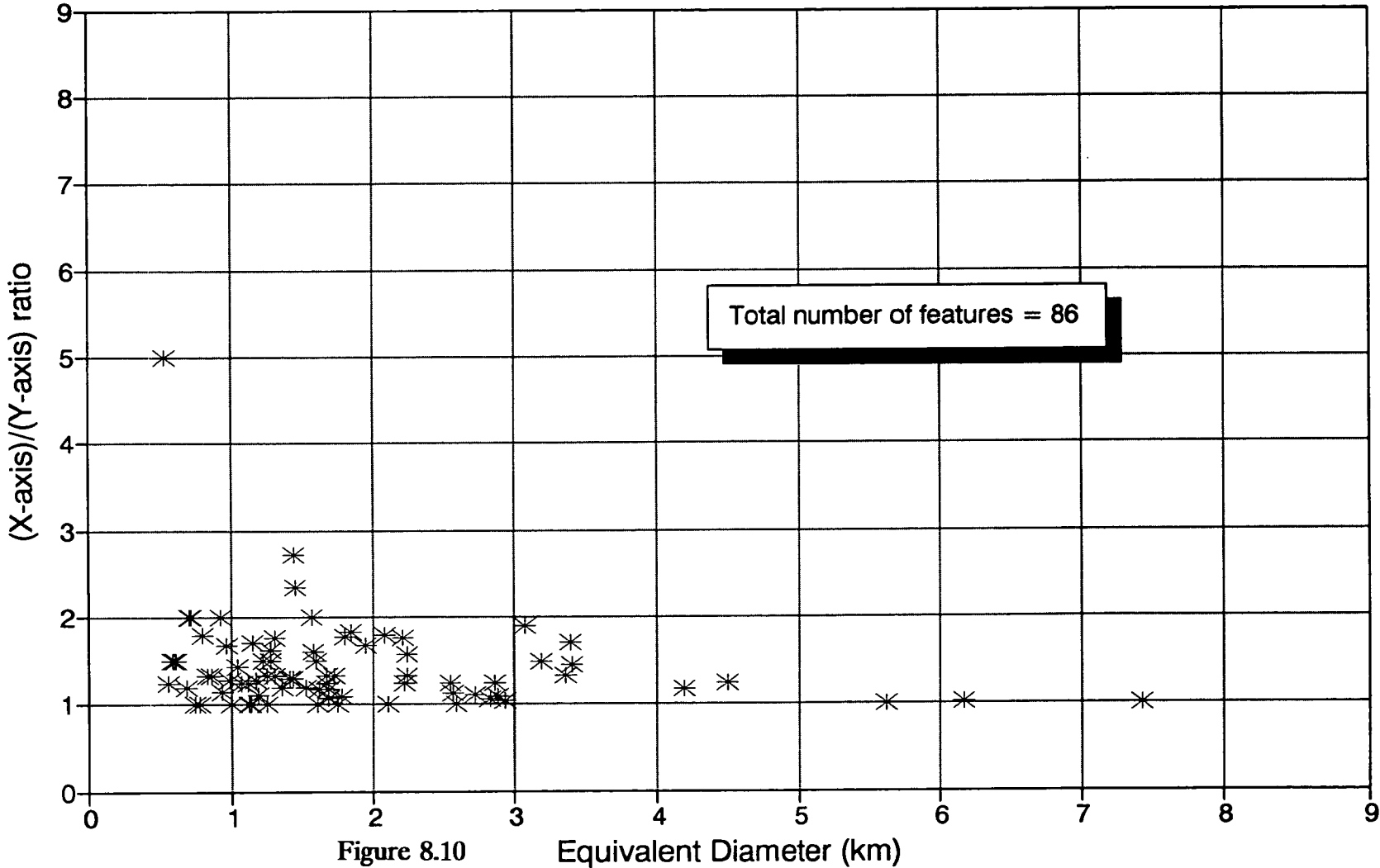


Figure 8.10

Equivalent Diameter (km)

Shape vs Size, 1988-1991 Ice Island Fragments

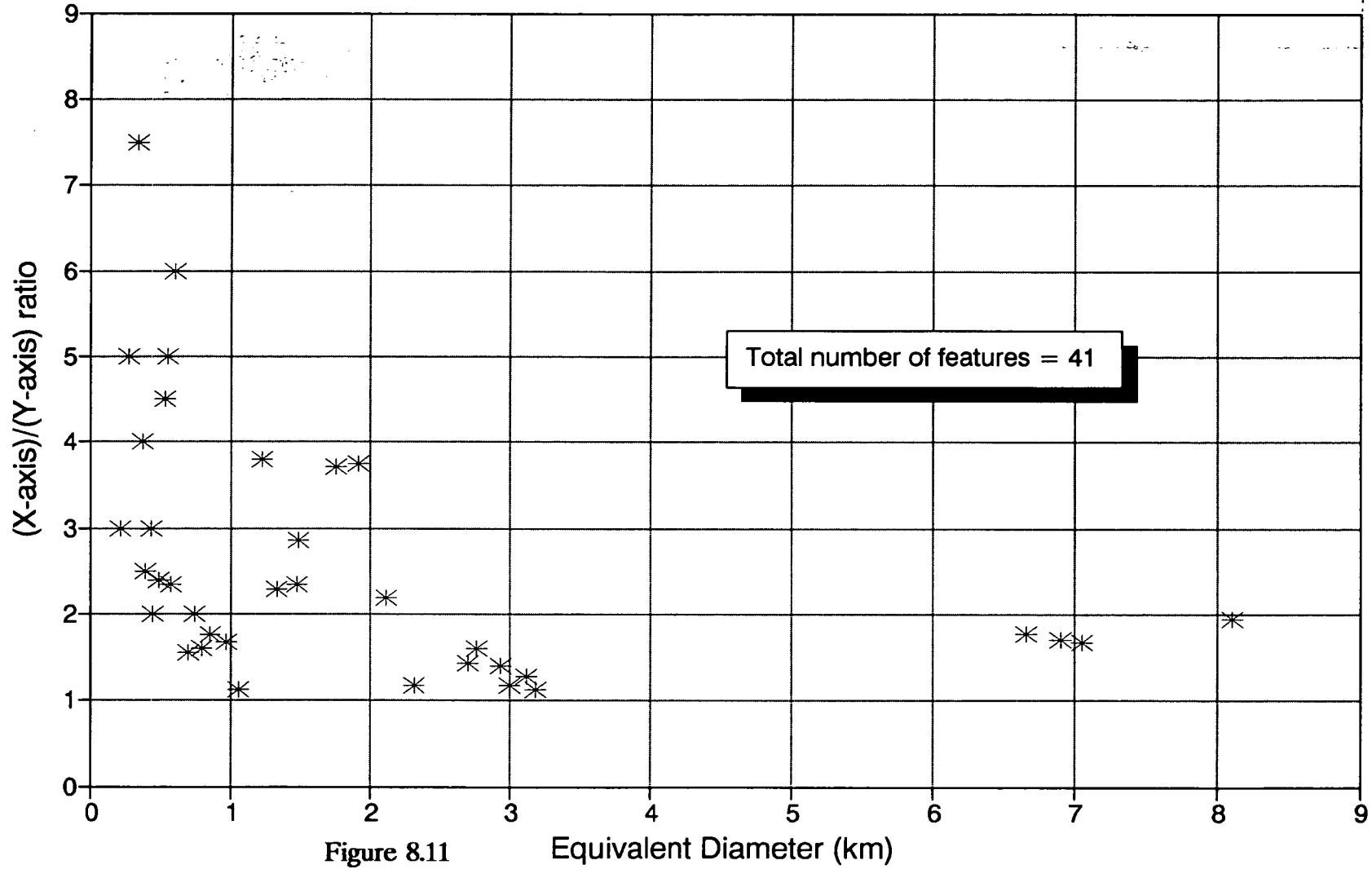


Figure 8.11

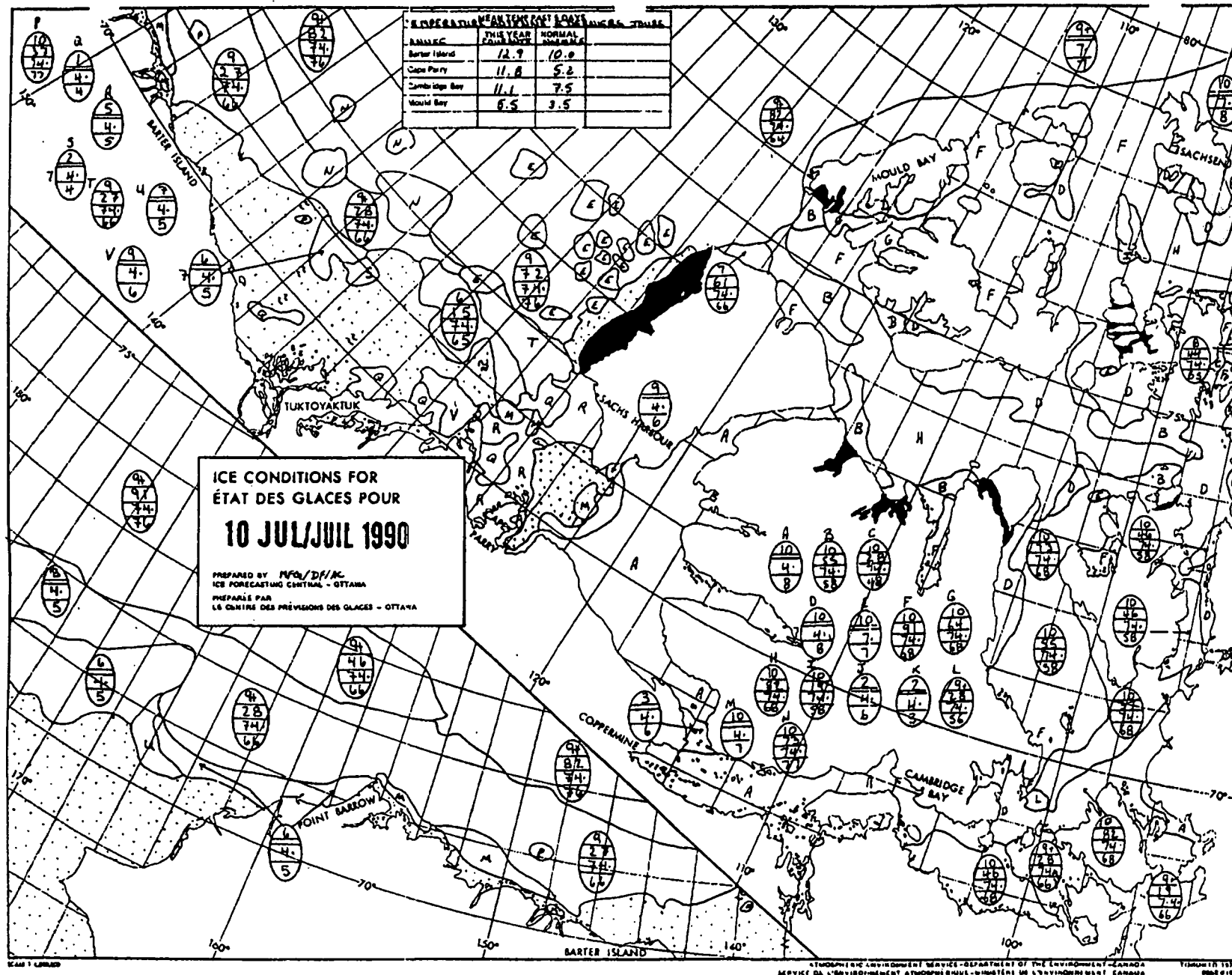


Figure 8.13: Detail of AES composite series ice chart used to monitor changes in fast ice limits.

In some years, this fast ice and the Sverdrup Basin ice would fracture and become mobile in the late September to early October period. During such periods, AES's charted line separating fast and mobile ice disappears in the channels connecting the Sverdrup Basin to the Arctic Ocean, i.e. Ballantyne Strait, Prince Gustaf Adolf Sea, Peary Channel.

The following three areas of recurring fast ice were evident from the analysis:

- a) The entire offshore band between Prince Patrick Island and Meighen Island.
- b) The Prince Patrick Island coast between Lands End and Cape Andreasen.
- c) The Borden Island coast between Cape Mackay and Cape Malloch.

These areas of fast ice are illustrated in Figure 8.14. A summary of inferred break-up appears in Table 8.3. This table shows the years when multi-year ice (i.e., ice with a minimum age of 2 years or more) broke off, for different coast line sections, and different ages of the multi-year ice. These breakups would result in more EIFs entering the polar pack.

Table 8.3: Inferred fast ice break-up along the outer coasts of the Queen Elizabeth Islands 1974 - 1991

| Minimum age of ice | Zone | | |
|--------------------|--------------------|------------------------------|---------------|
| | Archipelago Coasts | Prince Patrick Island | Borden Island |
| 2 years | 1980 1987 | 1977 1983 1985 1987 | 1989 1991 |
| 3 years | -- | 1980 (1992)* | 1980 |
| 4 years | -- | -- | 1987 |

* As of April 1992, the current Prince Patrick Island fast ice has been in place for past two seasons.

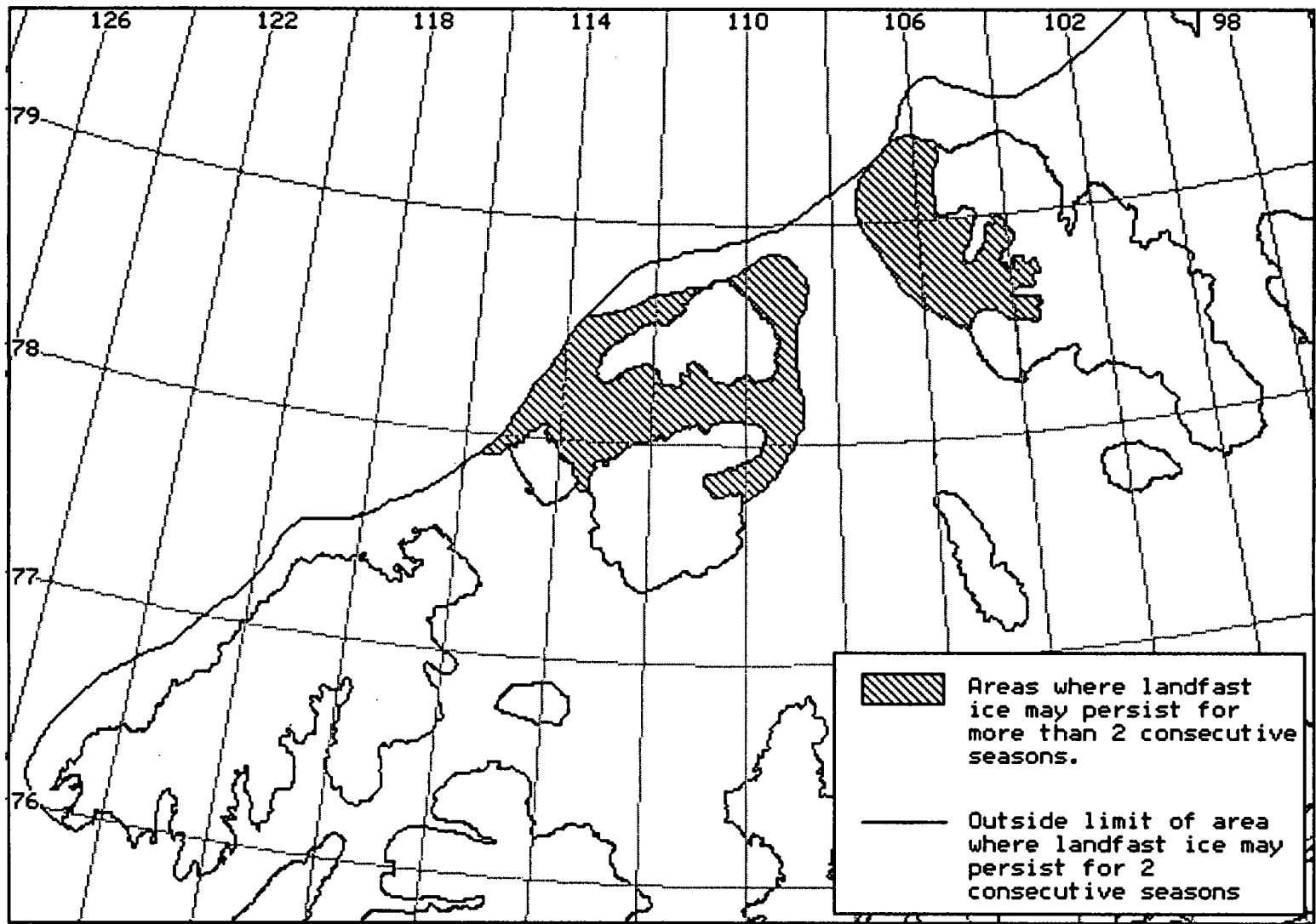


Figure 8.14 Multi-Year Fast Ice Extent

8.3.5 Ice Plugs

As indicated earlier, ice plugs were originally considered to be potential EIFs. However, after the review of EIFs indicated that these features must be 15 to 20 m thick, it became evident that ice plugs were not EIFs, since they never exceed 10 m in thickness. Hence, ice plugs were not investigated further in this study.

8.4 INTERACTION PROBABILITIES WITH EIFS IN THE SOUTHERN BEAUFORT SEA

8.4.1 Introduction

This section provides an estimate of the required density (features per 100 km²) of EIFs in the vicinity of Prince Patrick Island (the area investigated here), which would result in an ice feature-structure impact rate in the southern Beaufort Sea of 1 per year, 1 per 10 years, and 1 per 100 years. An estimate of the impact return period for the measured EIF density is also included. A calculation of this type is extremely difficult and subjective due to the many unknowns, and must be considered order-of-magnitude only.

8.4.2 Assumptions

There are three types of EIFs (i.e., ice features greater than 15 to 20 m thick within 2 km diameter floes): - *ice islands* which originate from the north coast of Ellesmere island, *re-entrant* ice which is formed from ridges and rubble and is attached to the outer edge of the ice islands and consolidated, and *multi-year hummock fields* which form predominately as rubble fields adjacent to the Queen Elizabeth Islands in the Beaufort Sea and consolidate with time. All three feature types move southward with the Beaufort Gyre, along the western edge of the Queen Elizabeth Islands and then westward through the southern Beaufort Sea area of interest. Thus, the density of extreme features in the area off Prince Patrick Island is related to the potential feature-structure impact rate in the Southern Beaufort Sea one or two years later. However, several poorly understood factors affect these EIFs and their density as they are transported into the potential production area to the south.

- i) As indicated earlier, many EIFs move out of the Beaufort Gyre via the channels between the Queen Elizabeth Islands. This effect is accommodated by f_i below.
- ii) The EIFs will break up and reduce in size on their passage south. Hence, if 2 km is the minimum size of an extreme feature of concern in the southern Beaufort Sea, one has to consider the density of larger features adjacent to Prince Patrick Island. There are no studies which address this question of size reduction. Hudson et al. (1980) note a reduction in the density of "extremely bumpy" features - identified as "rubble fields, MYHFs, and ice island fragments" by 80% between Prince Patrick and Banks Island, whereas Eley and Hudson (1982) measured no "extremely bumpy" features adjacent to Banks Island. "Bumpy" features - identified by Hudson et al. as ridged and old MY ice - suffer only a 35% reduction in density between Prince Patrick and Banks Islands.

As the distance between Prince Patrick and Banks Islands is only half the distance between Prince Patrick Island and the southern Beaufort Sea, there could be a further reduction by 0.2 in the EIF number density; hence, f_{ij} could be between 0.2 and $(0.2)^2$. De Poali et al (1982) (their Fig. 4.1), suggests that floes within 50 km of the North tip of Banks Island can spread out over about four times this distance when they travel west across the Beaufort Sea. Thus the number density of MYHFs greater than 2 km would probably reduce more than this as the MYHFs break up.

- iii) If we assume that the EIFs are uniformly distributed in the outer perimeter of the old pack ice, we can use the probability of old ice in the vicinity of the potential production sites to estimate the occurrence probability of EIFs. Danielewicz and Pilkington (1980) and more recent in-house data indicate that the probability of old ice occurrence is a function of the latitude. At a

longitude of 133° West, the percentage of the time that old ice is at a particular latitude is given by:

| Latitude | % Prob (f_{iii}) |
|----------|----------------------|
| 71° | 9 |
| 70.5° | 6.0 |
| 70° | 4 |

As the concentration of old ice in the pack off the Archipelago is typically 9+/10, these mean old ice concentrations take into account the probability of the ice moving southward into the production area and the resulting concentration decrease due to the ice spreading out. This spreading also decreases the density of EIFs.

8.4.3 Impact Rate

The impact rate of EIFs in the southern Beaufort Sea is:

$$N = (W + D) n V f_{ii} f_{iii} \quad / \text{ unit time}$$

where:

W is the structure width (=200 m)

D is the mean diameter of EIFs greater than 2 km diameter (=3,782 metres from data provided in fig. 8.7 to 8.9).

n is the density of EIFs over 2 km diameter at Prince Patrick Island (P.P.I.), also from Figs. 8.7 to 8.9.

V is the mean velocity of the gyre (=0.03 m/s)

f_{ii} is the reduction in the numbers of EIFs between P.P.I. and the southern Beaufort Sea (.04 to .2, see above)

f_{iii} is the probability that the pack will spread out over the production area with the resulting reduction in density of extreme features (4 to 9% - see above)

Hence

$$N = 0.2 - 0.98 n / \text{sec} (f_{ii} = 0.2; n \text{ in } /\text{m}^2) \text{ at } 70^\circ \text{ latitude}$$

$$= 6 - 31 n / \text{year} (n \text{ in } /\text{km}^2)$$

Return period $R \approx 1/N$ years

| Return Period (years) | Lat = 70° | Lat = 71° |
|-----------------------|----------------------------|---------------------------|
| | n(/km ²) | n(/km ²) |
| 1 | $3.2^{-16} \times 10^{-2}$ | $1.4^{-7} \times 10^{-2}$ |
| 10 | $3.2^{-16} \times 10^{-3}$ | $1.4^{-7} \times 10^{-3}$ |
| 100 | $3.2^{-16} \times 10^{-4}$ | $1.4^{-7} \times 10^{-4}$ |

These values of n represent the required EIF densities off PPI that would result in an impact every 1, 10, and 100 years at 70° and 71° latitude.

The measured value of EIFs adjacent to PPI is:

$$n = 2.6 \times 10^{-4} \text{ per km}^2 \text{ (see section 8.2.2)}$$

based on the 1988, 1989 and 1991 radar imagery data. Using the theory outlined here, the EIF return periods (calculated as the reciprocal of annual probability of impact) are thus about 123 - 615 years at 70° and 54 - 270 years at 71° for $f_{ii} = .2$ and $.04$, respectively.

If we use only EIF densities within 50 km of shore along the Queen Elizabeth Islands, we get a density of 6.0×10^{-4} , for return periods of 53 - 265 years at 70° and 23 - 115 years at 71°, for $f_{ii} = .2$ and 0.04 , respectively.

Hudson et al. (1980) identified "extremely bumpy" floes in aerial photography as MYHFs and ice islands. Very few floes were in this category - 48 adjacent to Prince Patrick island. No extremely bumpy floes greater than 1200 m in diameter were identified. Hudson et al. fitted the floe data to a negative exponential function which, when extrapolated to 2 km, indicates 3×10^{-5} floes/km². Note, however, that there are significantly more "bumpy" floes greater than 2 km (1.3×10^{-3}) and if any of these are MYHFs, this will seriously affect the statistics. Extrapolating results of Hudson and Eley (1982) (24 floes total) one gets 1.2×10^{-4} floes/km² greater than 2 km adjacent to Prince Patrick Island. Thus, Hudson et al.'s data span the data presented in the current study. These data cover an area which extends about 100 km out from the coast.

Hudson et al. only identified the MYHF or Ice Island and, as indicated, such features may not be EIFs unless they are attached to a large (greater than 2 km), thick multi-year floe. In winter when the ice surface is covered with snow (and hence white), it is difficult to determine the presence or size of any multi-year floe which might be frozen to a MYHF or ice island. SAR data, and also SPOT or photo imagery in summer, can identify such features. Thus many of Hudson et al.'s "extremely bumpy" floes may not have been EIFs.

De Paoli et al. (1982) quotes MYHF impact rates of 0.6 years at 71° and 3 years at 70° North, respectively, for MYHF's greater than 1 km. Fig. 8.7 indicates a decrease in EIF number density by a factor of six for a doubling in diameter of the feature; Hudson et al. (1980) reported a similar result. Thus the results presented in this study suggest an impact rate for MYHFs greater than 1 km of 4 to 9 years at 71° and 70°, respectively. These are 3 to 7 times longer than those reported by De Paoli et al.

CHAPTER 9

RECOMMENDATIONS FOR FUTURE DATA COLLECTION

9.1 GENERAL

The objectives of this project are to utilize SAR and other information sources to develop an EIF data base and provide guidelines for future data collection programs. Also, the data should be used for improved EIF impact rates. Recommendations are provided here for future SAR, aerial photography, and ground truthing programs. Data processing procedures are also discussed.

9.2 GENERAL SURVEY DETAILS

9.2.1 Area of interest

Figure 9.1 shows the area of interest. Both the 1980 and 82 air photo data and the new (1988-1991) SAR data reviewed here indicated that the EIFs tend to lie within 100 km of the shore. The data also indicate that the number of floes varies along the coast, with higher densities adjacent to the prominent land masses of the Queen Elizabeth Islands.

It is recommended that data collection be conducted along the entire coastline from Banks Island to Borden Island (Figure 9.1), as this region feeds the EIFs into the southern Beaufort Sea area. Our study shows that there are statistically significant variations in the numbers of features along this coast line, hence the entire area along the coast between Banks and Borden Islands should be covered to obtain the mean areal density of EIFs.

9.2.2 Frequency of Survey

It takes ice floes about 1½ to 2 years from Prince Patrick Island to the southern Beaufort Sea to travel this distance.

It is recommended that a flight along the region of interest should be conducted every two years to provide EIF statistics.

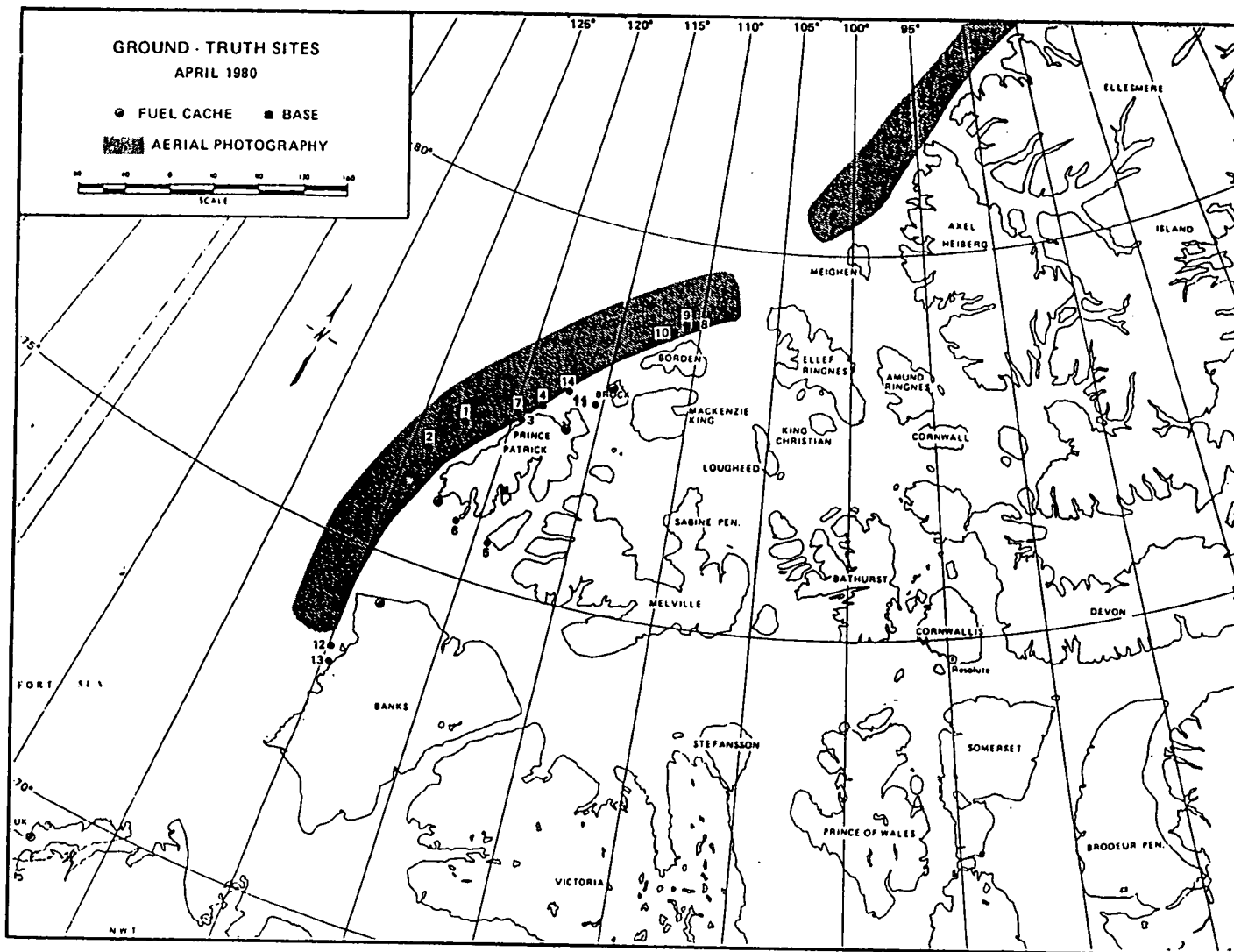


Figure 9.1: Area of interest for extreme ice features

9.3 SAR SURVEY (Aircraft /Satellite)

9.3.1. General

Sar imagery is clearly the method of choice, provided that guidelines are followed. Side-looking airborne radar (SLAR) and synthetic airborne radar (SAR) both penetrate cloud, fog, darkness, and provide a large area coverage, but only the SAR provides adequate spatial resolution for the detection of EIFs.

9.3.2 Resolution and Swath Width

This study has indicated that data of 12 m or better resolution (pixel size) is required for the detection of EIFs. The 15 m data from the STAR-2, obtained in January 1991, did not provide the level of ice surface information obtained from STAR-1 and STAR-2 12 m data. However, this difference in interpretability might be lessened or eliminated by further adjustment of the STAR-2 radar to optimize detection of EIFs (Intera, 1991, personal communication). With 12 or 15 m resolution data, the SAR swath is limited to about 50 km for STAR-1 and about 100 km for STAR-2.

It is recommended that the timing of the 15 m SAR setting on STAR-2 be optimized for the detection of EIFs. If no improvements are possible over the settings used in January 1991, the STAR-1 12 m SAR should be used for EIF studies.

9.3.3 Flight Path

In imagery reproduced in Canarctic (1990), the SAR aircraft flew over the Queen Elizabeth Islands into the nearshore regions of the polar pack. This flight path was found to be satisfactory. Multi-year hummock fields form with their ridges parallel to shore so, in principle, a flight parallel to the shore is more likely to identify the grounded features as the radar beam is perpendicular to the ridges. Once the MYHFs break off, they rotate and adopt a more or less random orientation, and a SAR flight along or perpendicular to the shore has an equal chance of picking up these features. However, one would still expect the MYHF texture to have a preferred orientation parallel to shore.

It is recommended that a SAR flight parallel to shore be carried out as such a flight would pick up more MYHFs than one perpendicular to shore.

9.3.4. Date of Flight

It is recommended that a SAR flight be conducted early to mid-winter, as this gives the optimum opportunity to recognize the various ice types and features. Also, the recent history of the ice of interest must be reviewed using NOAA or similar imagery, for the period prior to the SAR flight. In summer the ice surface is wet, which causes reflection (rather than scatter) of the radar waves.

In the fall, the new ice surface is often very rough due to wind or wave turbulence when the ice forms, resulting in high scattering of the radar, and an incorrect interpretation of the new ice. In early to mid-winter, when the ice is cold, these two problems are eliminated and the old ice (grey tone) is recognizable from the thin first year ice (very dark tone), and any open water (black tone). As indicated in Section 7.2, MYHFs and ice islands are also recognized by their shape and surface features (texture).

The interpretation keys to allow recognition of EIFs in SAR data are based on a comparison of SAR and SPOT data. **It is recommended** that these keys be verified by ground truthing or a simultaneous aerial photography program.

9.4 AERIAL PHOTOGRAPHY

9.4.1 Aircraft

Aerial photography is another method of obtaining information on EIFs. It generally provides good quality data with high resolution, and stereo photography also permits measurements of the height profile of the more prominent ice surface features. However, the disadvantages of this method are:

- it requires clear, daylight weather (no fog or cloud)
- should be carried out when the sun angle is fairly high, i.e. mid-summer in the Arctic

- relatively small aerial coverage - for useful aircraft altitudes - 3000 m for stereo and 6,000 m for non-stereo imagery, the size of the image is only about 3,000 and 6,000 m, respectively.
- it provides information on the surface features of the ice-ridges, etc., and the perimeters of the ice floes against open water or very thin ice. Except for surface features and floe shape, it does not distinguish multi-year floes from first year floes by their tone (colour), as the SAR does. Note that in SAR imagery one tends to identify "conglomerate multi-year floes", against the thick first year ice. Aerial photo images show the ice surface features, rather than floe perimeter, hence one tends to identify "single floes" within the conglomerate floes.

It is recommended that aerial photography be flown between April and October over the areas shown in Figure 9.1, to get optimum contrast, and mainly at 6000 m, no stereo overlap, to get optimum coverage. It is also recommended that some stereo coverage be obtained over the coastal area of Prince Patrick Island. As indicated earlier, simultaneous SAR and aerial photography would be invaluable to assist in verification of the SAR interpretation keys. DND has offered to collect aerial photography; this option should be pursued.

9.4.2 Spot Satellite

The SPOT satellite provides 10 m resolution imagery. These data have similar restrictions to aircraft photography, except that they do cover an area of 60 by 60 km.

Very few suitable images were obtained from a search of the SPOT data archive. However, this is because the satellite is only switched on by request in isolated areas.

It is recommended that SRI be requested to provide SPOT imagery for the area of interest along the coastal zone between Banks and Borden islands every summer. About 20 photos would be needed to cover the 600 km of coastline, from shore out to 100 km. (This would cost about \$20,000 which is less than a dedicated SAR flight). The ERS1 radar satellite

would likely be of little use due to its relatively poor resolution (30 m).

9.5 THE DATA

It is recommended that the data acquired be interpreted as outlined in Chapter 7 of this report. The resulting EIFs should be entered into the data base in the required format.

One of the major errors in calculating the EIF-structure impact rate in the Beaufort Sea is in the calculation of the numbers of features which reach the area from the coastal region of Prince Patrick Island and also the breakup of these features.

It is recommended that this be considered in more detail.

The EIF-structure impact rates are very approximate. **It is recommended** that an improved model be developed, as EIF impacts are a major design consideration.

CHAPTER 10

REFERENCES

AES, SAR Interpretation Manual, 1991

Arsenault, L.D., 1981a "The Current Extent Of The Ice Shelves Of Northern Ellesmere Island" CRRS 8114 Submitted to Dome Petroleum Limited (Referred to as 1981a)

Arsenault, L., 1981b, "SLAR and LANDSAT Measurements of Sea Ice Features off Prince Patrick to Ellef Ringnes Islands", CRRS Report 8113 to Dome Petroleum

Barton, R.A. and Croasdale, K.R., 1973, "Probability of Ice Islands Colliding with Fixed Offshore Structures in the Southern Beaufort Sea", (Part of APOA Project Imperial Internal Report IPRT-2ME-73).

Bercha, F.G. & Assoc. 1982 "SLAR Local and Regional Investigation of Katie's Floeberg 1981" Report for Gulf Canada Resources Ltd. July 1982

Cammaert, A.B., and D.B. Muggeridge, 1988, Ice Interaction with Offshore Structures, ed. by Van Nostrand Reinhold.

Cornett, S. 1987 "Beaufort Gyre Ice Trajectories" in Workshop on Extreme Ice Features Nov. 1986, NRC Technical Memorandum 144, June 1987

Crary, A.P., "Arctic Ice Island and Ice Shelf Studies"

a) Part I, Arctic, Volume 11, no. 1, pp. 3 - 42, 1958

b) Part II, Arctic, Volume 13, no 1, pp. 32 - 5, 1960

Croasdale, K.R., 1986, Extreme Ice Features - Structure Interaction, in Workshop on Extreme Ice Features, November 03-05, 1986, Banff, Alberta.

De Bastiani, P. 1987 "Canadian Arctic Marine Ice Atlas Winter 1986/87" Report for Canadian Coast Guard Northern, Transport Canada Report No. TP-8318-E

De Bastiani, P. 1990, Canadian Arctic Marine Ice Atlas - Winter 1987/88 with perspectives from 1987/87 and 1988/89, Atlas prepared for Canadian Coast Guard Northern Transport Canada Report No. TP-10224, Ottawa, March 1990

De Bastiani, P., (Government of NWT), 1990, Personal Communication

De Paoli, S., T.B. Morrison, R.W. Marcellus, 1982, " Analysis of Interaction Probabilities Between Large Ice Features and Offshore Structures in the Canadian Beaufort Sea" Report to Dome Petroleum and EIS Partners, Nov. 1982

- Dickins, D.F. 1982a "Multiyear Ice Floe Survey Data Report" report for Gulf Canada Resources Inc., May 1982
- Dickins, D.F. 1982b "Multiyear Thickness Distribution in the Beaufort Sea" report for Gulf Canada Resources Inc., Dec. 1982
- Eley, J., and R.D. Hudson, 1982, Multiyear Floe and Hummock Field Survey in the East Beaufort Sea, April 1982 Report for Canada Resources Ltd.
- Hattersley-Smith, G., "The Ward Hunt Ice Shelf - Recent Changes in the Ice Front", J. of Glaciology, Volume 4, no. 34, pp.413 - 242.
- Hattersley-Smith, G., "Note on Ice Shelves off the North Coast of Ellesmere Island", Arctic Circular, Volume XVII, no 1.
- Hibler, W.D., 1980, Modelling a Variable Thickness Ice Cover, Monthly Weather Review, Volume 108, No. 12, Dec. 1980.
- Hill, M.C., 1990, "Ice Interpretation, Queen Elizabeth Islands", February - May, 1989, for NRC
- Hudson, R.D., M. Metge, G.R. Pilkington, B.D. Wright, D. McGonigal, D. Schwab, 1980, "Final Report on the Field Studies and Aerial Mapping along the North-West Edge of the Canadian Archipelago". March/April 1980.
- Inkster, D.R., and R.T. Lowry, 1980, Ridge Height Measurements with SAR, in "Sea Ice Ridging and Pile-up Workshop", NRC TM 134.
- Intera Technologies, 1982, "SAR Program of Beaufort Sea" AOGA Project #144
- Intera Technologies, 1983, "SAR Program of Bering, Chukchi and Beaufort Sea Ice 1982" AOGA Project #177
- Intera, 1991, Intera Technologies Inc., Calgary, personal communication
- Jeffries, M.O. 1985a "Physical, Chemical and Isotopic Investigations of Ward Hunt Ice Shelf and Milne Ice Shelf, Ellesmere Island, NWT" PhD. Thesis - University of Calgary, April 1985
- Jeffries, M.O. 1985b "Ice Islands of the Arctic Ocean" Report to Gulf Canada Resources Inc., Sept. 1985
- Jeffries, M.O., 1986, "Structure and Growth of Arctic Ice Shelves and Ice Islands", in "Extreme Ice Features Workshop", NRC TM 141.

- Jeffries, M.O., W.M. Sackinger and H.D. Shoemaker, 1988 "Geometry and Physical Properties of Ice Islands" Ninth International Conference on Port and Ocean Engineering Under Arctic Conditions POAC '87. W.M. Sackinger and M.O. Jeffries (eds.) Geophysical Institute, University of Alaska, Fairbanks, 69-83.
- Jeffries, M.O., and W.M. Sackinger 1990a, "Near-Real-Time, Synthetic Aperture Radar Detection of a Calving Event at the Milne Ice Shelf, NWT. and the Contribution of Offshore Winds" in Second International Conference on Ice Technology (ITF '90) Cambridge, England, Sept. 1990.
- Jeffries, M.O. and W.M. Sackinger 1990b, "Ice Island Detection and Characterization with Airborne Synthetic Aperture Radar". *Journal of Geophysical Research*, v. 95, no. C4, pp. 5371-5377.
- Koenig, L.S., Greenway, K.R., Dunbar, M. and Hattersley-Smith, G., 1952 Arctic Ice Islands. *Arctic* Vol.5, No.2: 67-103.
- Leshack, L. 1978, Analysis of Under-Ice Profiles in the Southern Beaufort Sea, October 1978, Leshack Associates Ltd., Submitted to Dome Petroleum.
- McGonigal, D., 1985a, Kulluk Performance Monitoring, Fall 1983, Beaufort Sea Ice Conditions, 1983, report for Gulf Oil.
- McGonigal, D., 1985b, Beaufort Sea Grounded Ice Features and Seabed Scours, Vol.1, Field Program, April 1984, Report for Gulf Canada Resources Ltd.
- Mercer, J.B.,(Intera), 1990, Private Communication.
- Mullane, T.,(AES Ice Forecasting Centre Operations), 1990, Private Communication.
- Pilkington, G.R. and B. Danielewicz, 1986, Extreme Ice Features Workshop, Banff, Alberta, NRC T. M. 141.
- Pilkington, G.R. and M.C. Hill, 1990, AOGA Project 380: A Study of Floe Sizes in the US Beaufort Sea, CANATEC Consultants Ltd.
- Sackinger, W.M., M.O. Jeffries, Fuchong Li and Mingchi Lu, 1990, Interaction of Arctic Offshore Structures with Drifting Ice Islands and Thick Sea Ice Floes, in Second International Conference on Ice Technology (ITC '90), Cambridge, England, Sept. 1990.
- Sadler, H.E., and H.V. Serson, 1981, Observations of a Plug of Old Sea Ice in the Entrance of Nansen Sound, Ellesmere Island. RDB Report 81-5.

- Sanderson, T.J.O., 1988, Ice Mechanics, ed. by Graham and Trotman.
- Spedding, L.G., 1977. Ice Island Count. Southern Beaufort Sea, 1976, APOA Project #99, 1 PRT - 13 ME - 77, Imperial Oil Limited, Nov. 1977.
- Steen, J.W., 1989, SAR Interpretation Manual for Sea Ice, report by F.G. Bercha and Associates for CCRS.
- Thomas, B. and D. McGonigal, 1983, Katie's Floeberg 1981, Gulf Oil Houston Technology Centre Report No. 44RP008 for Gulf Canada Resources.
- Vaudrey, K., 1980/81, Katie's Floeberg Reports, for Gulf Oil Inc.
- Vaudrey, K.D. and B. Thomas, 1981, Katie's Floeberg 1980, report by K.D. Vaudrey and Associates for Gulf Canada Resources et al.
- Wadhams, P., 1979, Ice Islands in the Beaufort Sea, report to Dome Petroleum.
- Walker, E.R., and P. Wadhams, 1979, Thick Sea-ice Floes, Arctic, v 32, 2 p 140.
- WMO (World Meteorological Organization), 1970, WMO Sea-Ice Nomenclature. Geneva, 147 pp.
- Wright, B.D., Gulf Canada Resources Inc., personal communication.
- Wright, B.D., D.L. Schwab, and P. Gupta, 1983, Beaufort Sea Multi-year Ice Study, 1980. Gulf Canada Resources Inc., informal report, December, 1983.

APPENDIX A

Survey Fax and Recipients of Fax

FACSIMILE TRANSMISSION (FAX)

FROM: **CANATEC Consultants Ltd.**
Suite 110, 3553 - 31st Street N.W.,
University Research Park,
Calgary, Alberta, Canada T2L 2K7

Fax number (403) 289-0465

TO (604)380 2856

FAX NO.

DATE: 07 Dec 1990

TO: Mr Ron Verral

COMPANY: Defence Research Establishment Pacific

FROM: G. Roger Pilkington / Michel Metge, CANATEC

RE: Extreme Ice Features

Dear Ron:

CANATEC has been awarded a contract by ESRF (Environmental Studies Research Fund) to create a data base on Extreme Ice Features likely to reach the Beaufort Sea. It is proposed to use the AES STAR 2 "Round Robin" flights (see Figure 1) and to extend the flight paths slightly to cover the west coast of the Arctic Islands Archipelago. SPOT imagery may also be utilized.

- i) Do you know of any existing ground truth data (extreme features, height, thickness, type, extent, etc.) in the areas shown in Figure 1.
- ii) Do you plan or do you know anyone who is planning to be in the area of interest off the west coast of the Arctic island Archipelago in the winter or early spring of 1991. If so we would appreciate knowing which group, where the field party will be, and when, and whether it might be possible for the field party to ground truth some features seen on the STAR imagery. We will provide STAR data of the area of interest and a list of the most useful measurements.
- iii) Do you know of any existing data which might be useful for us to use in ground truthing the proposed January flight.

If you have any ideas (or leads) which might be useful, we would appreciate if you could fax them back to us by December 12.

Thank you very much.



This transmission consists of 2 pages (including this cover page). If the transmission is not complete, please call (403) 282-5321.

LIST OF RECIPIENTS OF THE FAX

| | | |
|-------------|------------|--------------------------------------|
| Dr. Bob | Frederking | NRC |
| Dr. Ian | Jordaan | Memorial University, Nfld |
| Dr. Jack | Clark | C-CORE |
| Mr. Don | Reed | ARCO |
| Mr. Jeff | Post | Chevron |
| Dr. Albert | Wang | EXXON |
| Mr. William | Hopkins | AOGA Office in Alaska |
| Mr. John | McCallum | Canadian Coast Guard |
| Dr. Touraj | Nasseri | C-FER |
| Dr. Walter | Spring | Mobil |
| Dr. Dave | Dickins | Dickins and Associates (Consultants) |
| Dr. Ken | Vaudrey | Vaudry & Associates (Consultants) |
| Mr. Ian | Sterling | Canadian Wildlife Service |
| Mr. Austin | Kovacs | CRREL |
| Mr. Frank | Hunt | Polar Shelf |
| Mr. Denis | Blanchet | CANMAR |
| Mr. Ron | Ritch | Fleet |
| Dr. Thomas | Curtin | Department of Navy |
| Dr. Roy | Verral | DND |

APPENDIX B

Results of SPOT Survey

| NO | HRV | SPOT MODE | ANGLE | SCENE CENTRE | | ORB | DATE RECORDED | | | CLOUD | QUAL | S | HDTID |
|----|-----|--------------|-------|--------------|--------------|-----|---------------|----|----|-------|------|---|----------|
| | | | | K/J | LAT/LONG | | DD | MM | YY | | | | |
| 2 | 2 | PD | -27.9 | 071/119 | 80 11/096 39 | 218 | 25 | 06 | 90 | 1111 | | P | P0701306 |
| 2 | 2 | PD | -27.9 | 076/120 | 81 01/093 05 | 218 | 25 | 06 | 90 | 1111 | | P | P0701305 |
| 2 | 2 | PD | -30.7 | 028/089 | 74 19/128 28 | 318 | 02 | 07 | 90 | 1111 | | P | P0701314 |
| 2 | 2 | PD | -30.7 | 030/090 | 74 47/127 49 | 318 | 02 | 07 | 90 | 0000 | | P | P0701314 |
| 2 | 2 | PD | -30.7 | 029/092 | 74 19/125 34 | 105 | 13 | 07 | 90 | 0002 | | P | P0701328 |
| 2 | 2 | PD | -30.7 | 032/094 | 74 47/124 55 | 105 | 13 | 07 | 90 | 0000 | | P | P0701328 |
| 2 | 2 | PD | -30.7 | 044/095 | 77 36/124 59 | 091 | 07 | 08 | 90 | 0000 | | P | P0701359 |
| 2 | 2 | PD | -26.5 | 071/119 | 80 09/096 29 | 289 | 21 | 08 | 90 | 1100 | S | P | P0701375 |
| 2 | 2 | PD | -30.7 | 044/095 | 77 36/124 58 | 091 | 28 | 09 | 90 | 0000 | | P | P0701421 |
| 2 | 2 | PD | -30.7 | 028/089 | 74 19/128 28 | 318 | 02 | 07 | 90 | 1111 | | P | P0701314 |
| 2 | 2 | PD | -30.7 | 030/090 | 74 47/127 49 | 318 | 02 | 07 | 90 | 0000 | | P | P0701314 |
| 2 | 2 | PD | -30.7 | 029/092 | 74 19/125 34 | 105 | 13 | 07 | 90 | 0002 | | P | P0701328 |
| 2 | 2 | PD | -30.7 | 032/094 | 74 47/124 55 | 105 | 13 | 07 | 90 | 0000 | | P | P0701328 |

Table B.1: Suitable SPOT Imagery for 1990

| NO. | HRV | SPOT MODE | ANGLE | SCENE CENTRE | | ORB | DATE RECORDED | | | CLOUD | QUAL | S | HDTID |
|-----|-----|-----------|-------|--------------|--------------|-----|---------------|----|----|-------|------|---|----------|
| | | | | K/J | LAT/LONG | | DD | MM | YY | | | | |
| 1 | 1 | PD | -1.0 | 070/118 | 80 06/098 17 | 205 | 12 | 06 | 89 | 0044 | | P | P0701035 |
| 1 | 1 | PD | -13.1 | 074/118 | 80 55/096 00 | 162 | 21 | 09 | 89 | 0022 | | P | P0701130 |
| 1 | 1 | PD | -15.2 | 066/114 | 80 00/103 36 | 091 | 16 | 09 | 89 | 0110 | | P | P0701125 |
| 1 | 1 | PD | -20.0 | 062/109 | 79 52/109 48 | 162 | 31 | 07 | 89 | 0000 | | P | P0701083 |
| 1 | 1 | PD | -15.2 | 063/113 | 79 38/105 35 | 091 | 16 | 09 | 89 | 0013 | S | P | P0701125 |
| 1 | 1 | PD | -20.0 | 059/108 | 79 28/111 34 | 162 | 31 | 07 | 89 | 0000 | | P | P0701083 |
| 1 | 1 | PD | -15.9 | 050/102 | 78 07/118 25 | 148 | 08 | 06 | 89 | 1111 | | P | P0701031 |
| 1 | 1 | PD | -30.4 | 044/095 | 77 36/124 41 | 091 | 04 | 06 | 89 | 0000 | | P | P0701027 |
| 1 | 1 | PD | -30.4 | 040/098 | 76 12/121 28 | 034 | 26 | 06 | 89 | 0000 | | P | P0701049 |
| 1 | 1 | PD | -30.4 | 042/099 | 76 40/120 39 | 034 | 26 | 06 | 89 | 0000 | | P | P0701049 |
| 1 | 1 | PD | -20.0 | 041/099 | 76 30/121 00 | 162 | 31 | 07 | 89 | 0000 | | P | P0701083 |
| 1 | 2 | PD | -30.7 | 040/098 | 76 12/121 43 | 034 | 17 | 08 | 89 | 1120 | | P | P0701099 |
| 1 | 2 | PD | -30.7 | 045/100 | 77 09/120 01 | 034 | 17 | 08 | 89 | 2110 | | P | P0701099 |
| 1 | 1 | PD | 7.3 | 030/093 | 74 20/124 54 | 049 | 01 | 06 | 89 | 0000 | | P | P0701024 |
| 1 | 1 | PD | -15.9 | 027/088 | 74 11/128 27 | 148 | 08 | 06 | 89 | 0000 | | P | P0701031 |
| 1 | 1 | PD | -15.9 | 030/090 | 74 39/127 35 | 148 | 08 | 06 | 89 | 1111 | | P | P0701031 |
| 1 | 1 | PD | -30.4 | 030/094 | 74 19/124 20 | 034 | 26 | 06 | 89 | 0000 | | P | P0701049 |
| 1 | 2 | PD | -30.7 | 029/092 | 74 19/125 32 | 105 | 22 | 08 | 89 | 0000 | | P | P0701104 |
| 1 | 2 | PD | -30.7 | 032/094 | 74 47/124 53 | 105 | 22 | 08 | 89 | 0000 | | P | P0701104 |

Table B.2: Suitable SPOT Imagery for 1989

| NO | HRV | SPOT MODE | ANGLE | SCENE CENTRE | | ORB | DATE RECORDED | | | CLOUD | QUAL | S | HDTID |
|----|-----|-----------|-------|--------------|--------------|-----|---------------|----|----|-------|------|---|----------|
| | | | | K/J | LAT/LONG | | DD | MM | YY | | | | |
| 1 | 2 | PD | -12.1 | 078/119 | 81 41/092 37 | 219 | 14 | 06 | 88 | 0099 | | P | P0700669 |
| 1 | 2 | PD | -15.5 | 075/117 | 81 23/096 08 | 233 | 11 | 07 | 88 | 0000 | | P | P0700727 |
| 1 | 2 | PD | -15.5 | 077/118 | 81 40/093 19 | 233 | 11 | 07 | 88 | 0000 | S | P | P0700727 |
| 1 | 2 | PD | -11.4 | 074/117 | 81 22/097 06 | 361 | 20 | 07 | 88 | 0000 | S | P | P0700745 |
| 1 | 1 | PD | -14.5 | 076/116 | 81 52/096 23 | 361 | 20 | 07 | 88 | 9900 | S | P | P0700745 |
| 1 | 1 | PD | -8.4 | 072/116 | 80 54/098 45 | 063 | 25 | 07 | 88 | 0000 | | P | P0700754 |
| 1 | 2 | PD | -15.5 | 067/113 | 80 24/103 31 | 233 | 11 | 07 | 88 | 0000 | | P | P0700727 |
| 1 | 1 | PD | -8.4 | 067/113 | 80 19/103 56 | 063 | 25 | 07 | 88 | 0000 | | P | P0700754 |
| 1 | 2 | PD | -8.0 | 061/110 | 79 40/109 14 | 134 | 08 | 06 | 88 | 0044 | | P | P0700656 |
| 1 | 1 | PD | -31.1 | 062/112 | 79 26/107 05 | 204 | 13 | 06 | 88 | 0000 | | P | P0700665 |
| 1 | 1 | PD | -31.1 | 064/112 | 79 53/105 45 | 204 | 13 | 06 | 88 | 0000 | | P | P0700665 |
| 1 | 1 | PD | -29.0 | 063/111 | 79 48/106 53 | 048 | 28 | 06 | 88 | 0044 | | P | P0700700 |
| 1 | 2 | PD | -15.5 | 060/110 | 79 18/109 29 | 233 | 11 | 07 | 88 | 0000 | | P | P0700727 |
| 1 | 2 | PD | -15.5 | 062/111 | 79 40/107 38 | 233 | 11 | 07 | 88 | 0000 | | P | P0700727 |
| 1 | 2 | PD | -11.4 | 062/109 | 79 50/109 36 | 361 | 20 | 07 | 88 | 3800 | | P | P0700745 |
| 1 | 1 | PD | -8.4 | 062/110 | 79 41/108 31 | 063 | 25 | 07 | 88 | 0000 | | P | P0700754 |
| 1 | 2 | PD | -15.5 | 055/107 | 78 30/112 49 | 233 | 11 | 07 | 88 | 0000 | | P | P0700727 |
| 1 | 2 | PD | -15.5 | 057/108 | 78 54/111 12 | 233 | 11 | 07 | 88 | 0000 | | P | P0700727 |
| 1 | 2 | PD | -11.4 | 059/108 | 79 29/111 39 | 361 | 20 | 07 | 88 | 0000 | | P | P0700745 |

Table B.3: Suitable SPOT Imagery for 1988

| NO | HRV | SPOT MODE | ANGLE | SCENE CENTRE | | ORB | DATE RECORDED | | | CLOUD | QUAL | S | HDTID |
|----|-----|-----------|-------|--------------|--------------|-----|---------------|----|----|-------|------|---|----------|
| | | | | K/J | LAT/LONG | | DD | MM | YY | | | | |
| 1 | 1 | PD | -8.4 | 059/109 | 79 20/110 36 | 063 | 25 | 07 | 88 | 0067 | | P | P0700754 |
| 1 | 2 | PD | -14.1 | 051/100 | 78 30/119 35 | 063 | 03 | 06 | 88 | 0000 | | P | P0700646 |
| 1 | 1 | PD | -13.8 | 051/101 | 78 28/119 25 | 063 | 03 | 06 | 88 | 1010 | | P | P0700646 |
| 1 | 2 | PD | -14.1 | 048/102 | 77 39/117 50 | 077 | 04 | 06 | 88 | 2100 | | P | P0700648 |
| 1 | 1 | PD | -23.4 | 050/100 | 78 19/119 32 | 233 | 11 | 07 | 88 | 1111 | | P | P0700727 |
| 1 | 2 | PD | -15.5 | 050/105 | 77 41/115 45 | 233 | 11 | 07 | 88 | 0000 | | P | P0700727 |
| 1 | 2 | PD | -15.5 | 052/106 | 78 05/114 20 | 233 | 11 | 07 | 88 | 0000 | | P | P0700727 |
| 1 | 1 | PD | -20.7 | 047/098 | 77 49/121 55 | 077 | 04 | 06 | 88 | 0011 | | P | P0700648 |
| 1 | 2 | PD | -15.5 | 041/094 | 76 54/124 56 | 361 | 24 | 06 | 88 | 0000 | | P | P0700693 |
| 1 | 1 | PD | -15.2 | 043/096 | 77 13/123 49 | 361 | 24 | 06 | 88 | 0000 | | P | P0700693 |
| 1 | 2 | PD | -15.5 | 044/096 | 77 19/123 41 | 361 | 24 | 06 | 88 | 0000 | | P | P0700693 |
| 1 | 1 | PD | -15.2 | 046/097 | 77 38/122 30 | 361 | 24 | 06 | 88 | 0000 | | P | P0700693 |
| 1 | 2 | PD | -15.5 | 046/098 | 77 45/122 21 | 361 | 24 | 06 | 88 | 0090 | | P | P0700693 |
| 1 | 2 | PD | -12.8 | 041/099 | 76 21/120 52 | 077 | 30 | 06 | 88 | 0000 | | P | P0700706 |
| 1 | 1 | PD | -18.6 | 042/095 | 76 54/124 01 | 148 | 05 | 07 | 88 | 1111 | | P | P0700716 |
| 1 | 1 | PD | -30.4 | 039/096 | 76 12/123 28 | 176 | 07 | 07 | 88 | 0402 | | P | P0700719 |
| 1 | 1 | PD | -11.8 | 043/095 | 77 16/124 19 | 205 | 09 | 07 | 88 | 0110 | | P | P0700723 |
| 1 | 1 | PD | -11.8 | 046/097 | 77 40/122 54 | 205 | 09 | 07 | 88 | 0000 | | P | P0700723 |

Table B.3 (cont'd)

| NO | HRV | SPOT MODE | ANGLE | SCENE CENTRE | | ORB | DATE RECORDED | | | CLOUD | QUAL | S | HDTID |
|----|-----|-----------|-------|--------------|--------------|-----|---------------|----|----|-------|------|---|----------|
| | | | | K/J | LAT/LONG | | DD | MM | YY | | | | |
| 1 | 1 | PD | -23.4 | 040/095 | 76 33/124 05 | 233 | 11 | 07 | 88 | 1111 | | P | P0700727 |
| 1 | 1 | PD | -23.4 | 043/097 | 77 00/123 04 | 233 | 11 | 07 | 88 | 1111 | | P | P0700727 |
| 1 | 1 | PD | -23.4 | 045/098 | 77 27/121 58 | 233 | 11 | 07 | 88 | 1111 | | P | P0700727 |
| 1 | 1 | PD | -23.4 | 048/099 | 77 54/120 48 | 233 | 11 | 07 | 88 | 1111 | | P | P0700727 |
| 1 | 2 | PD | -4.6 | 043/098 | 76 58/121 30 | 276 | 14 | 07 | 88 | 1111 | | P | P0700733 |
| 1 | 1 | PD | -8.4 | 039/096 | 76 16/123 20 | 063 | 25 | 07 | 88 | 2101 | | P | P0700754 |
| 1 | 2 | PD | -11.4 | 041/0* | 76 45/123 47 | 063 | 25 | 07 | 88 | 0304 | | P | P0700754 |
| 1 | 2 | PD | -11.4 | 044/097 | 77 10/122 28 | 063 | 25 | 07 | 88 | 0000 | | P | P0700754 |
| 1 | 1 | PD | -8.4 | 044/099 | 77 05/120 43 | 063 | 25 | 07 | 88 | 0000 | | P | P0700754 |
| 1 | 2 | PD | -11.4 | 046/099 | 77 34/121 05 | 063 | 25 | 07 | 88 | 0201 | | P | P0700754 |
| 1 | 1 | PD | -22.0 | 029/088 | 74 42/128 49 | 006 | 25 | 06 | 88 | 0000 | | P | P0700695 |
| 1 | 2 | PD | -12.8 | 028/092 | 74 10/125 59 | 077 | 30 | 06 | 88 | 0000 | | P | P0700706 |
| 1 | 2 | PD | -12.8 | 031/093 | 74 36/125 04 | 077 | 30 | 06 | 88 | 0000 | | P | P0700706 |
| 1 | 1 | PD | -26.2 | 028/089 | 74 16/127 54 | 091 | 01 | 07 | 88 | 0000 | | P | P0700707 |
| 1 | 2 | PD | -21.0 | 029/093 | 74 14/125 11 | 091 | 01 | 07 | 88 | 0000 | | P | P0700707 |
| 1 | 1 | PD | -26.2 | 030/091 | 74 45/127 11 | 091 | 01 | 07 | 88 | 0000 | | P | P0700707 |
| 1 | 2 | PD | -21.0 | 032/094 | 74 41/124 23 | 091 | 01 | 07 | 88 | 0000 | | P | P0700707 |
| 1 | 1 | PD | -18.6 | 029/088 | 74 40/129 00 | 148 | 05 | 07 | 88 | 0000 | | P | P0700716 |

Table B.3 (cont'd)

| NO | HRV | SPOT MODE | ANGLE | SCENE CENTRE | | ORB | DATE RECORDED | | | CLOUD | QUAL | S | HDTID |
|----|-----|--------------|-------|--------------|--------------|-----|---------------|----|----|-------|------|---|----------|
| | | | | K/J | LAT/LONG | | DD | MM | YY | | | | |
| 1 | 2 | PD | -24.4 | 028/089 | 74 16/127 57 | 162 | 06 | 07 | 88 | 1111 | | P | P0700718 |
| 1 | 1 | PD | -20.0 | 029/092 | 74 13/125 39 | 162 | 06 | 07 | 88 | 0001 | | P | P0700718 |
| 1 | 2 | PD | -24.4 | 030/090 | 74 44/127 12 | 162 | 06 | 07 | 88 | 1101 | | P | P0700718 |
| 1 | 1 | PD | -30.4 | 029/091 | 74 19/126 19 | 176 | 07 | 07 | 88 | 0000 | | P | P0700719 |
| 1 | 1 | PD | -23.4 | 027/089 | 74 15/128 23 | 233 | 11 | 07 | 88 | 1111 | | P | P0700727 |
| 1 | 2 | PD | -15.5 | 029/094 | 74 11/124 24 | 233 | 11 | 07 | 88 | 0100 | | P | P0700727 |
| 1 | 1 | PD | -23.4 | 030/090 | 74 43/127 38 | 233 | 11 | 07 | 88 | 1111 | | P | P0700727 |
| 1 | 1 | PD | -8.4 | 026/088 | 74 07/128 46 | 063 | 25 | 07 | 88 | 0000 | | P | P0700754 |
| 1 | 1 | PD | -8.4 | 029/090 | 74 33/127 48 | 063 | 25 | 07 | 88 | 0000 | | P | P0700754 |
| 1 | 1 | PD | -8.4 | 032/091 | 74 59/126 46 | 063 | 25 | 07 | 88 | 0000 | | P | P0700754 |

Table B.3 (cont'd)

| NO | HRV | SPOT MODE | ANGLE | SCENE CENTRE | | ORB | DATE RECORDED | | | CLOUD | QUAL | S | HDTID |
|----|-----|-----------|-------|--------------|--------------|-----|---------------|----|----|-------|------|---|----------|
| | | | | K/J | LAT/LONG | | DD | MM | YY | | | | |
| 1 | 1 | PD | -31.1 | 054/106 | 78 32/114 25 | 190 | 14 | 06 | 87 | 0000 | | P | P0700336 |
| 1 | 1 | PD | -31.1 | 054/106 | 78 32/114 25 | 190 | 10 | 07 | 87 | 0033 | | P | P0700370 |
| 1 | 1 | PD | -24.1 | 048/101 | 77 55/119 20 | 091 | 03 | 07 | 87 | 0000 | | P | P0700360 |
| 1 | 1 | PD | -28.3 | 053/104 | 78 28/116 12 | 105 | 04 | 07 | 87 | 0066 | | P | P0700362 |
| 1 | 1 | PD | -24.8 | 050/104 | 77 55/115 54 | 176 | 09 | 07 | 87 | 0000 | | P | P0700369 |
| 1 | 2 | PD | -21.0 | 052/107 | 77 50/113 22 | 176 | 09 | 07 | 87 | 0000 | | P | P0700369 |
| 1 | 1 | PD | -17.9 | 051/107 | 77 45/113 22 | 318 | 19 | 07 | 87 | 0000 | | P | P0700380 |
| 1 | 1 | PD | -24.8 | 053/105 | 78 22/114 40 | 176 | 04 | 08 | 87 | 0011 | | P | P0700399 |
| 1 | 1 | PD | -17.2 | 049/103 | 77 44/116 50 | 233 | 08 | 08 | 87 | 0022 | | P | P0700403 |
| 1 | 1 | PD | -24.1 | 038/096 | 76 07/123 33 | 091 | 03 | 07 | 87 | 1201 | | P | P0700360 |
| 1 | 1 | PD | -24.8 | 040/100 | 76 07/120 03 | 176 | 09 | 07 | 87 | 0000 | | P | P0700369 |
| 1 | 1 | PD | -7.0 | 042/100 | 76 39/120 22 | 361 | 12 | 09 | 87 | 0011 | | P | P0700436 |
| 1 | 1 | PD | -24.1 | 028/091 | 74 16/126 50 | 091 | 03 | 07 | 87 | 0112 | | P | P0700360 |
| 1 | 1 | PD | -24.1 | 031/092 | 74 43/126 05 | 091 | 03 | 07 | 87 | 0000 | | P | P0700360 |
| 1 | 1 | PD | -5.6 | 031/094 | 74 31/124 32 | 290 | 12 | 08 | 87 | 0010 | | P | P0700408 |
| 1 | 2 | PD | -4.6 | 031/095 | 74 31/124 01 | 290 | 12 | 08 | 87 | 0000 | | P | P0700408 |

Table B.4: Suitable SPOT imagery for 1987

ABBREVIATIONS USED IN SPOT TABLES

| | |
|---------|--|
| HRV | High Resolution Visible Imager |
| XS | Multi-spectral |
| PD | Panchromatic |
| Angle | Of camera to vertical + east - west of path |
| K/J | Are SPOT ref. grid zones (Fig. 6.2) |
| ORB | Orbit number |
| Cloud | Cloud cover in tenths in each of four quarters |
| Quality | Digital product quality |
| S | Station ID, P is Prince Albert |
| HDTID | Image ID # |

APPENDIX C

EIF DATA BASE

EXTREME ICE FEATURES, 1946-1988

| Latitude | Longitude | Date | Target | X-floe (km) | Y-floe (km) | X (km) | Y (km) | 1 cm= | Type |
|----------|-----------|--------|--------|----------------|----------------|-----------|-----------|--------|------|
| 73.0000 | 128.0000 | 999 | 5010 | 0.55 | 0.55 | 999.00 | 999.00 | 999.00 | HUM |
| 999.0000 | 999.0000 | 999 | 3021 | 7.87 | 7.87 | 999.00 | 999.00 | 999.00 | ISL |
| 999.0000 | 999.0000 | 460814 | 3001 | 29.00 | 24.00 | 999.00 | 999.00 | 999.00 | ISL |
| 999.0000 | 999.0000 | 470700 | 3004 | 24.70 | 24.70 | 999.00 | 999.00 | 999.00 | ISL |
| 999.0000 | 999.0000 | 480628 | 3005 | 11.00 | 10.00 | 999.00 | 999.00 | 999.00 | ISL |
| 999.0000 | 999.0000 | 500721 | 3002 | 29.00 | 27.00 | 999.00 | 999.00 | 999.00 | ISL |
| 999.0000 | 999.0000 | 500729 | 3003 | 14.00 | 7.00 | 999.00 | 999.00 | 999.00 | ISL |
| 999.0000 | 999.0000 | 560000 | 3006 | 13.00 | 9.00 | 999.00 | 999.00 | 999.00 | ISL |
| 999.0000 | 999.0000 | 610523 | 3007 | 6.00 | 4.00 | 999.00 | 999.00 | 999.00 | ISL |
| 999.0000 | 999.0000 | 620610 | 3011 | 13.00 | 9.00 | 999.00 | 999.00 | 999.00 | ISL |
| 999.0000 | 999.0000 | 620610 | 3012 | 18.00 | 8.00 | 999.00 | 999.00 | 999.00 | ISL |
| 999.0000 | 999.0000 | 620610 | 3010 | 13.00 | 9.00 | 999.00 | 999.00 | 999.00 | ISL |
| 999.0000 | 999.0000 | 620610 | 3008 | 9.00 | 16.00 | 999.00 | 999.00 | 999.00 | ISL |
| 999.0000 | 999.0000 | 620610 | 3009 | 9.00 | 8.00 | 999.00 | 999.00 | 999.00 | ISL |
| 999.0000 | 999.0000 | 670403 | 3016 | 23.00 | 10.00 | 999.00 | 999.00 | 999.00 | ISL |
| 999.0000 | 999.0000 | 670403 | 3013 | 12.00 | 5.00 | 999.00 | 999.00 | 999.00 | ISL |
| 999.0000 | 999.0000 | 670520 | 3017 | 1.60 | 1.60 | 999.00 | 999.00 | 999.00 | ISL |
| 999.0000 | 999.0000 | 681000 | 3018 | 10.20 | 10.20 | 999.00 | 999.00 | 999.00 | ISL |
| 999.0000 | 999.0000 | 690000 | 3019 | 8.94 | 8.94 | 999.00 | 999.00 | 999.00 | ISL |
| 999.0000 | 999.0000 | 710331 | 3020 | 7.20 | 2.00 | 999.00 | 999.00 | 999.00 | ISL |
| 999.0000 | 999.0000 | 730900 | 3022 | 3.16 | 3.16 | 999.00 | 999.00 | 999.00 | ISL |
| 999.0000 | 999.0000 | 740400 | 3014 | 12.00 | 5.00 | 999.00 | 999.00 | 999.00 | ISL |
| 999.0000 | 999.0000 | 751200 | 3015 | 7.00 | 3.00 | 999.00 | 999.00 | 999.00 | ISL |
| 999.0000 | 999.0000 | 780400 | 3023 | 17.00 | 8.00 | 999.00 | 999.00 | 999.00 | ISL |
| 72.2750 | 132.8500 | 800317 | 5001 | 1.10 | 0.80 | 999.00 | 999.00 | 999.00 | HUM |
| 76.4417 | 123.8750 | 800401 | 5002 | 3.00 | 3.00 | 1.00 | 0.25 | 999.00 | HUM |

EXTREME ICE FEATURES, 1946-1988

| Latitude | Longitude | Date | Target | X-floe (km) | Y-floe (km) | X (km) | Y (km) | 1 cm = | Type |
|-----------------|------------------|-------------|---------------|------------------------|------------------------|-------------------|-------------------|---------------|-------------|
| 77.2833 | 119.5000 | 800402 | 5003 | 1.80 | 0.30 | 999.00 | 999.00 | 999.00 | HUM |
| 77.4500 | 118.7500 | 800403 | 5004 | 1.00 | 0.50 | 999.00 | 999.00 | 999.00 | HUM |
| 77.3667 | 119.6667 | 800406 | 5007 | 2.00 | 2.00 | 1.50 | 1.00 | 999.00 | HUM |
| 77.5833 | 118.0000 | 800408 | 5014 | 1.50 | 1.50 | 999.00 | 999.00 | 999.00 | MYF |
| 78.8367 | 110.5500 | 800409 | 6008 | 999.00 | 999.00 | 999.00 | 999.00 | 999.00 | PIL |
| 78.9000 | 110.7000 | 800409 | 5008 | 0.26 | 0.2 | 999.00 | 999.00 | 999.00 | ISL |
| 78.8750 | 111.0333 | 800409 | 5009 | 999.00 | 999.00 | 999.00 | 999.00 | 999.00 | RDG |
| 78.8750 | 111.0333 | 800409 | 6009 | 999.00 | 999.00 | 999.00 | 999.00 | 999.00 | MLF |
| 73.5500 | 124.9000 | 800413 | 5012 | 0.18 | 0.14 | 999.00 | 999.00 | 999.00 | ISL |
| 999.0000 | 999.0000 | 830423 | 3026 | 2.40 | 2.10 | 999.00 | 999.00 | 999.00 | ISL |
| 999.0000 | 999.0000 | 830423 | 3027 | 4.50 | 1.00 | 999.00 | 999.00 | 999.00 | ISL |
| 999.0000 | 999.0000 | 830423 | 3024 | 10.5 | 3.90 | 999.00 | 999.00 | 999.00 | ISL |
| 999.0000 | 999.0000 | 830423 | 3025 | 3.90 | 2.70 | 999.00 | 999.00 | 999.00 | ISL |
| 999.0000 | 999.0000 | 830521 | 3030 | 2.40 | 0.75 | 999.00 | 999.00 | 999.00 | ISL |
| 999.0000 | 999.0000 | 830521 | 3029 | 2.70 | 1.00 | 999.00 | 999.00 | 999.00 | ISL |
| 999.0000 | 999.0000 | 830521 | 3028 | 2.70 | 0.60 | 999.00 | 999.00 | 999.00 | ISL |
| 999.0000 | 999.0000 | 831019 | 3031 | 999.00 | 999.00 | 999.00 | 999.00 | 999.00 | ISL |
| 999.0000 | 999.0000 | 840723 | 3032 | 0.50 | 0.25 | 999.00 | 999.00 | 999.00 | ISL |
| 999.0000 | 999.0000 | 850723 | 3033 | 0.15 | 0.40 | 999.00 | 999.00 | 999.00 | ISL |
| 82.7500 | 84.0000 | 880222 | 3034 | 7.20 | 3.60 | 999.00 | 999.00 | 999.00 | REI |

EXTREME ICE FEATURES DATA

| Latitude | Longitude | Date | Target | X-floe (km) | Y-floe (km) | X (km) | Y (km) | 1 cm = | Type | equ dia | X/Y |
|-----------------|------------------|-------------|---------------|------------------------|------------------------|-------------------|-------------------|---------------|-------------|----------------|------------|
| 78.2653 | -116.7407 | 880207 | 26 | 1.31 | 0.65 | 999.00 | 999.00 | 3.27 | HUM | 0.92490 | 2.00000 |
| 78.1388 | -119.4434 | 880207 | 25 | 1.96 | 1.31 | 999.00 | 999.00 | 3.27 | HUM | 1.60197 | 1.50000 |
| 78.7232 | -113.2614 | 880215 | 5 | 2.41 | 1.35 | 999.00 | 999.00 | 3.01 | HUM | 1.80600 | 1.77778 |
| 78.6129 | -114.6221 | 880215 | 4 | 1.33 | 1.04 | 999.00 | 999.00 | 2.96 | HUM | 1.17471 | 1.28571 |
| 78.8641 | -108.8044 | 880215 | 6 | 0.75 | 0.75 | 999.00 | 999.00 | 3.01 | HUM | 0.75250 | 1.00000 |
| 78.8316 | -108.5784 | 880215 | 7 | 2.11 | 2.11 | 999.00 | 999.00 | 3.01 | HUM | 2.10700 | 1.00000 |
| 77.7329 | -115.2549 | 880218 | 27 | 2.79 | 1.55 | 999.00 | 999.00 | 3.10 | HUM | 2.07954 | 1.80000 |
| 77.6827 | -115.5360 | 880218 | 28 | 1.86 | 1.71 | 999.00 | 999.00 | 3.10 | HUM | 1.78081 | 1.09091 |
| 80.3070 | -100.6834 | 880219 | 49 | 2.93 | 1.67 | 2.09 | 0.56 | 2.79 | HUM | 2.21449 | 1.75000 |
| 80.5229 | -100.7962 | 880219 | 51 | 1.67 | 1.40 | 999.00 | 999.00 | 2.79 | HUM | 1.52815 | 1.20000 |
| 78.2874 | -116.9787 | 880219 | 1 | 1.14 | 1.14 | 999.00 | 999.00 | 2.85 | HUM | 1.14000 | 1.00000 |
| 78.4362 | -115.2043 | 880219 | 3 | 2.85 | 2.28 | 2.00 | 1.71 | 2.85 | HUM | 2.54912 | 1.25000 |
| 78.4362 | -115.9755 | 880219 | 2 | 1.14 | 1.14 | 999.00 | 999.00 | 2.85 | HUM | 1.14000 | 1.00000 |
| 78.2191 | -106.6081 | 880220 | 53 | 1.87 | 1.50 | 999.00 | 999.00 | 3.74 | HUM | 1.67258 | 1.25000 |
| 83.4010 | -68.5355 | 880222 | 82 | 2.73 | 2.42 | 0.61 | 0.61 | 3.03 | HUM | 2.57104 | 1.12500 |
| 81.6130 | -93.6655 | 880222 | 91 | 2.23 | 1.11 | 999.00 | 999.00 | 3.18 | HUM | 1.57402 | 2.00000 |
| 81.5844 | -93.6758 | 880222 | 90 | 2.23 | 0.95 | 999.00 | 999.00 | 3.18 | HUM | 1.45726 | 2.33333 |
| 79.4753 | -110.9137 | 880725 | 91 | 1.75 | 1.75 | 999.00 | 999.00 | 1.25 | HUM | 1.75000 | 1.00000 |
| 79.4044 | -111.5709 | 880725 | 149 | 3.88 | 2.63 | 2.25 | 1.50 | 1.25 | HUM | 3.18934 | 1.47619 |
| 79.3515 | -110.7506 | 880725 | 154 | 5.63 | 5.63 | 4.75 | 3.75 | 1.25 | HUM | 5.62500 | 1.00000 |
| 79.6687 | -110.7579 | 880725 | 155 | 2.38 | 0.88 | 999.00 | 999.00 | 1.25 | HUM | 1.44157 | 2.71429 |
| 79.3875 | -110.3288 | 880725 | 156 | 3.00 | 2.88 | 999.00 | 999.00 | 1.25 | HUM | 2.93684 | 1.04348 |
| 79.5101 | -107.2275 | 880725 | 183 | 1.25 | 1.00 | 999.00 | 999.00 | 1.25 | HUM | 1.11803 | 1.25000 |
| 79.4910 | -109.3012 | 880725 | 160 | 0.75 | 0.63 | 999.00 | 999.00 | 1.25 | HUM | 0.68465 | 1.20000 |
| 79.5034 | -107.3850 | 880725 | 182 | 1.13 | 0.88 | 999.00 | 999.00 | 1.25 | HUM | 0.99216 | 1.28571 |
| 79.5709 | -108.7641 | 880725 | 162 | 1.88 | 1.50 | 1.75 | 0.50 | 1.25 | HUM | 1.67705 | 1.25000 |

EXTREME ICE FEATURES DATA

| Latitude | Longitude | Date | Target | X-floe (km) | Y-floe (km) | X (km) | Y (km) | 1 cm = | Type | equ dia | X/Y |
|----------|-----------|--------|--------|----------------|----------------|-----------|-----------|--------|------|---------|---------|
| 79.3425 | -110.0638 | 880725 | 165 | 1.75 | 1.63 | 999.00 | 999.00 | 1.25 | HUM | 1.68634 | 1.07692 |
| 79.5034 | -108.8113 | 880725 | 169 | 1.00 | 0.50 | 999.00 | 999.00 | 1.25 | HUM | 0.70711 | 2.00000 |
| 79.4336 | -109.6386 | 880725 | 158 | 1.50 | 0.88 | 1.38 | 0.63 | 1.25 | HUM | 1.14564 | 1.71429 |
| 78.6382 | -104.8133 | 890324 | 38 | 1.61 | 1.61 | 999.00 | 999.00 | 2.48 | HUM | 1.61200 | 1.00000 |
| 78.6494 | -104.9716 | 890324 | 39 | 2.48 | 1.36 | 999.00 | 999.00 | 2.48 | HUM | 1.83922 | 1.81818 |
| 78.6204 | -104.8395 | 890324 | 40 | 1.61 | 1.24 | 999.00 | 999.00 | 2.48 | HUM | 1.41382 | 1.30000 |
| 78.6248 | -104.4962 | 890324 | 41 | 0.74 | 0.50 | 999.00 | 999.00 | 2.48 | HUM | 0.60747 | 1.50000 |
| 78.6270 | -104.9452 | 890324 | 42 | 1.74 | 0.99 | 999.00 | 999.00 | 2.48 | HUM | 1.31229 | 1.75000 |
| 79.9224 | -102.6170 | 890324 | 141 | 1.26 | 1.13 | 999.00 | 999.00 | 2.51 | HUM | 1.19060 | 1.11111 |
| 79.8027 | -103.0154 | 890324 | 143 | 3.01 | 2.76 | 999.00 | 999.00 | 2.51 | HUM | 2.88377 | 1.09091 |
| 79.1381 | -107.5719 | 890324 | 43 | 1.49 | 1.24 | 0.50 | 0.50 | 2.48 | HUM | 1.35835 | 1.20000 |
| 79.7462 | -103.3398 | 890324 | 142 | 5.02 | 4.02 | 999.00 | 999.00 | 2.51 | HUM | 4.49002 | 1.25000 |
| 80.0466 | -101.1056 | 890324 | 147 | 2.51 | 1.51 | 1.51 | 0.75 | 2.51 | HUM | 1.94424 | 1.66667 |
| 79.1471 | -107.7211 | 890324 | 44 | 2.48 | 1.98 | 1.98 | 0.99 | 2.48 | HUM | 2.21818 | 1.25000 |
| 79.4887 | -101.3338 | 890324 | 146 | 1.26 | 1.00 | 999.00 | 999.00 | 2.51 | HUM | 1.12251 | 1.25000 |
| 82.1713 | -88.8378 | 890404 | 100 | 1.63 | 1.26 | 1.26 | 0.75 | 2.51 | HUM | 1.43092 | 1.30000 |
| 82.9656 | -67.1473 | 890404 | 64 | 0.75 | 0.50 | 999.00 | 999.00 | 2.50 | HUM | 0.61237 | 1.50000 |
| 83.1584 | -70.9570 | 890404 | 66 | 2.00 | 1.50 | 999.00 | 999.00 | 2.50 | HUM | 1.73205 | 1.33333 |
| 82.9903 | -67.5755 | 890404 | 63 | 1.00 | 0.88 | 999.00 | 999.00 | 2.50 | HUM | 0.93541 | 1.14286 |
| 83.2169 | -71.2161 | 890404 | 67 | 1.75 | 1.50 | 999.00 | 999.00 | 2.50 | HUM | 1.62019 | 1.16667 |
| 82.9026 | -65.5631 | 890404 | 61 | 1.00 | 0.75 | 999.00 | 999.00 | 2.50 | HUM | 0.86603 | 1.33333 |
| 77.5377 | -116.7443 | 890406 | 24 | 1.56 | 1.04 | 999.00 | 999.00 | 2.60 | HUM | 1.27373 | 1.50000 |
| 77.6903 | -111.2278 | 890406 | 15 | 1.25 | 0.75 | 999.00 | 999.00 | 2.50 | HUM | 0.96825 | 1.66667 |
| 77.7758 | -114.7824 | 890406 | 12 | 1.00 | 1.00 | 999.00 | 999.00 | 2.50 | HUM | 1.00000 | 1.00000 |
| 77.6655 | -115.8592 | 890406 | 9 | 1.25 | 1.25 | 999.00 | 999.00 | 2.50 | HUM | 1.25000 | 1.00000 |
| 77.8140 | -117.0401 | 890406 | 8 | 2.00 | 1.25 | 999.00 | 999.00 | 2.50 | HUM | 1.58114 | 1.60000 |

EXTREME ICE FEATURES DATA

| Latitude | Longitude | Date | Target | X-floe (km) | Y-floe (km) | X (km) | Y (km) | 1 cm= | Type | equ dia | X/Y |
|----------|-----------|--------|--------|----------------|----------------|-----------|-----------|-------|------|---------|---------|
| 77.7983 | -114.2442 | 890406 | 13 | 0.75 | 0.63 | 999.00 | 999.00 | 2.50 | HUM | 0.68465 | 1.20000 |
| 77.7780 | -114.0684 | 890406 | 14 | 1.00 | 0.88 | 999.00 | 999.00 | 2.50 | HUM | 0.93541 | 1.14286 |
| 77.7353 | -116.3526 | 890406 | 10 | 1.63 | 1.00 | 999.00 | 999.00 | 2.50 | HUM | 1.27475 | 1.62500 |
| 78.3130 | -117.2243 | 890406 | 20 | 1.21 | 0.96 | 999.00 | 999.00 | 2.41 | HUM | 1.07778 | 1.25000 |
| 78.1959 | -116.9431 | 890406 | 21 | 1.21 | 0.24 | 999.00 | 999.00 | 2.41 | HUM | 0.53889 | 5.00000 |
| 77.8568 | -115.8755 | 890406 | 11 | 1.50 | 1.00 | 999.00 | 999.00 | 2.50 | HUM | 1.22474 | 1.50000 |
| 77.5963 | -114.2222 | 890406 | 31 | 1.51 | 1.13 | 999.00 | 999.00 | 2.51 | HUM | 1.30423 | 1.33333 |
| 77.8673 | -117.3465 | 890406 | 32 | 1.13 | 1.13 | 999.00 | 999.00 | 2.51 | HUM | 1.12950 | 1.00000 |
| 77.8651 | -117.2045 | 890406 | 33 | 0.63 | 0.50 | 999.00 | 999.00 | 2.51 | HUM | 0.56125 | 1.25000 |
| 78.2349 | -116.9845 | 890406 | 22 | 1.08 | 0.60 | 999.00 | 999.00 | 2.41 | HUM | 0.80834 | 1.80000 |
| 77.5096 | -119.8409 | 890406 | 23 | 1.82 | 1.56 | 999.00 | 999.00 | 2.60 | HUM | 1.68499 | 1.16667 |
| 77.5646 | -115.0955 | 890406 | 29 | 1.51 | 1.13 | 999.00 | 999.00 | 2.51 | HUM | 1.30423 | 1.33333 |
| 78.2897 | -113.7493 | 890406 | 30 | 1.26 | 0.88 | 999.00 | 999.00 | 2.51 | HUM | 1.05001 | 1.42857 |
| 78.2978 | -117.4140 | 890406 | 18 | 0.96 | 0.72 | 999.00 | 999.00 | 2.41 | HUM | 0.83485 | 1.33333 |
| 77.6250 | -110.7063 | 890406 | 16 | 0.75 | 0.50 | 999.00 | 999.00 | 2.50 | HUM | 0.61237 | 1.50000 |
| 78.2414 | -117.4068 | 890406 | 19 | 0.72 | 0.48 | 999.00 | 999.00 | 2.41 | HUM | 0.59033 | 1.50000 |
| 78.2262 | -117.5713 | 890406 | 17 | 1.45 | 1.08 | 999.00 | 999.00 | 2.41 | HUM | 1.25227 | 1.33333 |
| 79.4181 | -103.4574 | 910126 | 2130 | 3.20 | 2.56 | 999.00 | 999.00 | 2.56 | HUM | 2.86217 | 1.25000 |
| 79.3859 | -104.0115 | 910126 | 2131 | 1.02 | 0.51 | 999.00 | 999.00 | 2.56 | HUM | 0.72408 | 2.00000 |
| 79.3512 | -109.3077 | 910126 | 131 | 0.78 | 0.78 | 999.00 | 999.00 | 2.60 | HUM | 0.78000 | 1.00000 |
| 79.5564 | -105.0368 | 910126 | 132 | 2.82 | 1.79 | 1.54 | 0.90 | 2.56 | HUM | 2.24639 | 1.57143 |
| 79.4074 | -108.7182 | 910126 | 130 | 2.86 | 2.60 | 999.00 | 999.00 | 2.60 | HUM | 2.72690 | 1.10000 |
| 80.0287 | -104.7926 | 910126 | 133 | 4.10 | 2.82 | 1.54 | 1.28 | 2.56 | HUM | 3.39622 | 1.45455 |
| 80.5645 | -98.6614 | 910126 | 115 | 4.22 | 2.23 | 1.74 | 0.99 | 2.48 | HUM | 3.06759 | 1.88889 |
| 80.6917 | -98.5083 | 910126 | 117 | 2.48 | 1.98 | 999.00 | 999.00 | 2.48 | HUM | 2.21818 | 1.25000 |
| 79.5338 | -101.4002 | 910126 | 2122 | 6.24 | 6.11 | 5.72 | 5.46 | 2.60 | HUM | 6.17466 | 1.02128 |

EXTREME ICE FEATURES DATA

| Latitude | Longitude | Date | Target | X-floe (km) | Y-floe (km) | X (km) | Y (km) | 1 cm= | Type | equ dia | X/Y |
|----------|-----------|--------|--------|----------------|----------------|-----------|-----------|-------|------|---------|---------|
| 80.2477 | -107.2729 | 910126 | 123 | 2.58 | 2.58 | 999.00 | 999.00 | 3.23 | HUM | 2.58400 | 1.00000 |
| 81.0122 | -111.2437 | 910126 | 127 | 4.52 | 3.88 | 999.00 | 999.00 | 3.23 | HUM | 4.18656 | 1.16667 |
| 80.1692 | -105.7699 | 910126 | 125 | 2.58 | 1.94 | 999.00 | 999.00 | 3.23 | HUM | 2.23781 | 1.33333 |
| 80.4134 | -108.3387 | 910126 | 126 | 3.88 | 2.91 | 999.00 | 999.00 | 3.23 | HUM | 3.35671 | 1.33333 |
| 79.5548 | -105.7500 | 910126 | 129 | 4.42 | 2.60 | 999.00 | 999.00 | 2.60 | HUM | 3.38999 | 1.70000 |
| 79.8698 | -107.7983 | 910126 | 124 | 2.91 | 2.75 | 999.00 | 999.00 | 3.23 | HUM | 2.82510 | 1.05882 |
| 79.5588 | -102.2982 | 910126 | 122 | 7.43 | 7.43 | 999.00 | 999.00 | 3.23 | HUM | 7.42900 | 1.00000 |
| 80.1373 | -105.0664 | 910126 | 128 | 1.94 | 1.45 | 999.00 | 999.00 | 3.23 | HUM | 1.67836 | 1.33333 |
| 79.4179 | -109.7977 | 880725 | 157 | 3.50 | 2.19 | 3.50 | 0.88 | 1.25 | ISL | 2.76699 | 1.60000 |
| 79.4978 | -107.4077 | 880725 | 181 | 0.63 | 0.31 | 999.00 | 999.00 | 1.25 | ISL | 0.44194 | 2.00000 |
| 79.4899 | -107.3311 | 880725 | 180 | 0.38 | 0.13 | 999.00 | 999.00 | 1.25 | ISL | 0.21651 | 3.00000 |
| 79.5202 | -107.1697 | 880725 | 184 | 0.88 | 0.56 | 999.00 | 999.00 | 1.25 | ISL | 0.70156 | 1.55556 |
| 79.3425 | -111.6241 | 880725 | 151 | 1.25 | 0.75 | 0.63 | 0.50 | 1.25 | ISL | 0.96825 | 1.66667 |
| 79.4865 | -107.5147 | 880725 | 179 | 0.75 | 0.25 | 999.00 | 999.00 | 1.25 | ISL | 0.43301 | 3.00000 |
| 79.5214 | -107.0965 | 880725 | 185 | 0.63 | 0.13 | 999.00 | 999.00 | 1.25 | ISL | 0.27951 | 5.00000 |
| 79.5180 | -107.0216 | 880725 | 186 | 0.75 | 0.19 | 999.00 | 999.00 | 1.25 | ISL | 0.37500 | 4.00000 |
| 79.5236 | -107.0237 | 880725 | 187 | 2.38 | 0.63 | 999.00 | 999.00 | 1.25 | ISL | 1.21835 | 3.80000 |
| 79.5405 | -106.8707 | 880725 | 188 | 0.75 | 0.31 | 999.00 | 999.00 | 1.25 | ISL | 0.48412 | 2.40000 |
| 79.5326 | -106.7818 | 880725 | 189 | 0.88 | 0.38 | 999.00 | 999.00 | 1.25 | ISL | 0.57282 | 2.33333 |
| 79.6620 | -107.8629 | 880725 | 163 | 0.38 | 0.13 | 999.00 | 999.00 | 1.25 | ISL | 0.21651 | 3.00000 |
| 79.6609 | -107.7778 | 880725 | 164 | 0.38 | 0.13 | 999.00 | 999.00 | 1.25 | ISL | 0.21651 | 3.00000 |
| 79.4764 | -107.5484 | 880725 | 178 | 0.63 | 0.13 | 999.00 | 999.00 | 1.25 | ISL | 0.27951 | 5.00000 |
| 79.4573 | -108.3325 | 880725 | 168 | 8.88 | 5.00 | 1.25 | 2.13 | 1.25 | ISL | 6.66146 | 1.77500 |
| 79.4944 | -107.8742 | 880725 | 175 | 0.63 | 0.25 | 999.00 | 999.00 | 1.25 | ISL | 0.39528 | 2.50000 |
| 79.5832 | -107.4854 | 880725 | 190 | 0.94 | 0.13 | 999.00 | 999.00 | 1.25 | ISL | 0.34233 | 7.50000 |
| 79.5225 | -108.4225 | 880725 | 172 | 0.75 | 0.19 | 999.00 | 999.00 | 1.25 | ISL | 0.37500 | 4.00000 |

EXTREME ICE FEATURES DATA

| Latitude | Longitude | Date | Target | X-floe (km) | Y-floe (km) | X (km) | Y (km) | 1 cm= | Type | equ dia | X/Y |
|-----------------|------------------|-------------|---------------|------------------------|------------------------|-------------------|-------------------|--------------|-------------|----------------|------------|
| 79.4438 | -107.6862 | 880725 | 174 | 1.13 | 1.00 | 0.25 | 0.13 | 1.25 | ISL | 1.06066 | 1.12500 |
| 79.4955 | -108.2190 | 880725 | 173 | 3.38 | 3.00 | 3.38 | 1.25 | 1.25 | ISL | 3.18198 | 1.12500 |
| 79.9744 | -103.1506 | 890324 | 137 | 2.01 | 0.88 | 999.00 | 999.00 | 2.51 | ISL | 1.32817 | 2.28571 |
| 80.0060 | -102.4757 | 890324 | 139 | 1.00 | 0.63 | 999.00 | 999.00 | 2.51 | ISL | 0.79373 | 1.60000 |
| 80.0060 | -102.1464 | 890324 | 140 | 0.63 | 0.25 | 999.00 | 999.00 | 2.51 | ISL | 0.39687 | 2.50000 |
| 80.0466 | -103.0500 | 890324 | 138 | 2.51 | 2.13 | 1.51 | 0.25 | 2.51 | ISL | 2.31411 | 1.17647 |
| 79.8298 | -104.2423 | 890324 | 148 | 9.04 | 5.27 | 9.04 | 2.01 | 2.51 | ISL | 6.90136 | 1.71429 |
| 79.9563 | -102.5319 | 890324 | 135 | 3.26 | 2.76 | 3.26 | 1.26 | 2.51 | ISL | 3.00152 | 1.18182 |
| 79.8434 | -102.9773 | 890324 | 134 | 3.51 | 2.76 | 3.51 | 1.00 | 2.51 | ISL | 3.11483 | 1.27273 |
| 79.9360 | -102.9050 | 890324 | 136 | 2.51 | 0.88 | 999.00 | 999.00 | 2.51 | ISL | 1.48494 | 2.85714 |
| 82.2300 | -87.6783 | 890404 | 99 | 1.13 | 0.25 | 999.00 | 999.00 | 2.51 | ISL | 0.53245 | 4.50000 |
| 79.2767 | -100.5000 | 910126 | 113 | 1.49 | 0.25 | 999.00 | 999.00 | 2.48 | ISL | 0.60747 | 6.00000 |
| 79.3861 | -101.1874 | 910126 | 112 | 3.47 | 2.48 | 3.47 | 1.49 | 2.48 | ISL | 2.93438 | 1.40000 |
| 79.4425 | -100.8963 | 910126 | 2111 | 3.38 | 0.91 | 999.00 | 999.00 | 2.60 | ISL | 1.75380 | 3.71429 |
| 79.3059 | -100.8592 | 910126 | 119 | 2.26 | 0.97 | 999.00 | 999.00 | 3.23 | ISL | 1.48017 | 2.33333 |
| 79.4565 | -102.9761 | 910126 | 2118 | 9.10 | 5.46 | 9.10 | 1.82 | 2.60 | ISL | 7.04883 | 1.66667 |
| 79.3910 | -101.4943 | 910126 | 2120 | 3.12 | 1.43 | 2.86 | 0.91 | 2.60 | ISL | 2.11225 | 2.18182 |
| 79.4425 | -102.2596 | 910126 | 2121 | 1.04 | 0.52 | 999.00 | 999.00 | 2.60 | ISL | 0.73539 | 2.00000 |
| 79.2767 | -100.6246 | 910126 | 114 | 1.24 | 0.25 | 999.00 | 999.00 | 2.48 | ISL | 0.55454 | 5.00000 |
| 79.4687 | -101.5712 | 910126 | 111 | 3.72 | 0.99 | 999.00 | 999.00 | 2.48 | ISL | 1.92100 | 3.75000 |
| 79.3757 | -102.1821 | 910126 | 120 | 3.23 | 2.26 | 3.23 | 0.97 | 3.23 | ISL | 2.70241 | 1.42857 |
| 79.4513 | -103.9659 | 910126 | 118 | 11.31 | 5.81 | 11.31 | 2.58 | 3.23 | ISL | 8.10724 | 1.94444 |
| 79.4425 | -103.2009 | 910126 | 121 | 1.13 | 0.65 | 999.00 | 999.00 | 3.23 | ISL | 0.85458 | 1.75000 |
| 80.9312 | -98.9565 | 880219 | 72 | 7.06 | 3.68 | 2.15 | 1.84 | 3.07 | REI | 5.10027 | 1.91667 |
| 80.3647 | -99.9996 | 880219 | 48 | 1.81 | 1.12 | 999.00 | 999.00 | 2.79 | REI | 1.42263 | 1.62500 |
| 80.2995 | -100.9630 | 880219 | 50 | 3.63 | 2.51 | 2.37 | 1.95 | 2.79 | REI | 3.01785 | 1.44444 |

EXTREME ICE FEATURES DATA

| Latitude | Longitude | Date | Target | X-floe (km) | Y-floe (km) | X (km) | Y (km) | 1 cm = | Type | equ dia | X/Y |
|----------|-----------|--------|--------|----------------|----------------|-----------|-----------|--------|------|---------|---------|
| 80.6880 | -101.0397 | 880219 | 71 | 3.07 | 1.54 | 1.84 | 0.61 | 3.07 | REI | 2.17082 | 2.00000 |
| 80.8787 | -100.0231 | 880219 | 69 | 3.07 | 1.84 | 1.54 | 0.77 | 3.07 | REI | 2.37801 | 1.66667 |
| 80.8372 | -99.1425 | 880219 | 70 | 2.76 | 1.38 | 999.00 | 999.00 | 3.07 | REI | 1.95374 | 2.00000 |
| 78.4648 | -101.8722 | 880220 | 50 | 5.80 | 4.11 | 3.74 | 1.31 | 3.74 | REI | 4.88353 | 1.40909 |
| 78.6970 | -107.3797 | 880220 | 54 | 4.11 | 2.81 | 2.99 | 1.12 | 3.74 | REI | 3.39702 | 1.46667 |
| 78.2561 | -105.8483 | 880220 | 52 | 4.68 | 2.62 | 999.00 | 999.00 | 3.74 | REI | 3.49845 | 1.78571 |
| 83.2613 | -73.7508 | 880222 | 92 | 1.61 | 1.29 | 0.97 | 0.97 | 3.22 | REI | 1.44003 | 1.25000 |
| 83.1338 | -70.3528 | 880222 | 86 | 0.91 | 0.91 | 999.00 | 999.00 | 3.03 | REI | 0.90900 | 1.00000 |
| 83.1284 | -70.4126 | 880222 | 85 | 0.91 | 0.45 | 999.00 | 999.00 | 3.03 | REI | 0.64276 | 2.00000 |
| 82.9811 | -66.2830 | 880222 | 84 | 1.82 | 1.82 | 1.52 | 0.61 | 3.03 | REI | 1.81800 | 1.00000 |
| 83.0329 | -67.8315 | 880222 | 83 | 1.52 | 1.52 | 999.00 | 999.00 | 3.03 | REI | 1.51500 | 1.00000 |
| 79.2683 | -109.8060 | 880725 | 166 | 2.25 | 0.94 | 999.00 | 999.00 | 1.25 | REI | 1.45237 | 2.40000 |
| 79.4201 | -108.3976 | 880725 | 167 | 2.00 | 1.63 | 999.00 | 999.00 | 1.25 | REI | 1.80278 | 1.23077 |
| 79.5079 | -107.6200 | 880725 | 177 | 3.13 | 1.88 | 2.50 | 0.69 | 1.25 | REI | 2.42061 | 1.66667 |
| 79.4550 | -109.1719 | 880725 | 159 | 6.13 | 4.38 | 1.88 | 2.50 | 1.25 | REI | 5.17657 | 1.40000 |
| 79.5022 | -107.7904 | 880725 | 176 | 1.38 | 0.75 | 999.00 | 999.00 | 1.25 | REI | 1.01550 | 1.83333 |
| 79.8908 | -102.9174 | 890324 | 144 | 3.39 | 2.51 | 2.76 | 2.51 | 2.51 | REI | 2.91636 | 1.35000 |
| 79.7101 | -103.5987 | 890324 | 145 | 2.76 | 1.51 | 1.51 | 0.63 | 2.51 | REI | 2.03913 | 1.83333 |
| 83.4970 | -76.3646 | 890404 | 94 | 1.70 | 1.57 | 1.31 | 0.26 | 2.61 | REI | 1.62994 | 1.08333 |
| 83.1799 | -76.6358 | 890404 | 93 | 1.44 | 1.31 | 1.31 | 0.26 | 2.61 | REI | 1.36870 | 1.10000 |
| 83.1202 | -70.3180 | 890404 | 65 | 0.75 | 0.63 | 999.00 | 999.00 | 2.50 | REI | 0.68465 | 1.20000 |
| 83.1400 | -77.9496 | 890404 | 97 | 1.31 | 1.04 | 999.00 | 999.00 | 2.61 | REI | 1.16723 | 1.25000 |
| 83.1048 | -77.3331 | 890404 | 96 | 1.96 | 1.31 | 999.00 | 999.00 | 2.61 | REI | 1.59829 | 1.50000 |
| 83.0508 | -77.8200 | 890404 | 95 | 2.09 | 1.17 | 999.00 | 999.00 | 2.61 | REI | 1.56600 | 1.77778 |
| 82.8182 | -82.3043 | 890404 | 98 | 1.57 | 1.44 | 999.00 | 999.00 | 2.61 | REI | 1.49933 | 1.09091 |
| 82.9184 | -65.0007 | 890404 | 62 | 1.25 | 0.75 | 999.00 | 999.00 | 2.50 | REI | 0.96825 | 1.66667 |

EXTREME ICE FEATURES DATA

| Latitude | Longitude | Date | Target | X-floe (km) | Y-floe (km) | X (km) | Y (km) | 1 cm= | Type | equ dia | X/Y |
|-----------------|------------------|-------------|---------------|------------------------|------------------------|-------------------|-------------------|--------------|-------------|----------------|------------|
| 81.5743 | -91.8919 | 890404 | 102 | 1.76 | 1.51 | 1.51 | 0.63 | 2.51 | REI | 1.62667 | 1.16667 |
| 81.3574 | -96.9204 | 890404 | 103 | 2.01 | 0.38 | 999.00 | 999.00 | 2.51 | REI | 0.86949 | 5.33333 |
| 82.8869 | -65.9441 | 890404 | 60 | 2.50 | 1.63 | 999.00 | 999.00 | 2.50 | REI | 2.01556 | 1.53846 |
| 83.4217 | -70.4549 | 890404 | 68 | 3.00 | 1.50 | 1.38 | 0.75 | 2.50 | REI | 2.12132 | 2.00000 |
| 82.0380 | -89.7652 | 890404 | 101 | 1.76 | 1.26 | 999.00 | 999.00 | 2.51 | REI | 1.48494 | 1.40000 |
| 80.3235 | -99.5009 | 910126 | 116 | 2.48 | 2.23 | 2.48 | 0.87 | 2.48 | REI | 2.35273 | 1.11111 |

APPENDIX D

ICE TERMINOLOGY

DEFINITIONS

ICE TERMINOLOGY

The following definitions are used by C.S.A. Preliminary Standard S471-M1989 General Requirements, Design Criteria, the Environment, and Loads.

Environmental Loads - A variable load associated with natural environmental phenomena.

Fast Ice - ice that forms and remains fast along the coast where it is attached to the shore (landfast ice), to an ice wall, to an ice front, or between shoals or grounded icebergs.

First-year Ice - sea ice of not more than one winter's growth.

Fixed Offshore Structure - A structure that is designed and constructed to be fixed to the seabed, or a subsea berm, at an offshore location, and which may be a pile-supported, gravity-based, earthfill, fill-retention, or hybrid structure.

Fixed Offshore Production Structure - A fixed offshore structure associated with the production of oil or gas.

Floe - any relatively flat piece of sea ice 20 m or more across that may be categorized according to its horizontal extent as follows:

| | | |
|--------|---|-------------------|
| Giant | - | over 10 km across |
| Vast | - | 2 - 10 km |
| Big | - | 500 - 2000 m |
| Medium | - | 100 - 500 m |
| Small | - | 20 - 100 m |

Hummock Field - an area of broken ice hillocks that has been forced upwards by pressure (see also Rubble Field).

Ice Island - a large piece of floating ice more than 5 m above sea level that has a thickness of 30 - 50 m and an area of a few thousand square metres to 500 km² or more, which has broken away from an Arctic ice shelf.

Ice Scour - the indentation and or scraping of the seabed by ice (also referred to as gouging).

Multi-Year Hummock Field - a hummock field made up of multi-year ice (see also Hummock field).

Multi-Year Ridge - a ridge that has survived one or more melt seasons (see also Ridge).

Rare Environmental Event - an environmental event of short duration that occurs at discrete points in time with an annual probability of occurrence of less than 0.5.

Ridge - a linear ice feature of broken ice blocks, created by pressure due to relative motion that can be categorized as a shear ridge or a compression ridge.

Rubble Field - the floating or grounded accumulation of broken blocks of first-year ice, generally contiguous with a natural or man-made obstruction (see also Hummock Field).

Sea Ice - any form of ice originating from the freezing of sea water.

Other definitions used in this report:

Re-entrant ice - ice which adheres to the outer edge of the ice shelf, thickens and becomes part of the ice shelf. Re-entrant ice does not show the characteristic lineal patterns seen on the surface of ice islands.

Ice Shelf - a floating ice sheet of considerable thickness showing 2 to 50 m or more above sea level, attached to the coast. Usually of great horizontal extent and with a level, or gently undulating surface. Nourished by annual snow accumulation and also the seaward extension of land glaciers. Limited areas may be aground.

Multi-year Landfast Ice - in this report this refers to the landfast ice which forms along the shoreline of the Queen Elizabeth Islands and the north shore of Ellesmere Island and remains there for more than two years, becoming multi-year ice.



This publication is printed on paper containing recovered waste.